

**Leaf movement:
auxin-mediated light signalling
over spatial scales**

Jesse Küpers

Thesis committee

Prof. dr. C. Fankhauser

Prof. dr. R. Offringa

Dr. V.A. Willemsen

Prof. dr. K.H.W.J. ten Tusscher

Prof. dr. J.C.M. Smeekens

ISBN: 978-94-6458-083-9

Cover & Lay-out: Publiss | www.publiss.nl

Print: Ridderprint | www.ridderprint.nl

© Copyright 2022: Jesse Küpers

Plant Ecophysiology, Utrecht University

All rights reserved. No part of this publication may be reproduced, stored in a retrieval system, or transmitted in any form or by any means, electronic, mechanical, by photocopying, recording, or otherwise, without the prior written permission of the author.

Leaf movement: auxin-mediated light signalling over spatial scales

**Bladbeweging: langeafstandssignalering van licht via
auxine**
(met een samenvatting in het Nederlands)

Proefschrift

ter verkrijging van de graad van doctor aan de
Universiteit Utrecht
op gezag van de
rector magnificus, prof.dr. H.R.B.M. Kummeling,
ingevolge het besluit van het college voor promoties
in het openbaar te verdedigen op

maandag 28 maart 2022 des middags te 2.15 uur

door

Jesse Jaap Küpers

geboren op 5 juli 1992
te Winterswijk

Promotor:

Prof. dr. R. Pierik

Dit proefschrift werd (mede) mogelijk gemaakt met financiële steun van de Nederlands organisatie voor Wetenschappelijk Onderzoek (GSU 831.15.003) en Limagrain Nederland B.V.

Contents

Chapter 1	General introduction	7
Chapter 2	Photoreceptors regulate plant developmental plasticity through auxin	21
Chapter 3	Neighbour detection at the leaf tip regulates upward leaf movement through spatial auxin-abscisic acid dynamics	41
Chapter 4	Far-red light enrichment at the leaf tip induces tissue-specific transcriptomes, hormone signalling and petiole hyponasty	59
Chapter 5	PIN-dependent transport facilitates tissue-specific auxin accumulation in the petiole to regulate hyponasty upon remote far-red light enrichment	81
Chapter 6	Gibberellin action and BAP/D module activation are required for the petiole hyponasty response to leaf tip-derived auxin	101
Chapter 7	Transient early weed competition reduces maize development and yield	115
Chapter 8	General discussion	131
Appendix	References	140
	Samenvatting	155
	Acknowledgements	156
	Curriculum Vitae	166
	Publications	167



Chapter 1

General introduction

Jesse J. Küpers, Kasper van Gelderen and Ronald Pierik

Plant Ecophysiology, Dept. Biology, Utrecht University, 3584CH Utrecht, The Netherlands

*A modified version of this chapter has been published as:
Küpers, J.J., van Gelderen, K., & Pierik, R. (2018). Location matters: Canopy light responses over spatial scales. *Trends in plant science*, 23(10), 865-873.*

<https://doi.org/10.1016/j.tplants.2018.06.011/>

Abstract

Plants use light as a signal to determine neighbour proximity in dense vegetation. Far-red light reflected from neighbour plants elicits a wide array of growth responses throughout the plant. Recently, various light quality-induced signals have been discovered that travel between organs and tissue layers. These signals share upstream and downstream components, but can have opposing effects on cell growth. The question is how plants can coordinate these spatial signals into various growth responses in remote tissues. This coordination allows plants to adapt to the environment and understanding the underlying mechanisms could allow precision engineering of crops. To achieve this understanding, plant photobiology research will need to focus increasingly on spatial signalling at the whole-plant level.

Spatial light signal transduction to adapt to heterogeneous light environments

Plants absorb sunlight to power photosynthesis. In addition, light is used as a signal by which plants determine neighbour proximity at high plant density. Chlorophyll preferentially absorbs blue (B: $\lambda = 400\text{-}500\text{ nm}$) and red (R: $\lambda = 600\text{-}700\text{ nm}$) light, whereas far-red (FR: $\lambda = 700\text{-}800\text{ nm}$) is reflected (Fraser *et al.*, 2016). Reflection of FR reduces the R to FR ratio (R/FR), providing an early neighbour detection signal (Ballaré *et al.*, 1990) that precedes the depletion of B and R light, which together indicate canopy shade (de Wit *et al.*, 2016). Plants use specialised photoreceptors to detect these changes in light quality and respond with extensive developmental plasticity (Fraser *et al.*, 2016) (Table 1.1). Seedlings elongate their hypocotyl and bend towards better light conditions (Fankhauser & Christie, 2015; Fraser *et al.*, 2016). Mature plants elongate their stems and petioles and increase leaf angles to the horizontal (Roig-Villanova & Martínez-García, 2016). Collectively, these responses enhance light capture of individual plants when competing with neighbours. Since light distribution in a vegetation canopy is heterogeneous (Chelle *et al.*, 2007), different leaves of an individual plant may experience different light signals. It is generally assumed that responses to light quality changes are coordinated at the individual organ level (de Kroon *et al.*, 2005), which has been corroborated by predominantly young seedling-focused photobiology studies. However, studies on seedlings cannot address the intrinsic developmental complexity of adult plants. Insights from a variety of studies challenge the conception that light responses would occur mostly local.

Spatial aspects of light responses were previously discussed by Martínez-García and co-workers (Bou-Torrent *et al.*, 2008) and huge progress has been made since. Petiole elongation (Pantazopoulou *et al.*, 2017), lamina (leaf blade) growth inhibition (de Wit *et al.*, 2015) and reduced indirect defence against herbivores through extrafloral nectar production (Izaguirre *et al.*, 2013) are local light signal responses to perception of FR light enrichment within the same organ (local, Table 1.1). Another seemingly local response to both FR (Goyal *et al.*, 2016) and B (Ding *et al.*, 2011; Preuten *et al.*, 2013) light enrichment is hypocotyl bending (phototropism). However, phototropism may require spatial light-signal transduction across cell layers (intra-organ, Table 1.1). Other light responses to FR enrichment, such as hypocotyl elongation (Tanaka *et al.*, 2002; Procko *et al.*, 2014) and upward petiole movement (petiole hyponasty) (Michaud *et al.*, 2017; Pantazopoulou *et al.*, 2017) depend on FR perception in the cotyledons and leaf tip respectively, indicating spatial signalling between and within organs. Moreover, root development and flowering are regulated by low R/FR perception in the leaves, indicating true inter-organ light

quality signal transduction across the extreme ends of plants (Table 1.1) (Chen *et al.*, 2016; Endo *et al.*, 2016; van Gelderen *et al.*, 2018). Other responses, such as reduced axillary branching in response to low R/FR need additional work to elucidate the exact spatial aspects (González-Grandío *et al.*, 2017; Holalu & Finlayson, 2017).

A mechanism by which light signals could move between organs would be the transduction of light itself through plant tissues. Relatively woody stems of mature *Arabidopsis* (*Arabidopsis thaliana*) plants and certain tree species can indeed channel light, especially FR, through the plant tissue (Sun *et al.*, 2003; Lee *et al.*, 2016). This light could then affect phytochrome activity in for example the roots (Lee *et al.*, 2016). Another study, using *Arabidopsis* seedlings, found no evidence for physiological effects of putative FR light transmission from shoot to root or vice-versa (van Gelderen *et al.*, 2018). Further studies are required to identify which tissues transduce light and what the ecological significance of this is. Various recent studies, however, have identified light signal transmission via intermediates, such as plant hormones and mobile transcription factors.

Table 1.1. Spatial aspects of different plant developmental responses to light quality.

Light quality response	Regulatory distance	Light quality signal	References
Hypocotyl elongation	Inter-organ	Low R/FR cotyledons	(Tanaka <i>et al.</i> , 2002; Keuskamp <i>et al.</i> , 2010; Procko <i>et al.</i> , 2014, 2016; Das <i>et al.</i> , 2016; Kohnen <i>et al.</i> , 2016)
	Intra-organ	Low R/FR hypocotyl	(Procko <i>et al.</i> , 2016; Zheng <i>et al.</i> , 2016)
Hypocotyl bending	Intra-organ	Unilateral B / FR hypocotyl	(Preuten <i>et al.</i> , 2013; Goyal <i>et al.</i> , 2016)
Petiole elongation	Intra-organ	EODFR ^a lamina	(Kozuka <i>et al.</i> , 2010)
	Local	Low R/FR petiole	(Pantazopoulou <i>et al.</i> , 2017)
Lamina growth inhibition	Local	Low R/FR lamina	(de Wit <i>et al.</i> , 2015)
Reduced extrafloral nectar from leaf	Local	Low R/FR whole branch	(Izaguirre <i>et al.</i> , 2013)
Petiole hyponasty	Intra-organ	Low R/FR leaf tip	(Michaud <i>et al.</i> , 2017; Pantazopoulou <i>et al.</i> , 2017)
Reduced lateral root outgrowth	Inter-organ	Low R/FR shoot	(Salisbury <i>et al.</i> , 2007; Silva-Navas <i>et al.</i> , 2015; Chen <i>et al.</i> , 2016; van Gelderen <i>et al.</i> , 2018)
Floral transition	Inter-organ	Low R/FR leaf	(Cerdán & Chory, 2003; Endo <i>et al.</i> , 2005; Notaguchi <i>et al.</i> , 2008)
Reduced axillary branching	Local	Low R/FR axillary bud	(González-Grandío <i>et al.</i> , 2017; Holalu & Finlayson, 2017)
	Inter-organ	Low R/FR SAM ^b	

^a EODFR= end-of-day far-red treatment. ^b SAM=shoot apical meristem

Here, we will comparatively discuss spatial light signal transduction and responses in seedlings that consist of the embryonic tissues, i.e. cotyledons, hypocotyl and main root, versus adult plants that also have true leaves, a complex root system and floral organs. We will discuss how light quality signalling affects several aspects of plant development, from local cell growth to long-distance regulation of meristem outgrowth and flowering induction, and how this spatial integration helps plants optimally adjust to their dynamic environment.

Inter-organ signalling regulates hypocotyl elongation

Early work in cucumber (*Cucumis sativus* L.) (Black & Shuttleworth, 1974) and mustard (*Sinapis alba* L.) (Casal & Smith, 1988a,b) showed that R/FR perception in the cotyledons and first leaves largely determines hypocotyl and internode elongation. It was later found that in addition to signalling from the leaves, local low R/FR perception in the internodes themselves also regulates the elongation of this organ (Ballaré *et al.*, 1990).

Inter-organ signalling between leaves and stems also occurs in *Arabidopsis* seedlings. Seedlings perceive horizontal reflection of FR by nearby neighbours as a low R/FR ratio which causes phytochrome-dependent induction of auxin biosynthesis (Tao *et al.*, 2008) in the cotyledons (Tanaka *et al.*, 2002; Procko *et al.*, 2014). Here, phyB inactivation releases the repression of the bHLH transcription factors PHYTOCHROME INTERACTING FACTOR 4 (PIF4), PIF5 and PIF7, which in turn rapidly activate expression of YUCCA flavin monooxygenase indole-3-acetic acid (IAA) synthesis genes *YUC2*, *YUC5*, *YUC8* and *YUC9* (Hornitschek *et al.*, 2012; Li *et al.*, 2012) (Figure 1.1 B). YUCCAs then stimulate *de novo* IAA synthesis in low R/FR (Won *et al.*, 2011; Nito *et al.*, 2015; Kohnen *et al.*, 2016; Müller-Moulé *et al.*, 2016). After synthesis in the cotyledons, IAA is transported to the hypocotyl by PIN-FORMED (PIN) auxin-transport proteins, where it leads to induction of auxin responsive genes and elongation (Tanaka *et al.*, 2002; Keuskamp *et al.*, 2010; Procko *et al.*, 2014; Nito *et al.*, 2015; Kohnen *et al.*, 2016).

In the hypocotyl, PIN-FORMED 3 (PIN3) relocates from a basal to a more lateral orientation in low R/FR (Keuskamp *et al.*, 2010), thereby allowing IAA transport from the vasculature towards the elongating epidermal cells. In the epidermis, IAA stimulates cell growth, in part through brassinosteroid-dependent signalling (Das *et al.*, 2016; Procko *et al.*, 2016). Moreover, epidermal IAA perception promotes the expression of the SMALL AUXIN UP-RNA 19 (SAUR19) subfamily of SAUR genes (Procko *et al.*, 2016). SAUR19 activates plasma membrane H⁺-ATPases (Spartz *et al.*, 2014), which leads to apoplast acidification and cell growth (Fendrych *et al.*, 2016) (Figure 1.1 A). This process is reinforced by enhanced expression of cell wall modifying enzymes, such as expansins

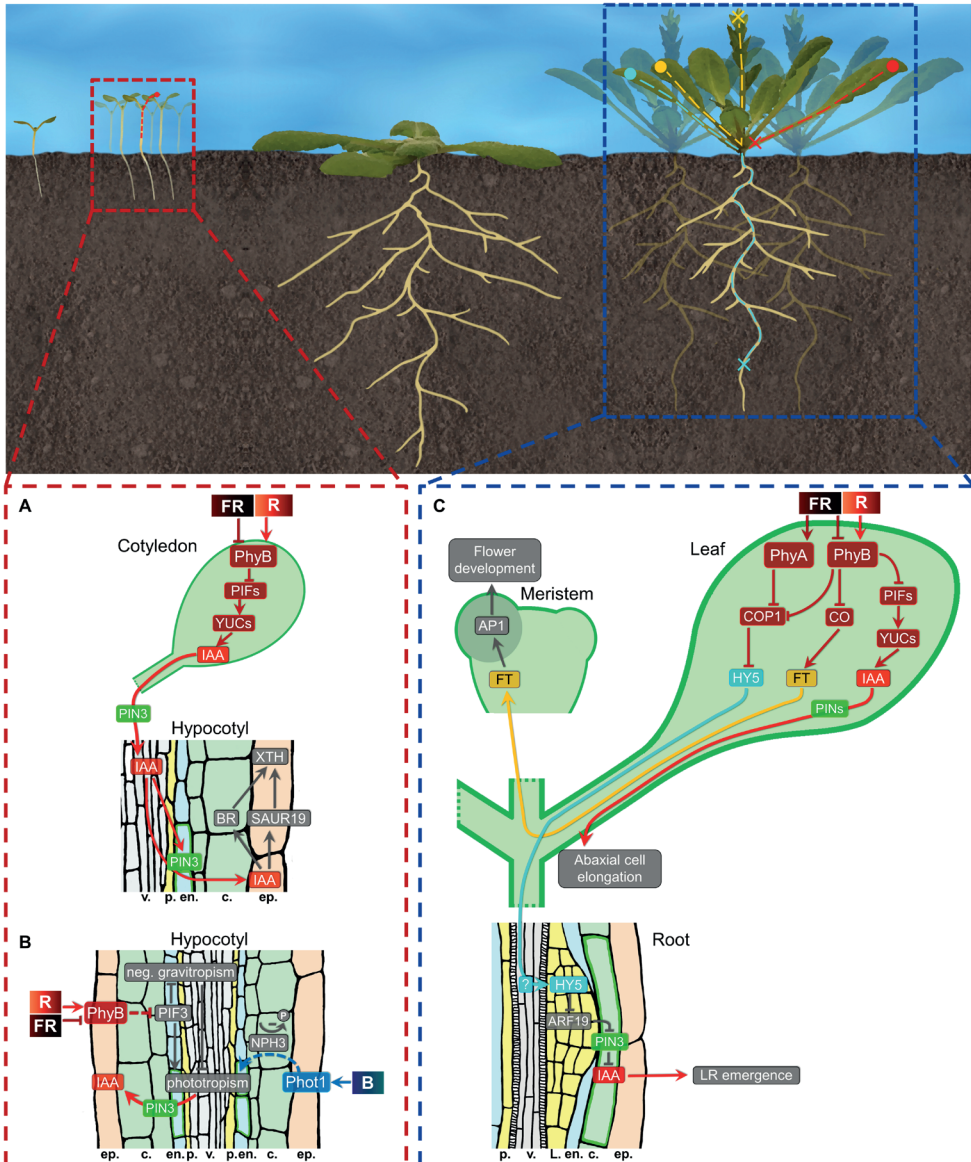
and XYLOGLUCAN ENDOTRANSGLUCOSYLASE/HYDROLASEs (XTHs) (Sasidharan *et al.*, 2010) that are activated by the reduced pH (Arsuffi & Braybrook, 2018). Since the epidermis restricts hypocotyl growth (Kutschera & Niklas, 2007; Procko *et al.*, 2016), epidermis-specific cell elongation allows for hypocotyl elongation. Besides inter-organ IAA transport, local auxin metabolism in the hypocotyl is also regulated by FR enrichment via repressed expression of the auxin conjugating IAA-amido synthetase *GRETCHEN HAGEN 3.17 (GH3.17)* (Zheng *et al.*, 2016). The resulting IAA accumulation occurs independently of IAA synthesis in the cotyledons and stimulates hypocotyl elongation. Although GH3.17-dependent modulation of auxin levels clearly happens locally in the hypocotyl, it is currently unknown whether the regulation of *GH3.17* is entirely local or if it involves inter-organ signalling from the cotyledons.

Intra-organ light signalling in hypocotyl phototropism, elongation and gravitropism

The flow of auxin from the cotyledon to the hypocotyl and then from the vasculature towards the epidermis is a great example of an intra-organ signal traversing organ boundaries and cell layers. Another example of the latter is hypocotyl phototropism, the process in which seedlings bend towards light. Hypocotyl phototropism mainly occurs in the upper part of the hypocotyl and appears to be a local response (Fankhauser & Christie, 2015). B light is sensed by the AGC kinase phototropin 1 (phot1) in the elongation zone, which triggers a more lateral distribution of PIN3 on the plasma membrane (Ding *et al.*, 2011). Subsequently, a relative auxin increase on the shaded compared to the illuminated side of the hypocotyl elongation zone arises, which results in uneven growth and bending (Figure 1.1 C) (Ding *et al.*, 2011; Preuten *et al.*, 2013).

►**Figure 1.1. Spatial light signal transduction in a competitive light environment.** The top image shows *Arabidopsis* seedlings and adult plants in (non)competitive environments and the route of spatial signals in these plants. The colours of the long distance signals are matched in the sections below (A-C). The red or blue dashed box around the plant in competition corresponds to the dashed boxes below. **(A)** Scheme depicting the inter-organ signal (IAA, red) triggering epidermal cell and hypocotyl elongation in low R/FR. **(B)** Intra-organ signalling affecting R-light induced negative gravitropism and B-light-induced phototropic response. The spread of PIF3 degradation and NPH3 dephosphorylation act as intra-organ epidermis-to-endodermis signals. **(C)** Long distance low R/FR-induced signals in adult plants. FT (yellow) moves from leaf to meristem to initiate early flowering, IAA (red) moves from leaf tip to petiole to induce abaxial cell elongation and leaf hyponasty and HY5 (light blue) moves from shoot to root to reduce lateral root emergence. The tissue layers are described below the figures (v. = vasculature, p. = pericycle, en. = endodermis, c. = cortex, ep. = epidermis, L. = lateral root primordium). Acronyms: R, Red light; FR, Far-Red light; B, Blue light; PhyA – PhyB, phytochrome; PIF, PHYTOCHROME INTERACTING FACTOR; YUC, YUCCA flavin monooxygenase; IAA, auxin, Indole-3-Acetic Acid; PIN, PIN-FORMED; BR, Brassinosteroid; SAUR19, SMALL AUXIN UP RNA 19; XTH, Xyloglucan Endotransglucosylase/Hydrolase; Phot1, Phototropin1; NPH3, NON-PHOTOTROPIC HYPOCOTYL3; CO, CONSTANS; FT, FLOWERING LOCUS T; AP1, APETALA1; COP1, CONSTITUTIVE PHOTOMORPHOGENESIS1; HY5, ELONGATED HYPOCOTYL5; ARF19, AUXIN RESPONSE FACTOR19.

Moreover, phot1 signalling in the hypocotyl leads to dephosphorylation of NON-PHOTOTROPIC HYPOCOTYL3 (NPH3), which is necessary for phototropism (Pedmale & Liscum, 2007; Preuten *et al.*, 2013; Haga *et al.*, 2015). Interestingly, epidermal phot1 expression causes a spread of NPH3 dephosphorylation through the entire seedling (Preuten *et al.*, 2013) (Figure 1.1 B). Dephosphorylation causes NPH3 to dissociate from phot1 and the plasma membrane, a mechanism important in phototropism signalling.



NPH3 is part of an E3-ligase complex that is suggested to modulate PIN3 (re)cycling (Roberts *et al.*, 2011) and the vacuolar degradation of PIN2 in the root (Wan *et al.*, 2012). However, the exact way in which NPH3 molecular function and dephosphorylation affects phototropism is unclear (Haga *et al.*, 2015).

In addition to B light, R/FR signalling also affects hypocotyl phototropism. In etiolated seedlings, phyB activation allows phototropism by inhibiting hypocotyl negative gravitropism (Kim *et al.*, 2011). Gravitropism and phototropism are both bending responses of the hypocotyl. However, they are conflicting processes because they constitute growth in different directions; upward in negative gravitropism and sideways in phototropism. Negative gravitropism depends upon PIF-mediated biogenesis of gravity-sensing amyloplasts and can be suppressed by red light via phyB dependent degradation of PIFs (Kim *et al.*, 2011, 2016). It was recently shown that epidermal phyB expression can elicit the degradation of endodermal PIFs, implying an unknown intra-organ signal that traverses cell layers (Figure 1.1 B) (Kim *et al.*, 2016). When a seedling is established in light, phyB suppresses PIFs, thereby decreasing auxin biosynthesis and growth. When such a seedling is close to competing plants, the resulting reduced R/FR relieves PIF suppression, thereby promoting auxin biosynthesis and allowing hypocotyl elongation and phototropism (Goyal *et al.*, 2016).

There are interesting signal transduction overlaps between hypocotyl elongation and phototropism. Both processes need auxin signalling in the epidermis and rely upon a redistribution of PIN3 to transport auxin sideways (Keuskamp *et al.*, 2010; Ding *et al.*, 2011; Procko *et al.*, 2016). Moreover, both processes involve spatial intra-organ signals between endo- and epidermis that are yet to be identified and that include NPH3 dephosphorylation and PIF degradation (Preuten *et al.*, 2013; Goyal *et al.*, 2016; Kim *et al.*, 2016; Procko *et al.*, 2016).

Local and spatial far-red signalling responses regulate light foraging in adult leaves

When the seedling grows to a fully-fledged plant, the light environment it perceives becomes more heterogeneous over the scale of the entire organism, especially in dense stands (Chelle *et al.*, 2007). Different parts of the shoot will experience different light qualities and it is of great relevance to study the sites of light quality perception versus response. Whole-plant exposure to low R/FR conditions promotes petiole elongation and upward leaf movement (hyponasty), which improves the plant's competitive ability during light competition (Roig-Villanova & Martínez-García, 2016).

Recently, two independent studies found that upward petiole movement (hyponasty) in response to low R/FR is regulated via intra-organ signal transduction (Michaud *et al.*, 2017; Pantazopoulou *et al.*, 2017). Localised FR irradiation revealed that hyponasty was fully induced by low R/FR perception in the very tip of the leaf, whereas FR treatment to the petiole itself failed to induce any hyponastic growth. This showed that an intra-organ signal moves from the leaf tip to the petiole base, where differential growth between the abaxial and adaxial sides leads to upward bending of the petiole (Polko *et al.*, 2012, 2015; Rauf *et al.*, 2013; Pantazopoulou *et al.*, 2017). In the leaf tip, inactivation of phyB triggers *de novo* IAA synthesis through PIF7-dependent *YUC* transcription. IAA is subsequently transported by PIN3, PIN4 and PIN7 to the petiole base (Figure 1.1 C) (Michaud *et al.*, 2017; Pantazopoulou *et al.*, 2017). It is currently unknown how auxin from the leaf tip establishes differential growth in the petiole base.

Contrastingly, unidirectional petiole elongation was shown to occur in response to FR enrichment of the petiole but not by FR enrichment of the leaf tip (Pantazopoulou *et al.*, 2017). Although this is clearly a local response, there may still be spatial signal transduction across cell layers (similar to phototropism), or perhaps from the lamina towards the petiole as observed in an end-of-day FR study (Kozuka *et al.*, 2010).

Low R/FR treatment of a single leaf had no effects on petiole elongation or hyponasty of systemic leaves that were not exposed to low R/FR (Michaud *et al.*, 2017; Pantazopoulou *et al.*, 2017), indicating that low R/FR-induced growth responses are regulated within the individual leaf. This modular response to low R/FR allows plants to meet the demands of a light environment that is heterogeneous over the scale of different organs of a single plant. Nevertheless, light quality also controls developmental responses well beyond the leaf module, all the way into the root system (van Gelderen *et al.*, 2018).

Inter-organ light signalling controls root development

When discussing spatial signal transduction over longer distances within individual plants, no distance is longer than that from shoot to root. Plants need to coordinate the growth of both organs to their respective environments in order to balance challenges in light and nutrient uptake (Pierik & Testerink, 2014). Roots can detect and respond to light themselves (Salisbury *et al.*, 2007; Silva-Navas *et al.*, 2015), but low R/FR detected by the shoot can also regulate main root growth and lateral root emergence via a mobile signal that travels from shoot to root (van Gelderen *et al.*, 2018). Central in this response is the light-regulated bZIP transcription factor ELONGATED HYPOCOTYL5 (HY5) which

can move from shoot to root (Chen *et al.*, 2016). Low R/FR detected by phytochrome in the shoot leads to local *HY5* upregulation and protein stabilization, most likely through inhibition of CONSTITUTIVE PHOTOMORPHOGENESIS1 (COP1) (Sheerin *et al.*, 2015; Pacin *et al.*, 2016; van Gelderen *et al.*, 2018). It was subsequently found that HY5 accumulates in the lateral root primordia, where it represses lateral root emergence by downregulating AUXIN RESPONSE FACTOR19 (ARF19) (van Gelderen *et al.*, 2018) (Figure 1.1 C). This is a clear example of inter-organ, long distance signalling where one part of the plant detects the light and a signal is transmitted to remotely regulate development.

Local and inter-organ low R/FR signalling regulates the flowering phenotype

Another adult plant response to low R/FR that involves long distance signal transfer is accelerated flowering. Although early flowering reduces the total seed yield (Procko *et al.*, 2014), it ensures at least some reproduction in competitive environments. The early flowering response occurs in the shoot apical meristem and is induced by phyB inactivation in the leaves (Cerdán & Chory, 2003). PhyB inactivation in the mesophyll releases the repression of *CONSTANS* (*CO*), which leads to enhanced *FLOWERING LOCUS T* (*FT*) transcription in the vasculature (Endo *et al.*, 2005; Notaguchi *et al.*, 2008), indicating intra-organ transport of the light signal across cell layers. After translation, FT protein is transported towards the shoot apical meristem (Jaeger & Wigge, 2007; Notaguchi *et al.*, 2008), where floral transition is stimulated through induction of *APETALA1* (*AP1*) and related floral identity genes (Wigge *et al.*, 2005) (Figure 1.1 C). Low R/FR-induced early flowering thus also involves long-distance inter-organ light signal transduction.

Besides flowering initiation, low R/FR can also repress the development of axillary buds to branches on the inflorescence stem. Low R/FR promotes the *BRANCHED1* -dependent accumulation of abscisic acid (ABA) in the bud, thereby delaying bud outgrowth (González-Grandío *et al.*, 2013, 2017). Although low R/FR may also regulate bud-outgrowth long distance via auxin, this remains to be studied (Holalu & Finlayson, 2017).

Conclusions and future directions

As discussed above, several light quality responses in seedlings and adult plants depend on spatial transduction of light signals perceived in different parts of the plant. Although some growth responses are truly local and happen in the same cells that perceive the signal, it is becoming apparent that multiple light-induced signals travel within and

between organs, allowing precise coordination of growth at the whole-organism level (Figure 1.1). The regulation of root growth by shoot-detected low R/FR for example allows an organ that does not perceive light itself to adjust its growth to match the environment. Interestingly, in the shoot, both hypocotyl elongation and petiole hyponasty are largely regulated by distal light quality signals in the cotyledons and leaf tip respectively. The spatial separation between light perception and response in the leaves might allow plants to distinguish between shade caused by their own leaves and shade caused by neighbours. Both have the same light quality, but neighbours first shade the leaf tip, whereas the plant's own leaves, at least in rosette plants such as *Arabidopsis*, first shade the petiole base (Pantazopoulou *et al.*, 2017).

Spatial light signal transduction often occurs through transport of auxin between different cell layers and organs, for example in hypocotyl elongation, phototropism and upward leaf movement. Additionally, small proteins such as HY5 or FT are involved in light-induced inter-organ long distance signalling. Most likely there are other small proteins and hormones that can fulfil similar roles in other light responses. Indeed, gibberellin and ABA are candidates for intra and inter-organ signal transduction (Regnault *et al.*, 2015; Tal *et al.*, 2016) and future studies will likely elucidate how they control spatially explicit responses to light cues.

Plant responses to light quality have mostly been studied in very young seedlings under whole-seedling, homogeneous irradiation. Although this seedling model successfully aided the unravelling of shade avoidance signalling pathways, seedlings have limited spatial and developmental complexity. Therefore, it is important to study adult plants if we are to understand plants in their full environmental and developmental complexity. This will increase the potential to contribute to challenges of global food production and efficient land use. Elucidating the exact roles of specific organs and cell types in spatial light signal transduction will help to precisely engineer crops for optimal performance in current and future cropping systems.

Thesis outline

In this thesis, the spatial aspects of light signalling using the petiole hyponasty response to neighbour detection in the leaf tip, are investigated. **Chapter 2** reviews in detail the roles of photoreceptors and auxin on the regulation of plant developmental plasticity. It provides a detailed description of the complex integration of light and auxin signalling in diverse light environments and developmental stages.

Chapter 3 shows that in adult *Arabidopsis*, adaptive growth responses to FR enrichment depend on where in the plant the signal is perceived. Here, phytochrome signalling, followed by auxin synthesis and transport are shown to be required for the petiole hyponasty response to FR enrichment at the leaf tip. A potential role for abscisic acid as an inhibitor of excessive petiole hyponasty is also discovered.

Chapter 4 outlines a tissue-specific time-course transcriptomics approach to study how FR enrichment at the remote leaf tip can induce petiole hyponasty through asymmetrical petiole growth. It is revealed how leaf tip-derived auxin triggers an auxin response in the petiole that is strongest on the abaxial side. Moreover, various other hormones including gibberellin are shown to display tissue-specific signalling patterns that may influence auxin-mediated growth.

Chapter 5 consolidates our understanding of auxin distribution and signalling in the petiole upon FR enrichment at the leaf tip. Using various methods, it is shown that PIN proteins orchestrate auxin accumulation in the abaxial petiole, thereby triggering petiole hyponasty.

The involvement of gibberellin in petiole hyponasty that was suggested in **Chapter 4** is investigated in **Chapter 6**. This chapter shows that gibberellin synthesis likely occurs in the petiole through enhanced expression of the gibberellin synthesis genes *GA20OX1* and *GA20OX2* in response to leaf tip-derived auxin. This results in degradation of the downstream growth repressing DELLA protein RGA and allows for auxin-mediated petiole hyponasty. Here it is also shown that ARF and PIF proteins are required for the petiole hyponasty response to auxin.

Most of our work focusses on unravelling the mechanisms behind FR-induced petiole hyponasty in *Arabidopsis*. **Chapter 7** however presents work on the effect of early light competition in maize (*Zea mays*). It shows that the presence of weeds during maize seedling development severely hampers whole plant and seed biomass. Correlation analysis revealed that early stem diameter was a good indicator for final plant yield.

Chapter 8 concludes the thesis with a general discussion that integrates findings from the different chapters and makes suggestions for future directions in shade avoidance research.



Chapter 2

Photoreceptors regulate plant developmental plasticity through auxin

Jesse J. Küpers*, Lisa Oskam* and Ronald Pierik

Plant Ecophysiology, Dept. Biology, Utrecht University, 3584CH Utrecht, The Netherlands

** Authors contributed equally to this manuscript*

*A modified version of this chapter has been published as:
Küpers, J.J., Oskam, L., & Pierik, R. (2020). Photoreceptors regulate plant
developmental plasticity through auxin. *Plants*, 9(8), 940.*

<https://doi.org/10.3390/plants9080940/>

Abstract

Light absorption by plants changes the composition of light inside vegetation. Blue and red (R) light are used for photosynthesis whereas far-red (FR) and green light are reflected. A combination of UV-B, blue and R/FR-responsive photoreceptors collectively measures the light and temperature environment and adjusts plant development accordingly. This developmental plasticity to photoreceptor signals is largely regulated through the phytohormone auxin. The phytochrome, cryptochrome and UV RESISTANCE LOCUS 8 (UVR8) photoreceptors are inactivated in shade and/or elevated temperature, which releases their repression of PHYTOCHROME INTERACTING FACTOR (PIF) transcription factors. Active PIFs stimulate auxin synthesis and reinforce auxin signalling responses through direct interaction with AUXIN RESPONSE FACTORS (ARFs). It was recently discovered that shade-induced hypocotyl elongation and petiole hyponasty depend on long-distance auxin transport towards target cells from the cotyledon and leaf tip, respectively. Other responses, such as phototropic bending, are regulated by auxin transport and signalling across only a few cell layers. In addition, photoreceptors can directly interact with components in the auxin signalling pathway, such as AUXIN/INDOLE ACETIC ACIDS (AUX/IAAs) and ARFs. Here we will discuss the complex interactions between photoreceptor and auxin signalling, addressing both mechanisms and consequences of these highly interconnected pathways.

Introduction

The phytohormone auxin is long known to steer plant growth and development to ensure optimal light capture. In 1880 Charles and Francis Darwin noticed and experimented on the phototropic bending of *Phalaris canariensis* coleoptiles towards a light source (Darwin & Darwin, 1880). They observed that covering the coleoptile tip with tinfoil or a dark painted glass tube reduced their capacity to bend their coleoptile base, regardless of what light was locally perceived at the coleoptile base. Moreover, a tiny slit in the paint induced directed bending towards a weak light source even when the coleoptile base was brightly illuminated from another side. They concluded that “*when seedlings are freely exposed to a lateral light some influence is transmitted from the upper to the lower part, causing the latter to bend*”. Later experiments by Peter Boysen-Jensen, Frits Went and many others revealed that light-directed growth depends on the transport of a water-soluble chemical from the coleoptile tip towards the dark side of the coleoptile base. This chemical was named auxin (Went & Thimann, 1937). Ever since, auxin has been studied intensively in plant biology and certainly also in relation to light cues. We now know how auxin is synthesised, (de)conjugated, transported, sensed and responded to. Here, we discuss recent updates on auxin-mediated growth responses to photoreceptor stimuli. We will discuss how light sensing intimately regulates all aspects of auxin biology, ranging from auxin synthesis from the amino acid tryptophan to transcription factors controlling the expression of auxin-responsive genes. We will also review the current understanding of how these photoreceptor-dependent modifications of auxin biology regulate the developmental plasticity needed for optimal performance under heterogeneous light conditions.

Photoreceptors to sense temperature and light quality, quantity and direction

Light capture is essential for plant development as it fuels photosynthesis. Therefore, plants display elaborate plasticity to fine-tune their growth to the prevailing light conditions. Elongation and phototropic bending of the hypocotyl towards light, as well as upward leaf movement and petiole elongation enhance access to light in dense vegetation and are thus adaptive shade avoidance growth responses (Galvão & Fankhauser, 2015). Plant leaves absorb blue (B) and red (R) light for photosynthesis whilst reflecting far-red (FR), resulting in a low ratio of R to FR light (R/FR) and low B light in vegetational shade (Ballaré *et al.*, 1990; Franklin, 2008). These light composition changes are carefully monitored by several classes of wavelength-specific photoreceptors (Galvão & Fankhauser, 2015). Among those are R/FR perceiving phytochromes, blue

light sensitive cryptochromes and phototropins and UV-B responsive UV RESISTANCE LOCUS 8 (UVR8). The extent to which adaptive photoreceptor-driven growth responses are induced depends on the combined light-induced photoreceptor activation and their shared control of auxin signalling (Figure 2.1).

Phytochromes

There are five phytochromes (phyA-E) in *Arabidopsis*. The growth response to low R/FR mainly occurs through inactivation of phyB, with minor additional function for phyD and phyE (reviewed in Legris *et al.*, 2019). PhyB is synthesised as inactive Pr and photoconverted to active Pfr by R light. Darkness and relative high abundance of FR will cause a reversion back to Pr. PhyB photoconversion results in a ratio of Pfr/Pr that resembles the R/FR (Legris *et al.*, 2019). Besides the role of phyB in light signalling, thermal acceleration of the conversion of Pfr to Pr stimulates the growth response to high ambient temperature (Jung *et al.*, 2016; Legris *et al.*, 2016), which enhances leaf cooling (Crawford *et al.*, 2012). In contrast to phyB, phyA is active in very low R/FR and prevents excessive growth in such unfavourable conditions (Martínez-García *et al.*, 2014). Active phyB translocates to the nucleus where it interacts with and inactivates several PHYTOCHROME INTERACTING FACTOR (PIF) bHLH transcription factors. PhyB inactivates PIF1, PIF3, PIF4 and PIF5 through phosphorylation, ubiquitination and degradation, while PIF7 gets phosphorylated and inactivated without rapid degradation (reviewed in Leivar & Monte, 2014). Inactivation of phyB releases PIF repression, resulting in enhanced target gene expression, auxin synthesis and growth.

Cryptochromes

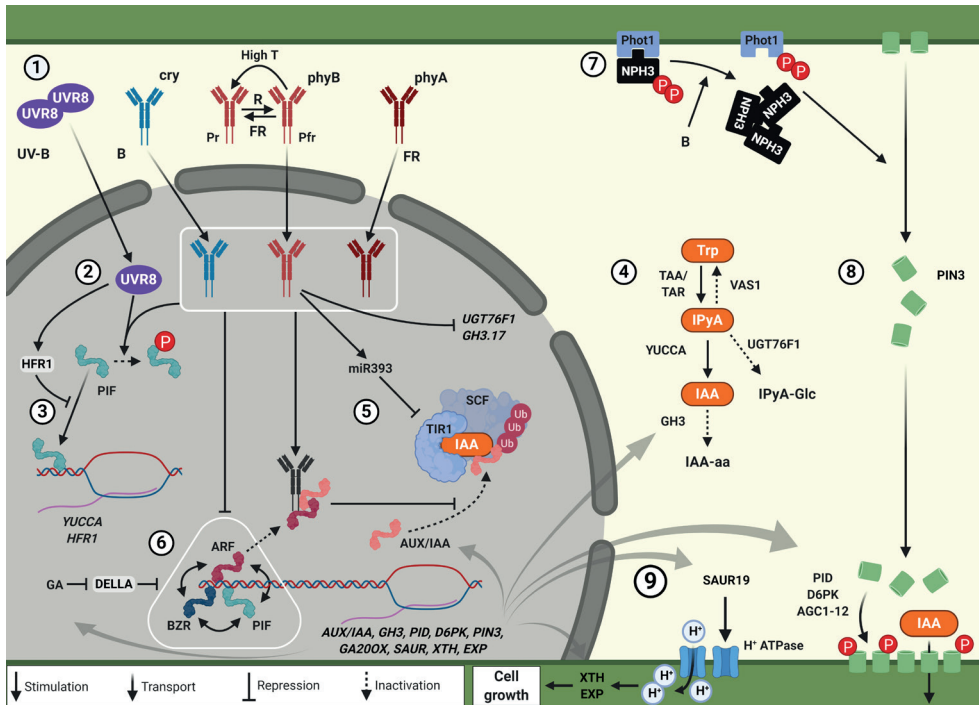
Next to the decreased R/FR, the fluence rate of blue light is also decreased in shade. Perception of low B by the flavoproteins cryptochrome 1 (cry1) and cry2 results in hypocotyl elongation and enhanced low R/FR-mediated petiole elongation in *Arabidopsis* (Keller *et al.*, 2011; Keuskamp *et al.*, 2011; de Wit *et al.*, 2016; Pedmale *et al.*, 2016). In blue light, cry1 and cry2 interact with PIF4 and PIF5 and repress their transcriptional activity (Ma *et al.*, 2016; Pedmale *et al.*, 2016). While PIF7 plays a major role in low R/FR-mediated hypocotyl elongation through stimulating auxin synthesis, with additional roles for PIF4 and PIF5, it is less strictly required for hypocotyl elongation in low B (de Wit *et al.*, 2016; Pedmale *et al.*, 2016). However, cryptochrome inactivation has recently been shown to affect hypocotyl phototropism towards blue light via PIF4, PIF5 and PIF7 and YUCCA-mediated auxin synthesis (Boccaccini *et al.*, 2020).

Phototropins

Phototropism, or bending towards a light source, primarily depends on blue light-induced autophosphorylation of the plasma membrane-associated AGCVIII kinases phototropin 1 (phot1) and phot2 (Fankhauser & Christie, 2015). Whilst phot1 regulates bending in a wide range of blue light intensities, phot2 primarily functions in high blue light. Unilateral blue light perception by phot1 leads to dephosphorylation of the key interacting protein NON-PHOTOTROPIC HYPOCOTYL 3 (NPH3) (Fankhauser & Christie, 2015). Dephosphorylated NPH3 dissociates from the phot1 membrane complex to form cytosolic aggregates which occur most strongly in the illuminated side of the hypocotyl (Sullivan *et al.*, 2019). This NPH3 dephosphorylation asymmetry is mirrored by auxin reporters (Ding *et al.*, 2011; Zhang *et al.*, 2017; Haga *et al.*, 2018; Boccaccini *et al.*, 2020). Asymmetric auxin concentrations allow for phototropic hypocotyl bending through auxin-mediated cell elongation on the shaded side of the hypocotyl (Wang *et al.*, 2020). Although most research regarding phototropism has focused on hypocotyl bending, phototropin-mediated bending towards blue light also occurs in inflorescence stems and petioles (Kagawa *et al.*, 2009). Furthermore, besides bending to blue light, inflorescences and hypocotyls also bend towards unilateral UV-B using the UV-B receptor UVR8 (Vandenbussche *et al.*, 2014; Vanhaelewyn *et al.*, 2019) (reviewed in Legris & Boccaccini, 2020).

UVR8

Upon UV-B irradiation, the inactive UVR8 dimer monomerises and relocates to the nucleus where it stabilises the growth repressing transcription factor ELONGATED HYPOCOTYL 5 (HY5) (reviewed in Liang *et al.*, 2019). This HY5 accumulation reduces gibberellic acid (GA) signalling by promoting GA inactivation through increased *GA2OX1* transcription (Hayes *et al.*, 2014). Moreover, as UV-B sensing by UVR8 serves as a signal for full sunlight, UVR8 signalling inhibits the elongation responses to low R/FR and high temperature through degradation of PIF4 and PIF5 (Hayes *et al.*, 2014, 2017; Sharma *et al.*, 2019; Tavridou *et al.*, 2020). Moreover, UVR8 signalling stabilises LONG HYPOCOTYL IN FAR-RED 1 (HFR1), which negatively regulates PIF4 and PIF5 activity (Tavridou *et al.*, 2020). The combined inactivation of PIFs and accumulation of HY5 reduces auxin and gibberellin signalling and thereby dampens the growth response to low R/FR and elevated temperature.



Photoreceptor control of auxin synthesis and conjugation

Photoreceptor signalling regulates local and systemic auxin concentrations at three levels of regulation: biosynthesis, (de)conjugation and transport (Figure 2.1) (reviewed in Casanova-Sáez & Voß, 2019). Bioactive auxin, indole-3-acetic acid (IAA), is mainly synthesised in a two-step pathway from its tryptophan (Trp) precursor (Tao *et al.*, 2008; Stepanova *et al.*, 2008, 2011; Mashiguchi *et al.*, 2011; Won *et al.*, 2011). Trp is converted to indole-pyruvic acid (IPyA) by TRYPTOPHAN AMINOTRANSFERASE OF ARABIDOPSIS 1 (TAA1) and TAA1-RELATED proteins (TARs) (Tao *et al.*, 2008; Stepanova *et al.*, 2008; Won *et al.*, 2011). IPyA is next converted to IAA in a rate limiting step by YUCCA (YUC) flavin monooxygenases (Mashiguchi *et al.*, 2011; Stepanova *et al.*, 2011; Won *et al.*, 2011). Although a *taa1* mutant was also characterised in a shade avoidance mutant screen as *shade avoidance 3 (sav3)*, TAA1 and TAR expression are not typically stimulated by low R/FR (Tao *et al.*, 2008). On the other hand, low R/FR and high ambient temperature do stimulate YUCCA gene expression through PIF4, PIF5 and PIF7 (Franklin *et al.*, 2011; Hornitschek *et al.*, 2012; Sun *et al.*, 2012; Li *et al.*, 2012; Hayes *et al.*, 2014; Müller-Moulé *et al.*, 2016; Fiorucci *et al.*, 2020). Indeed, low R/FR and elevated temperature promote IAA accumulation in the shoot (Tao *et al.*, 2008; Franklin *et al.*, 2011; Hornitschek *et al.*, 2012; Li

◀Figure 2.1. Photoreceptors regulate cell growth through altered auxin synthesis, transport and signalling. ① Wavelength-specific activation of the photoreceptors UV RESISTANCE LOCUS 8 (UVR8), cry, phyB and phyA triggers their nuclear accumulation. PhyB activation by red light is reversed by far-red light and spontaneous conversion that is accelerated at high temperature. ② Active photoreceptors trigger PHYTOCHROME INTERACTING FACTOR (PIF) phosphorylation, which leads to degradation for PIF4 and PIF5 and inactivation for PIF7. ③ Free PIFs bind to promoters of *YUCCAs*, *HFR1* and many other target genes and stimulate their expression. HFR1, which is stabilised in UV-B via UVR8, inhibits DNA binding of PIFs. ④ Auxin synthesis mainly occurs in a two-step pathway. Trp is first converted to IPyA by TAA1 and TARs. IPyA is next converted to active IAA auxin via YUCCA. Negative feedback on IPyA levels occurs through reversal to Trp via VAS1 and IPyA glycosylation by UGT76F1. IAA is also inactivated by conjugation to amino acids via GH3 proteins. ⑤ In the nucleus, IAA interacts with the TIR1/AFB receptors of the SCF^{TIR1/AFB} receptor complex. Upon IAA binding, SCF^{TIR1/AFB} ubiquitinates AUXIN/INDOLE ACETIC ACID (AUX/IAA) proteins, which leads to AUX/IAA degradation. In the absence of IAA, AUX/IAAs inhibit auxin signalling by interacting with AUXIN RESPONSE FACTORS (ARFs), preventing their DNA binding and transcriptional activity. ARF activity is further reduced by photoreceptor stabilisation of AUX/IAAs, and the formation of a transcriptionally inactive photoreceptor-AUX/IAA-ARF complex. PhyB inactivation in persistent shade enhances auxin signalling through reduced expression of the *TIR1*-targeting *mir393*. ⑥ The transcriptional activity of ARFs is reinforced by the formation of a trans-activating transcription factor module together with BZR and PIF. BZR1, ARF and PIF are all inhibited by interaction with growth-repressive DELLA proteins, forming the BAP/D module. DELLA repression is alleviated by GA-mediated DELLA degradation in persistent shade conditions. Besides DELLAs, various active photoreceptors have also been shown to inhibit the activity of BZR1, ARF and PIF. Active BZR1, ARF and PIF target many shared and unique target genes, including genes involved in auxin inactivation and transport, as well as gibberellin synthesis and cell growth. ⑦ Phot1 associates with NPH3 at the plasma membrane. Phot1 activation by unilateral blue light leads to phot1 autophosphorylation. This triggers NPH3 dephosphorylation and a loss of PIN3 from the outer endodermal plasma membrane on the illuminated side of the hypocotyl (for details see Figure 2.2). ⑧ Polar redistribution of PIN3 occurs in response to photoreceptor cues. Moreover, PIN3 can be phosphorylated by PID, D6PK and AGC1-12 kinases that are required for various photoreceptor-mediated growth responses. Polar localisation of PIN3 allows for directed auxin flow towards target tissues (for details see Figure 2.2). ⑨ Auxin stimulates apoplast acidification through SAUR19-mediated activation of H⁺-ATPases. This enhances the activity of cell wall modifying enzymes and results in acid growth. This figure was created using BioRender.com.

et al., 2012), and even in elongating hypocotyls specifically (Keuskamp *et al.*, 2010; Procko *et al.*, 2014).

The conversion of IPyA to IAA is described to be rate-limiting in IAA synthesis. Reduced IPyA levels inhibit IAA synthesis and auxin-mediated hypocotyl elongation in shade and elevated temperature (Zheng *et al.*, 2013; Chen *et al.*, 2020). IPyA can be reverted to Trp by the aminotransferase REVERSAL OF SAV3 PHENOTYPE 1 (VAS1), which inhibits shade-induced hypocotyl elongation (Zheng *et al.*, 2013). Moreover, IPyA glycosylation via UDP-GLYCOSYLTRANSFERASE 76F1 (UGT76F1) also reduces hypocotyl elongation (Chen *et al.*, 2020). PIF4 stabilisation in elevated temperature reduces *UGT76F1* expression leading to lower levels of glycosylated IPyA, which ultimately increases IAA levels in elevated temperature (Chen *et al.*, 2020).

Although seedlings elongate their hypocotyls in low R/FR, it has been shown in *Brassica rapa* seedlings that low R/FR triggers auxin synthesis in the cotyledons, which, indeed,

are the classic sites of auxin synthesis (Procko *et al.*, 2014). Auxin then is transported to the hypocotyl to promote elongation (Figure 2.2) (Keuskamp *et al.*, 2010). Consistently, transcriptome surveys in *Arabidopsis* indicate light sensing and auxin synthesis in the cotyledons, whereas mostly downstream responses are observed in the hypocotyl (Das *et al.*, 2016; Kohnen *et al.*, 2016). Another example of spatial separation between the location of light sensing and growth response can be observed in adult *Arabidopsis* plants. Low R/FR light perception at the leaf tip locally triggers auxin synthesis through PIF7-mediated upregulation of *YUC8* and *YUC9* expression (Pantazopoulou *et al.*, 2017). The newly synthesised auxin is subsequently transported towards the petiole base, where petiole hyponasty is induced (Figure 2.2) (Michaud *et al.*, 2017; Pantazopoulou *et al.*, 2017).

Auxin synthesis upon phytochrome inactivation in seedlings mainly takes place in the cotyledons. However, auxin levels in the elongating hypocotyl may also be locally regulated by altered auxin conjugation and inactivation. Amino acid conjugation to auxin is mediated by clade II members of the GRETCHEN HAGEN 3 (GH3) family of acyl acid-amido synthetases (Staswick *et al.*, 2005). These GH3s reduce free IAA levels by IAA conjugation with different amino acids (Staswick *et al.*, 2005). Because of functional redundancy, only higher order mutants display increased IAA concentrations (Staswick *et al.*, 2005; Porco *et al.*, 2016). In a mutant screen for suppressors of the R/FR-irrespective *sav3* phenotype, REVERSE OF SAV3 PHENOTYPE 2 (VAS2) was identified and shown to be GH3.17 (Zheng *et al.*, 2016). GH3.17 conjugates IAA to glutamic acid (Glu) which is irreversible and leads to IAA degradation. The expression of *GH3.17* is only mildly reduced by shade in the hypocotyl (Zheng *et al.*, 2016), asking the question if this is a major node of regulation during shade avoidance. Perhaps a concerted downregulation of multiple GH3's would indicate a major point of regulation. Importantly, the *vas2/gh3.17* mutant could elongate its hypocotyl in shade even without auxin transport from the cotyledons (Zheng *et al.*, 2016), indicating the potential for modulation of auxin concentrations in physiologically meaningful ranges without de novo synthesis.

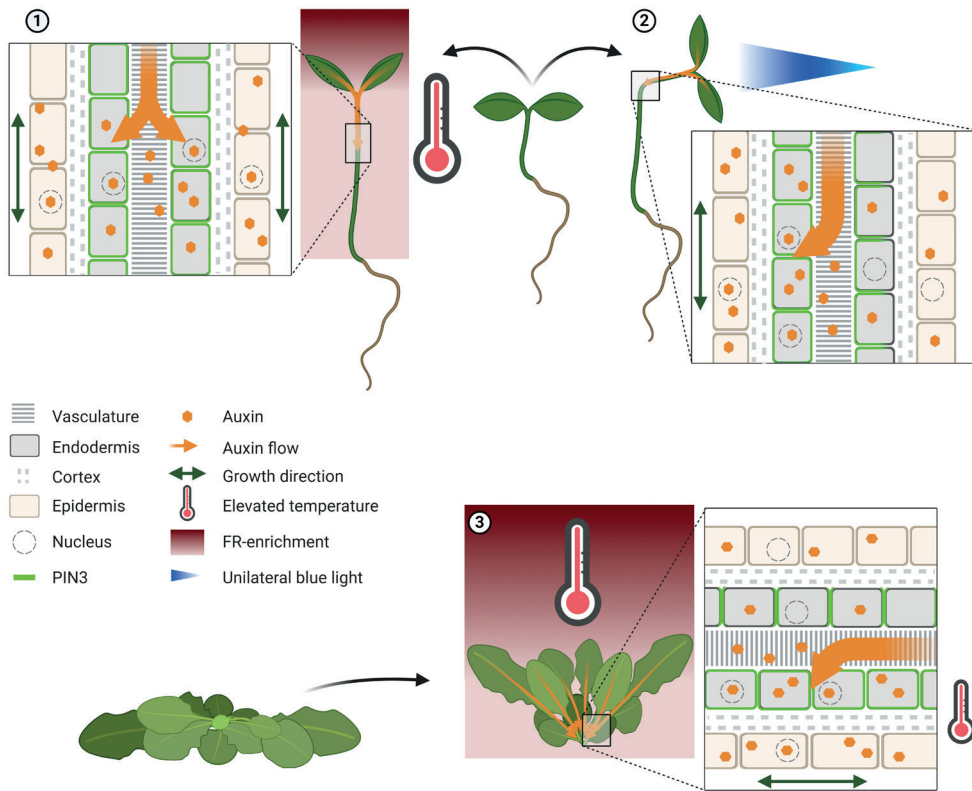


Figure 2.2. Photoreceptor control of auxin distribution patterns. Phenotypic changes of seedlings and adult plant after photoreceptor (de)activation are shown relative to plants grown under control conditions. Inserts depict a cellular representation of auxin localisation in either hypocotyl or petiole. ① Hypocotyl elongation of seedlings after photoreceptor phyB inactivation by elevated temperature and FR-enriched light. De novo synthesised auxin is transported from the cotyledons towards the hypocotyl, where an even distribution of PIN3 proteins between the different sides of the hypocotyl endodermis facilitates both downward and lateral auxin transport, allowing auxin accumulation throughout the hypocotyl. This is different from the control white light situation where PIN3 localisation mostly facilitates rootward auxin transport. ② Unilateral blue light (here from the right) results in phot-dependent phototropic bending towards the light source. This occurs through asymmetric localisation of PIN3 proteins in the endodermis, favouring auxin transport towards the non-illuminated side. The resulting auxin gradient promotes differential cell elongation that results in bending towards the light. ③ Adult plant exposure to supplemental FR or elevated temperature results in upward leaf movement. PIN3 localisation towards the abaxial sides of the abaxial endodermal layer was observed at elevated temperatures, and this would lead to auxin accumulation on the abaxial side of the petiole. In both elevated temperature and FR-enriched light, auxin and polar auxin transport are required for the hyponastic leaf movement. This figure was created using BioRender.com.

Photoreceptor control of auxin transport

As mentioned earlier, cotyledon- and leaf-generated auxin has to be transported to specific target cells in order to initiate shade avoidance responses. Importantly, polar auxin transport (PAT) is required to relay photoreceptor information through the plant (reviewed in Adamowski & Friml, 2015). In PAT, auxin can enter the cell via passive influx as protonated auxin (Adamowski & Friml, 2015), or through AUXIN1/LIKE AUX1 (AUX/LAX) auxin influx permeases (reviewed in Péret *et al.*, 2012), and is directed to the neighbouring cell via polarly localised PIN-FORMED 1 (PIN1) - PIN4 and PIN7 efflux carriers (Petráček *et al.*, 2006; Wisniewska *et al.*, 2006). Polar auxin transport through PINs is essential for photoreceptor-mediated growth responses including hypocotyl elongation, phototropic bending and petiole hyponasty. Moreover, the ATP-BINDING CASSETTE TRANSPORTERS OF THE B SUBFAMILY (ABCB) auxin transporters are also involved in the regulation of auxin transport during photomorphogenesis and phototropic bending (Lin & Wang, 2005; Nagashima *et al.*, 2008; Christie *et al.*, 2011).

Auxin transport through PIN proteins is essential for low B and low R/FR mediated hypocotyl elongation (Keuskamp *et al.*, 2010, 2011). In seedlings, low R/FR leads to redistribution of PIN3 in the hypocotyl endodermis from a downward apical orientation towards a more lateral outward orientation (Figure 2.2) (Keuskamp *et al.*, 2010). This redirects the cotyledon-generated downward auxin flow towards the hypocotyl epidermis where cell elongation allows for elongation of the whole organ (Keuskamp *et al.*, 2010; Procko *et al.*, 2016). This lateral PIN3 redistribution occurs similarly on all sides of the hypocotyl, leading to uniform and upward growth. In contrast, phototropism and petiole hyponasty are the result of differential growth between two sides of the responsive organ.

Hypocotyl phototropism towards unilateral blue light is the result of enhanced auxin signalling on the shaded side of the hypocotyl (Friml *et al.*, 2002b; Ding *et al.*, 2011; Zhang *et al.*, 2017; Haga *et al.*, 2018; Boccaccini *et al.*, 2020). The observed auxin asymmetry is reduced in *pin3* and *phot1* mutants (Ding *et al.*, 2011), and PIN1, PIN3, PIN4 and PIN7 are all required for normal phototropic bending (Haga & Sakai, 2012; Willige *et al.*, 2013). Unilateral light triggers clathrin-mediated internalisation of PIN3 from the outer endodermal membrane in the illuminated side (Figure 2.1) (Ding *et al.*, 2011; Zhang *et al.*, 2017). The ensuing asymmetric PIN3 localisation redirects the auxin flow towards the shaded side, stimulating growth towards the light by enhanced cell elongation on the shaded side (Figure 2.2).

Phototropic hypocotyl bending is not limited to dark-grown seedlings. In fact, de-etiolation by blue or red light renders the seedling more responsive to subsequent unilateral blue light, possibly through inactivation of PIFs by cry and phy (Sullivan *et al.*, 2019). Moreover, phyB and cry1 inactivation in shade stimulate phot1-mediated hypocotyl bending towards blue light when compared to white light conditions (Goyal *et al.*, 2016; Boccaccini *et al.*, 2020). This regulation requires auxin synthesis via PIF4, PIF5 and PIF7-dependent regulation of YUCCAs (Goyal *et al.*, 2016; Boccaccini *et al.*, 2020). In this model, the increased auxin flow into the hypocotyl from the cotyledons (Keuskamp *et al.*, 2010; Procko *et al.*, 2014) can feed into a phot1-mediated PIN3 asymmetry and increase auxin concentrations on the shaded side.

In addition to phototropin-mediated blue light signalling, UV-B signalling via UVR8 can also regulate phototropic bending (Vandenbussche *et al.*, 2014; Vanhaelewyn *et al.*, 2019). Although unilateral UV-B does result in an auxin signalling gradient in hypocotyls, this seems to depend less strictly on polar auxin transport than does blue light-dependent phototropism (Vandenbussche *et al.*, 2014). A UVR8-dependent HY5 gradient was observed between the UV-B-illuminated and non-illuminated side of the hypocotyl (Vandenbussche & Van Der Straeten, 2014) and this could differentially affect auxin response between these two sides (Vandenbussche *et al.*, 2014), although further experiments are needed to resolve this. Similar mechanisms may regulate inflorescence bending towards UV-B light, where the observed HY5 gradient is mirrored by auxin and GA signalling gradients (Vanhaelewyn *et al.*, 2019).

During hyponastic leaf bending, PIN-mediated auxin transport from the leaf tip towards the petiole base is essential (Michaud *et al.*, 2017; Pantazopoulou *et al.*, 2017). Indeed, blocking auxin transport from the leaf tip using local application of the polar auxin transport inhibitor NPA, strongly impaired this response (Pantazopoulou *et al.*, 2017). Although PIN3 is a major regulator in hyponastic leaf movement, it acts redundantly with PIN4 and PIN7 in this response (Michaud *et al.*, 2017; Pantazopoulou *et al.*, 2017). So far, it is unknown if and how an abaxial/adaxial auxin response gradient builds up in the petiole base itself in response to auxin coming from the leaf tip under low R/FR conditions. However, this has been studied in the hyponastic growth response to elevated ambient temperature (Park *et al.*, 2019). In such conditions, PIN3 was shown to concentrate on the outer side of the abaxial endodermis (Park *et al.*, 2019), suggesting directed auxin flow towards the elongating, abaxial side of the petiole (Figure 2.2). PIN3 accumulation on the abaxial endodermis requires functional PIF4 and ASYMMETRIC LEAVES 1 (AS1), an important regulator of abaxial/adaxial cell identity (Park *et al.*, 2019). Removal of the

lamina prior to high temperature exposure abolished petiole hyponasty, suggesting that auxin transport from the lamina to the petiole may be required for temperature-induced petiole hyponasty (Park *et al.*, 2019). More subtle manipulations, for example locally using the polar auxin transport inhibitor NPA, would help ascertain that this is really the case.

Besides PIN-mediated auxin transport, regulated diffusion through plasmodesmata may stimulate rapid directional auxin transport from leaf tip to petiole base (Gao *et al.*, 2020). The direction of the auxin flow depends on higher permeability for auxin in the longitudinal versus transverse direction of the cells along the petiole and midrib of the lamina (Gao *et al.*, 2020). Impaired glucan-mediated control of plasmodesmata aperture in the GLUCAN SYNTHASE LIKE 8 (GSL8) mutant *gs18* reduced the leaf hyponasty response to auxin application to the leaf tip (Gao *et al.*, 2020). It remains to be investigated if plasmodesmata aperture is regulated by photoreceptor signalling and light or temperature treatments.

Regulation of PIN relocalisation by photoreceptor signalling

Although our understanding of photoreceptor effects on PIN localisation is quite extensive, the exact mechanisms remain uncertain. PIN polarization is regulated by subcellular trafficking of PINs, which is a constant process that is influenced by light, but also other environmental stimuli such as gravity, temperature and salinity (Adamowski & Friml, 2015). Regulation of PIN localisation, as well as activation via phosphorylation, occurs through different components such as ARF-GEF GNOM and three families of protein kinases, AGC kinases, MITOGEN ACTIVATED PROTEIN (MAP) KINASES (MPKs) and CA²⁺/CALMODULIN-DEPENDENT PROTEIN KINASE-RELATED KINASES (CRKs) (Adamowski & Friml, 2015; Barbosa *et al.*, 2018). Several members of the AGCVIII kinase family, to which phototropin also belongs, have been implied to regulate auxin transport and PIN phosphorylation during phototropism (Ding *et al.*, 2011; Willige *et al.*, 2013; Haga *et al.*, 2018). Transcript levels of one of these AGCVIII kinases, *PINOID* (*PID*), were found to be reduced by light (Ding *et al.*, 2011). This was linked to reduced PIN3 asymmetry in seedlings mis-expressing *PID* (Ding *et al.*, 2011). However, the quadruple *pid pid2 wag1 wag2* mutant only has reduced phototropism in R light pre-treatment conditions but bends normally in other treatments (Haga *et al.*, 2014). Petiole hyponasty, induced by elevated temperature, was found to be correlated with PIF4-induced *PINOID* (*PID*) expression in the elongating abaxial side of the petiole, where auxin is thought to accumulate (Park *et al.*, 2019). In such conditions, ectopic *35S::PID* expression disturbed PIN3 localisation and inhibited temperature-mediated leaf hyponasty (Park *et al.*, 2019).

Other AGCVIII kinases that are required for hypocotyl bending include D6 PROTEIN KINASE (D6PK), D6PK LIKE 1 (D6PKL1), D6PKL2 and D6PKL3 as well as AGC1-12 (Willige *et al.*, 2013; Haga *et al.*, 2018). Similar to PID, both D6PKs and AGC1-12 are able to phosphorylate the PIN1 hydrophilic loop in vitro (Haga *et al.*, 2018). However, D6PKs and AGC1-12 phosphorylate at least one unique PIN1 serine residue that is not phosphorylated by PID, which might distinguish them from PID in regulating hypocotyl bending (Haga *et al.*, 2018). The function of D6PKs and AGC1-12 in regulating hypocotyl bending appears to extend beyond phototropism as their mutants also show decreased gravitropism (Haga *et al.*, 2018). Moreover, expression of *D6PK* and *D6PKL1* is specifically induced by low R/FR in hypocotyls and *d6pk01* mutant and *D6PK* overexpressing seedlings display reduced hypocotyl elongation in low R/FR (Kohnen *et al.*, 2016).

Phytochrome signalling regulates auxin perception

Photoreceptors not only influence auxin concentrations, but also regulate downstream auxin perception and signalling. Auxin perception mainly occurs via the nuclear TRANSPORT INHIBITOR RESISTANT1 (TIR1) and AUXIN SIGNALLING F-BOX (AFB) receptors of the SKP-CULLIN-F-BOX (SCF)^{TIR1/AFB} ubiquitin ligase complex that form a receptor complex with their AUXIN/INDOLE ACETIC ACID (AUX/IAA) coreceptors (Figure 2.1) (Salehin *et al.*, 2015) although other mechanisms of auxin perception have also been implied (reviewed in Gallei *et al.*, 2020). In persistent low R/FR, TIR1 and AFB2 are required for hypocotyl elongation and their transcript levels are increased (Pucciariello *et al.*, 2018). Increased *TIR1* and *AFB2* transcripts coincide with reduced *microRNA393* (*mir393*) expression. *mir393* targets *TIR1*, *AFB2* and *AFB3* transcripts, reducing auxin signalling in adverse environmental conditions (reviewed in Weijers & Wagner, 2016). Reduced *mir393* expression in persistent low R/FR suggests enhanced auxin activity, consistent with higher activity of the auxin reporter DR5::GUS in *mir393a mir393b* double mutant seedlings in persistent low R/FR (Pucciariello *et al.*, 2018).

Once the SCF^{TIR1/AFB} complex binds auxin, it interacts with and ubiquitinates the auxin signalling repressors AUX/IAAs, which are subsequently degraded (Salehin *et al.*, 2015). This releases AUX/IAA repression of auxin related gene expression and cell growth (Salehin *et al.*, 2015). Recent studies have established that photoreceptor activation by light prevents AUX/IAA degradation and thereby lessens the auxin induced growth response (Xu *et al.*, 2018; Yang *et al.*, 2018; Mao *et al.*, 2020).

Photoreceptor-mediated AUX/IAA stabilisation reduces ARF activity

Cry1 reduces hypocotyl growth and DR5::GUS auxin reporter activity through blue light intensity-dependent stabilisation of AUX/IAAs (Figure 2.1) (Xu *et al.*, 2018). Activated cry1 binds AUX/IAAs and thereby reduces their interaction with TIR1 (Xu *et al.*, 2018). Comparable to cry1, phyB can interact with and stabilise AUX/IAAs with increasing R light intensity (Xu *et al.*, 2018).

Unlike phyB, phyA is stabilised in deep shade and represses excessive auxin-induced gene expression and hypocotyl elongation in such unfavourable conditions (Martínez-García *et al.*, 2014; Yang *et al.*, 2018). Just like cry1 and phyB, phyA can interact with AUX/IAAs in the nucleus, tentatively preventing TIR1-dependent degradation (Yang *et al.*, 2018). AUX/IAA protein levels are reduced in mild shade, presumably due to reduced phyB activity, but in deep shade strong phyA activity outcompetes TIR1 for AUX/IAA binding (Yang *et al.*, 2018).

AUX/IAAs repress auxin signalling through inhibition of the Auxin Response Factor (ARF) transcription factor-mediated gene expression (Weijers & Wagner, 2016). The transcription activating class A ARFs consisting of ARF5, ARF6, ARF7, ARF8 and ARF19, constitute the main AUX/IAA targets (Weijers & Wagner, 2016). Of these class A ARFs, ARF6, ARF7 and ARF8 are redundantly required for auxin mediated hypocotyl elongation in low R/FR and high temperature (Reed *et al.*, 2018). In a recent study, ARF6 and ARF8 were found to interact with phyB in R light and cry1 in blue light, resulting in reduced ARF6/ARF8 DNA binding (Mao *et al.*, 2020). In correspondence with the observed light-induced stabilisation of AUX/IAAs by phyB and cry1 (Xu *et al.*, 2018), phyB and cry1 were shown to stimulate AUX/IAA-ARF interaction and AUX/IAAs were shown to strengthen the photoreceptor mediated inhibition of ARF DNA binding (Figure 2.1) (Mao *et al.*, 2020). In shade, the combination of increased IAA concentration and reduced light would disrupt the growth-repressive photoreceptor-AUX/IAA-ARF complex, thereby allowing for ARF-mediated gene expression and hypocotyl elongation.

Photoreceptor control of the BAP/D module

In shade and elevated temperature, auxin concentrations increase rapidly. However, this increase is often transient and lost on the second day of treatment (Bou-Torrent *et al.*, 2014; de Wit *et al.*, 2015; Pucciariello *et al.*, 2018). A subsequent increase of auxin sensitivity is required to maintain auxin signalling for a longer duration in low R/FR (Pucciariello *et al.*, 2018). Moreover, other hormones may further stimulate growth beyond the first day

(Bou-Torrent *et al.*, 2014). The synthesis of gibberellic acid (GA) is increased in low R/FR through enhanced *GA20-OXIDASE* transcription (Hisamatsu *et al.*, 2005; Bou-Torrent *et al.*, 2014; Gommers *et al.*, 2017). Increasing GA concentrations promote degradation of growth-repressive DELLA proteins. DELLAs are nuclear localised repressors that inhibit the activity of many transcription factors including the BR responsive growth promoters BRASSINAZOLE RESISTANT 1 (BZR1) and its close homolog BRI1-EMS-SUPPRESSOR 1 (BES1) as well as ARFs and PIFs (de Lucas *et al.*, 2008; Feng *et al.*, 2008; Bai *et al.*, 2012; Oh *et al.*, 2014). These transcription factors together with their DELLA repressor constitute the BZR-ARF-PIF/DELLA (BAP/D) module (Figure 2.1) (Oh *et al.*, 2014). Similar to PIF and ARF, the third TF of this group, BZR1, is also inactivated upon light-activation of phyB and cry (Wang *et al.*, 2018; Dong *et al.*, 2019; He *et al.*, 2019).

BZR1, ARF6 and PIF4 stimulate cell growth through induction of many shared target genes, and they interact and reinforce each other's activity at those targets (Oh *et al.*, 2012, 2014). These interactions would explain why PIFs and BZR stimulate auxin sensitivity (Sun *et al.*, 2012; Oh *et al.*, 2014). However, each member of the BAP module also has its own specific targets (Oh *et al.*, 2014), as illustrated by the observation that *arf6 arf7 arf8*, although not responsive to exogenous IAA, maintains the hypocotyl elongation response to exogenous BR and GA treatment (Reed *et al.*, 2018). All taken together, this implies a complex growth promoting network of interacting transcription factors that are stimulated by auxin, gibberellin and brassinosteroid signalling, whilst being repressed by active phy and cry photoreceptors.

Auxin-modulated cell growth

The auxin-mediated cell elongation response to unilateral light, shade, neighbour proximity signals and high temperature depends on enhanced expression of *SAUR19-24*, members of the *SMALL AUXIN UP RNA* family (Franklin *et al.*, 2011; Spartz *et al.*, 2012; Kohlen *et al.*, 2016; Wang *et al.*, 2020). In the Arabidopsis hypocotyl *SAUR19* expression is limited to the epidermis which is the cell layer that restricts hypocotyl growth (Procko *et al.*, 2016), and in unilateral blue light *SAUR19* expression only occurs on the shaded side of the hypocotyl (Wang *et al.*, 2020). Activation of *SAUR19* stimulates H⁺-ATPase proton pumps, which leads to rapid apoplast acidification and acid growth (Figure 2.1) (Spartz *et al.*, 2014; Fendrych *et al.*, 2016; Arsuuffi & Braybrook, 2018). In shade-exposed Arabidopsis petioles, apoplast acidification happens within minutes (Sasidharan *et al.*, 2010). The acidification is accompanied by enhanced expression and activity of cell wall-modifying proteins, such as XYLOGLUCAN ENDOTRANSGLUCOSYLASE/HYDROLASES (XTHs) and

expansins (Sasidharan *et al.*, 2008, 2010; Arsuffi & Braybrook, 2018). At least part of the *XTH* induction in *Arabidopsis* is auxin-dependent (Sasidharan *et al.*, 2014), but PIFs can also directly regulate *XTH* expression (Hornitschek *et al.*, 2009; Pedmale *et al.*, 2016).

Preventing excessive growth

We described before how cryptochrome and phytochrome inactivation both stabilise BZR/ARF/PIF proteins and increase auxin and gibberellin levels. In such conditions, the negative regulators AUX/IAA and DELLA are removed. Furthermore, auxin sensitivity increases in persistent shade. It would, therefore, seem pertinent for the plant to employ precise and dedicated negative feedback to prevent excessive growth.

This is achieved in deep shade by activation of phyA which leads to stabilisation of AUX/IAAs (Yang *et al.*, 2018). In addition, several of the most strongly upregulated transcripts in shade include negative regulators of auxin and shade signalling. Such transcripts include *AUX/IAAs*, *GH3s*, *PIL1*, *HFR1*, *PAR1* and *PAR2* (de Wit *et al.*, 2014; Buti *et al.*, 2020) which are also frequently used as marker genes for auxin response and photoreceptor inactivation. *PIL1*, *HFR1* and *PARs* are bHLH proteins that can physically interact with PIFs, reducing PIF binding to target gene promoters, including auxin-associated genes (reviewed in Buti *et al.*, 2020). Enhanced *AUX/IAA* expression and protein accumulation would reduce the auxin response by reducing ARF transcriptional activity (Weijers & Wagner, 2016). However, in specific conditions *AUX/IAAs* may indirectly stimulate the auxin response. PIF4 was shown to increase the expression of *IAA19* and *IAA29* in persistent shade (Pucciariello *et al.*, 2018). The expression of these *AUX/IAAs* appears to stimulate hypocotyl growth, possibly through inhibiting auxin-induced expression of the stronger negative growth regulator *IAA17* (Pucciariello *et al.*, 2018). It would be interesting to further tease apart the interaction between *AUX/IAAs* in variable conditions.

Future perspectives

We have reviewed here how auxin is a central node of photoreceptor-dependent regulation of plant development plasticity. Multiple interactions have been identified between photoreceptor activity and auxin biology, spanning all levels ranging from auxin synthesis, to response. Although it may seem as if most of photoreceptor-driven auxin biology is understood, much of this is still relatively early days. We will outline a few future perspectives for this field in the coming years, but this is by no means complete.

Auxin biology itself is still only partly understood. The massive diversity in auxin synthesis, transport and response factors makes it difficult to understand the complete interactome of photoreceptors with auxin. Even if we know that, for example, ARF6 and ARF8 interact with PIF4, there are countless other ARFs (and PIFs) for which this still needs to be resolved. The high redundancy as well as diversification within these protein families helps plants to respond to various and subtle changes in environmental and developmental signals. The many possible interactions of these auxin-associated proteins with photoreceptor signalling enable subtleties in developmental plasticity that we may not appreciate to their full potential yet. Resolving the multiple possible points of crosstalk will undoubtedly unravel novel subtleties in developmental plasticity.

In order to address the full potential of auxin-driven developmental plasticity to light, a challenge in future research will be to pair relatively simple study systems on etiolated seedlings exposed to monochromatic light, with light-grown adult plants and the full multi-colour perspective of natural daylight. With the exception of the studies of phyA-AUX/IAA interaction (Yang *et al.*, 2018), the work on photoreceptor regulation of AUX/IAAs and ARFs has for example been done in monochromatic light. It would be interesting to see if phyB-ARF-AUX/IAA binding is reduced with decreasing R/FR in white light backgrounds and if cry1-ARF-AUX/IAA binding is reduced with reducing blue light intensity. Furthermore, given the fluctuating levels of blue, red and far-red inside natural vegetations, these photoreceptors may even interactively regulate ARF and AUX/IAA activity. Moreover, the observed interactions have mainly been studied in seedlings. The ease of use of the seedling system fully justifies the chosen method. However, experimentation in adult plants can provide more detailed insights in the spatiotemporal activity of these regulatory mechanisms (Michaud *et al.*, 2017; Pantazopoulou *et al.*, 2017; Küpers *et al.*, 2018).

Finally, much is to be resolved about whole plant coordination of spatially distinct light signals. For example, one leaf may be exposed to other light cues than another leaf (Chelle *et al.*, 2007). Given its mobility, and the tight control over this, auxin transport would be an obvious candidate mediator of such integration. Indeed, PIN proteins are known to facilitate auxin transport from site of light detection to the site of action (Michaud *et al.*, 2017; Pantazopoulou *et al.*, 2017). Analogous to the root tip, where different PINs have unique localisation domains and mediate auxin transport in specific directions (Petránek & Friml, 2009), it will be helpful to extend our understanding of the localisation domains, and their plasticity in response to different photoreceptor cues, of the different PINs in the different shoot organs. Photoreceptor-regulated transcription of the PIN-phosphorylating AGCVIII kinases *PID* and *D6PK* has been reported in some conditions

(Ding *et al.*, 2011; Kohnen *et al.*, 2016; Park *et al.*, 2019). Moreover, misexpression of *PID*, but not *D6PK*, has been shown to alter PIN3 localisation (Zourelidou *et al.*, 2009; Ding *et al.*, 2011; Park *et al.*, 2019). It will be interesting to see how our understanding of AGCVIII kinase-mediated PIN regulation by photoreceptor signalling develops. Generating new mutant alleles and higher order mutants and testing those in various conditions might considerably deepen our understanding of photoreceptor-controlled auxin transport.



Chapter 3

Neighbour detection at the leaf tip regulates upward leaf movement through spatial auxin-abscisic acid dynamics

Jesse J. Küpers, Chrysoula K. Pantazopoulou, Marco Bentlage, Emilie Reinen & Ronald Pierik

Plant Ecophysiology, Dept. Biology, Utrecht University, 3584CH Utrecht, The Netherlands

Parts of this chapter have been published in:
Pantazopoulou C.K., Bongers F.J., Küpers J.J., Reinen E., Das D., Evers J.B., Anten N.P.R., Pierik R. (2017). Neighbor detection at the leaf tip adaptively regulates upward leaf movement through spatial auxin dynamics. *Proceedings of the National Academy of Sciences*, 114(28), 7450–7455.

<https://doi.org/10.1073/pnas.1702275114/>

Abstract

The uneven distribution of leaves in a vegetation stand causes heterogeneous distribution of light. This also leads to heterogeneous distribution of the ratio of red to far-red light (R/FR), that generally decreases at high density. In response to low R/FR, plants display adaptive shoot growth responses to enhance light capture and survival in dense stands. Here we investigated the effects of heterogeneous R/FR distribution by local FR enrichment. We found that FR enrichment of the petiole locally stimulates petiole elongation while FR enrichment at the leaf tip triggers upward leaf movement (hyponasty) through differential growth in the distal petiole base. Regarding petiole hyponasty, we suggest that the spatial distance between leaf tip and petiole base is bridged by auxin synthesis and transport. Moreover, we provide evidence to suggest that abscisic acid signalling may act as a dimmer switch to prevent excessive hyponasty in unfavourable environments.

Introduction

Light distribution in dense vegetation stands is heterogeneous due to different absorption and reflection of specific wavelengths of light. Red (R, $\lambda = 600\text{--}700$ nm) and blue (B, $\lambda = 400\text{--}500$ nm) light are absorbed by leaves and used in photosynthesis, while far-red (FR, $\lambda = 700\text{--}800$ nm) light is reflected (Fraser *et al.*, 2016). This leads to heterogeneous light quality distribution between and even within individual leaves (Chelle *et al.*, 2007). The specific reflection of FR reduces the ratio of R/FR light around the plant and provides an early signal for neighbour proximity that precedes actual light competition (Ballaré *et al.*, 1990). As light is essential for photosynthesis and survival, plants respond to FR enrichment with adaptive shade avoidance growth responses. These adaptive responses serve to increase light capture by raising the photosynthetic leaves and include hypocotyl elongation in seedlings as well as upward leaf movement and elongation of petioles and stems in adult plants (Franklin, 2008; Pierik & De Wit, 2014). Plants are modular organisms, suggesting that FR-induced growth responses would be restricted to the sensing organ (de Kroon *et al.*, 2005). This might benefit survival as excessively erect leaves intercept less light and this would benefit undesired weed growth (Pantazopoulou *et al.*, 2021). In addition, rapid elongation growth decreases plant stability, fitness and disease resistance (Franklin, 2008; Procko *et al.*, 2014; Courbier *et al.*, 2020).

Localised FR enrichment is known to regulate remote organ elongation responses in seedlings: *Brassica rapa* seedlings sense FR enrichment primarily in the cotyledons, which then stimulates elongation of the hypocotyl (Procko *et al.*, 2014). This spatial separation was previously suggested in *Arabidopsis thaliana* (*Arabidopsis*) where large parts of the signalling pathway regulating FR-induced growth have been revealed (Tanaka *et al.*, 2002). Perception of low R/FR leads to the inactivation of the R/FR sensitive phytochrome (phy) photoreceptors, mainly phyB (Roig-Villanova & Martínez-García, 2016). This in turn leads to the accumulation of PHYTOCHROME INTERACTING FACTOR (PIF) bHLH transcription factors (Leivar & Monte, 2014). Active PIFs, mainly PIF4, PIF5 and PIF7, stimulate growth by activating target gene expression including various *YUCCA* auxin synthesis genes (Hornitschek *et al.*, 2012; Li *et al.*, 2012; Goyal *et al.*, 2016; Kohnen *et al.*, 2016). *YUCCA* proteins stimulate the rate-limiting conversion of inactive indole-pyruvic acid to active indole-acetic acid (IAA) downstream of TRYPTOPHAN AMINOTRANSFERASE OF ARABIDOPSIS 1 (TAA1) (Tao *et al.*, 2008; Stepanova *et al.*, 2008; Won *et al.*, 2011; Müller-Moulé *et al.*, 2016). Cotyledon-derived auxin is transported via the PIN-FORMED 3 (PIN3) polar auxin transport protein towards the hypocotyl epidermis, where it stimulates hypocotyl growth (Keuskamp *et al.*, 2010; Procko *et al.*, 2016). To complement these

findings on spatial FR signalling in seedlings, studies involving larger and more mature plants would improve our understanding of how plants integrate light signalling across spatial scales (**Chapter 1**).

To this end, we study the effect of local FR enrichment on leaf responses in adult *Arabidopsis*. We show that FR enrichment induces adaptive petiole growth responses only in the treated leaf and that within the leaf there is spatial separation between the induction of petiole elongation and hyponasty. FR enrichment at the petiole induces local petiole elongation, while FR enrichment at the remote leaf tip triggers petiole hyponasty. We demonstrate that PIF-mediated auxin synthesis and transport from the leaf tip towards the petiole are required for FR-induced petiole hyponasty. We also investigate a potential repressive role for abscisic acid (ABA) in the control of FR-induced petiole hyponasty.

Results

Site of R/FR perception determines hyponasty vs. petiole elongation

Using a FR spotlight setup (Figure 3.1 A) we exposed different leaf regions to local FR enrichment in white light (WL) background and measured the effect on petiole angle and elongation. FR enrichment to the leaf tip (FR_{tip}) induced hyponasty to a similar degree as whole-plant FR enrichment (FR_{whole}), while FR treatment of the petiole (FR_{petiole}) did not elicit any hyponasty (Figure 3.1 B, D). Although FR_{petiole} induced no hyponasty, it induced maximal petiole elongation (similar to FR_{whole}), whereas FR_{tip} did not elicit any petiole elongation (Figure 3.1 C). Shifting the FR spotlight to the middle of the lamina (FR_{lamina}) did not elicit any petiole elongation and hyponasty responses, whereas combined FR enrichment of the leaf tip and petiole (FR_{tip+petiole}) only induced petiole elongation without any hyponasty.

To investigate whether local perception of FR enrichment in specific leaves has systemic effects, we exposed two other leaves, one younger and one older, to FR (FR_{other}) and measured petiole angle and elongation of our focal leaf. We found that such distal FR supplementation had no effect on petiole angle or elongation in the non-treated leaf (Figure 3.2 A, B). Interestingly, a R spotlight on the whole lamina of one leaf under FR_{whole} conditions reduced leaf angle of that specific leaf compared to its angles in just FR_{whole} (Figure 3.2 C), corroborating the observation that the leaf angle response is local to the treated leaf. As the R spotlight did not extend to the petiole, petiole elongation remained at the same high level as in FR_{whole} (Figure 3.2 D).

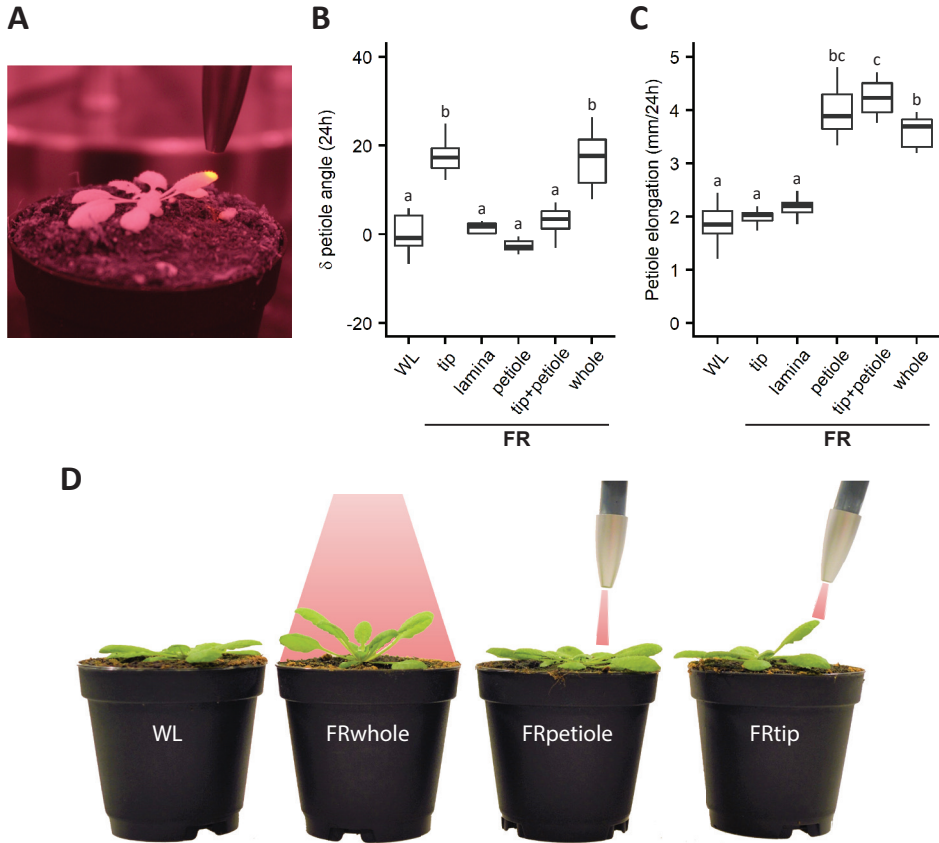


Figure 3.1. Location of FR detection determines growth response. (A) Infra-Red (IR) image of spotlight FR illumination on the *Arabidopsis thaliana* leaf tip. Quantification of differential petiole angle (B) and petiole elongation (C) after 24h in the indicated local FR enrichment light treatments. $n = 7$, different letters indicate significant difference according to one-way ANOVA + Tukey ($p < 0.05$). (D) Representative pictures of plant phenotypes after 24h in the indicated light treatments.

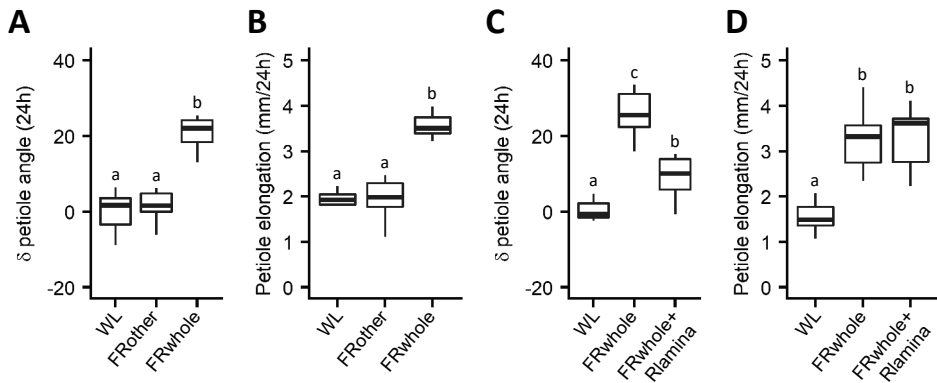


Figure 3.2. Petiole growth responses to FR enrichment occur in a modular, per-leaf manner. (A & B) Quantification of differential petiole angle (A) and petiole elongation (B) after 24h in WL, FRwhole and a treatment in which one older and one younger leaf received FR to the whole lamina (FRother). (C & D) Quantification of differential petiole angle (C) and petiole elongation (D) after 24h in WL, FRwhole and a treatment in which the measured leaf received R to the lamina in FRwhole background. (A - D) $n = 10$, different letters indicate significant difference according to one-way ANOVA + Tukey ($p < 0.05$).

FR enrichment at the leaf tip induces petiole hyponasty by auxin synthesis via phy-PIF-YUC

We confirmed that the hyponastic response to FRtip requires functional phytochrome when we found that the response was absent in the *phyB phyD phyE* triple mutant (Figure 3.3 A). We therefore studied the involvement of the key PIFs that are known to regulate shade-avoidance growth responses in the shoot. The *pif4 pif5* mutant showed no petiole hyponasty response to FRtip but responded normally to FRwhole, whereas *pif7* lacked petiole hyponasty in both FRtip and FRwhole conditions (Figure 3.3 B). As one of the functional roles of PIFs is to enhance auxin synthesis, we analysed petiole hyponasty in the auxin synthesis mutants *wei8* and *yuc2 yuc5 yuc8 yuc9* and found that neither mutant responded to FRtip and only *wei8* became slightly hyponastic in FRwhole (Figure 3.3 C, D). Circumventing *de novo* IAA synthesis, we applied IAA to the leaf tip (IAAtip) and observed petiole hyponasty in Col-0 (Figure 3.3 E). A similar dose-response relation was found for *pif7*, but *pif4 pif5* was less responsive to IAAtip.

Since PIFs are transcription factors, we analysed the expression of potential targets in auxin synthesis (*TAA1*, *YUC8* and *YUC9*), auxin transport (*PIN3*) and auxin response (*INDOLE-3-ACETIC ACID INDUCIBLE 19* (*IAA19*) and *IAA29*) in the mutant backgrounds (Figure 3.4). *TAA1* expression was slightly reduced by FR in the leaf tip in *pif4 pif5* but not significantly

in Col-0 or *pif7*. Expression of *YUC8* and *YUC9* as well as *PIN3* was induced in the leaf tip by FRtip in both Col-0 and *pif4 pif5* but not in *pif7*. The auxin responsive transcripts *IAA19* and *IAA29* were induced in the leaf tip as well as the petiole base in Col-0 and *pif4 pif5* but not in *pif7*. Collectively, these data suggest that FRtip induces auxin biosynthesis via PIF7 and YUCCAs in the leaf tip which is afterwards transported towards the petiole base to induce auxin signalling and growth.

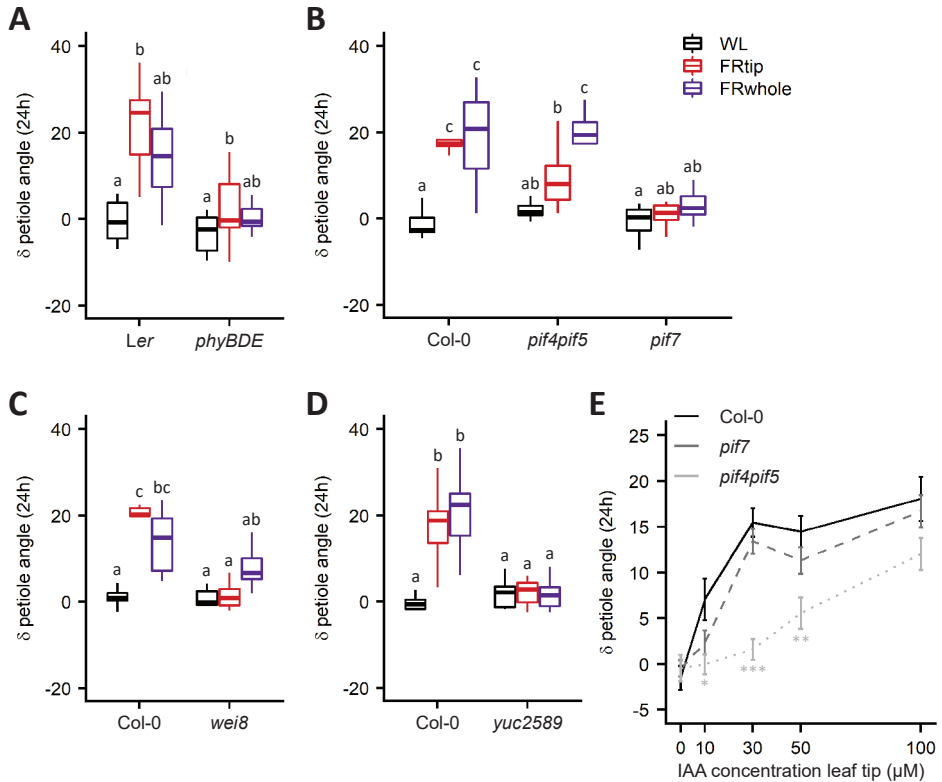


Figure 3.3. Phytochrome inactivation at the leaf tip stimulates petiole hyponasty through PIFs and auxin. (A – D) Quantification of differential petiole angle after 24 h in the indicated light treatments in *Ler* and *phyB phyD phyE* (A, $n = 7$), Col-0, *pif4 pif5* and *pif7* (B, $n = 10$), Col-0 and *wei8* (C, $n = 7$) and Col-0 and *yuc2 yuc5 yuc8 yuc9* (D, $n = 10$), different letters indicate significant difference according to two-way ANOVA + Tukey ($p < 0.05$). **(E)** Quantification of differential petiole angle after 24 h IAA treatment to the leaf tip at the indicated concentrations in Col-0, *pif4 pif5* and *pif7*. $n = 14$, error bars represent SEM, asterisks indicate significant difference between mutant and Col-0 (t-test, * $p < 0.05$, ** $p < 0.01$, *** $p < 0.001$). *phyBDE* = *phyB phyD phyE*, *yuc2589* = *yuc2 yuc5 yuc8 yuc9*.

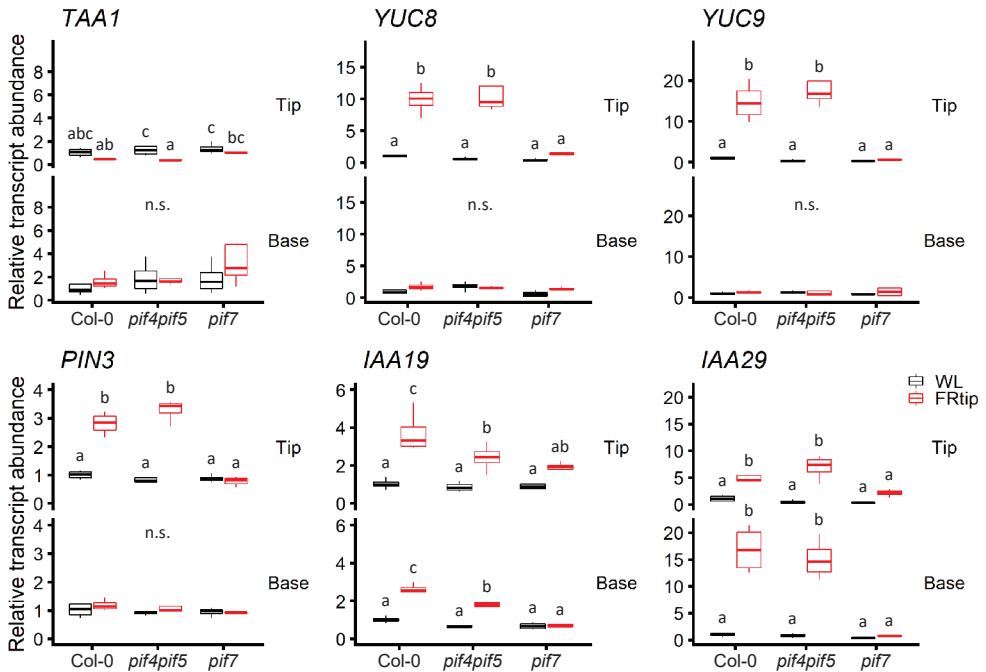


Figure 3.4. PIF7 stimulates expression of genes associated with auxin synthesis, transport and response in FRtip. Transcript abundance in after 5h in WL and FRtip of the auxin synthesis (*TAA1*, *YUC8* and *YUC9*), auxin transport (*PIN3*) and auxin response genes (*IAA19* and *IAA29*) in the leaf tip (Tip) and petiole base (Base) of Col-0, *pif4 pif5* and *pif7*. Transcript abundance was calculated relative to the Col-0 leaf tip in WL. $n = 4$, leaf material harvested from 10 plants per sample, different letters indicate significant difference according to two-way ANOVA + Tukey ($p < 0.05$).

Tip to base auxin transport facilitates petiole hyponasty

Consistent with a potential role for auxin transport in FR-induced petiole hyponasty, the auxin efflux mutant *pin3* showed a reduced response, and the *pin3 pin4 pin7* triple mutant that is also missing two closely related homologous PINs completely lost petiole hyponasty in FR enrichment and IAAtip treatment (Figure 3.5 A, B).

Next, we visualised auxin activity with the DR5::LUC auxin reporter and observed clear luciferase induction in the abaxial side of the petiole of the treated leaf in FRtip and on both sides of the petiole in IAAtip (Figure 3.5 C, D). In contrast with this leaf-specific induction, luciferase activity was increased throughout the plant in FRwhole exposed rosettes (Figure 3.5 C).

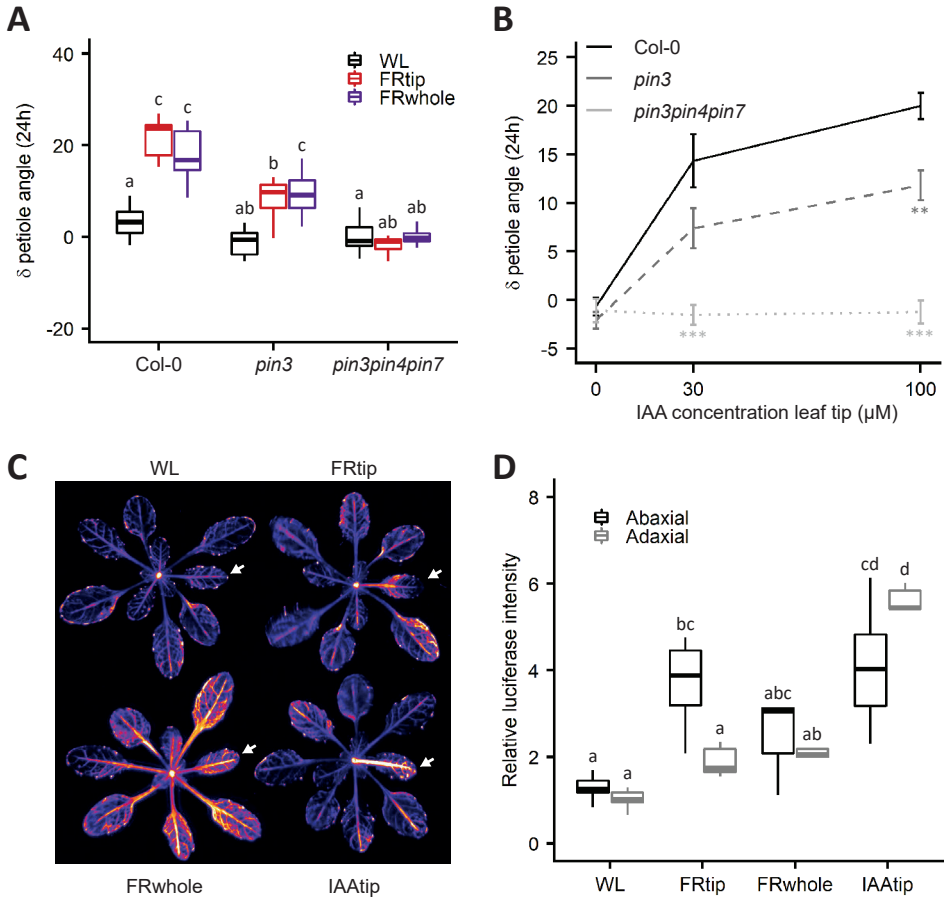


Figure 3.5. The petiole hyponasty response to FR enrichment at the leaf tip requires PIN-mediated auxin transport. (A) Quantification of differential petiole angle after 24h in the indicated light treatments in Col-0, *pin3* and *pin3 pin4 pin7*. $n = 10$, different letters indicate significant difference according to two-way ANOVA + Tukey ($p < 0.05$). (B) Quantification of differential petiole angle after 24h IAA treatment to the leaf tip at the indicated concentrations in Col-0, *pin3* and *pin3 pin4 pin7*. $n = 10$, error bars represent SEM, asterisks indicate significant difference between mutant and Col-0 (t-test, $*p < 0.05$, $**p < 0.01$, $***p < 0.001$). (C & D) Representative images of abaxial rosettes (C) and quantification of luciferase signal on the abaxial and adaxial side of the petiole (D) of DR5::LUC after 7h in the indicated light treatments. The focal leaf in (C) is indicated with the arrowhead. $n = 5$, different letters indicate significant difference according to two-way ANOVA + Tukey ($p < 0.05$).

Abscisic acid as an inhibitor of FRtip-induced petiole hyponasty

Previously published transcriptome analysis of leaf tip material in FR enrichment suggested activation of abscisic acid (ABA) signalling (Pantazopoulou et al., 2017). When we exogenously applied ABA to the leaf tip (ABAtip) we found that this reduced FRtip-

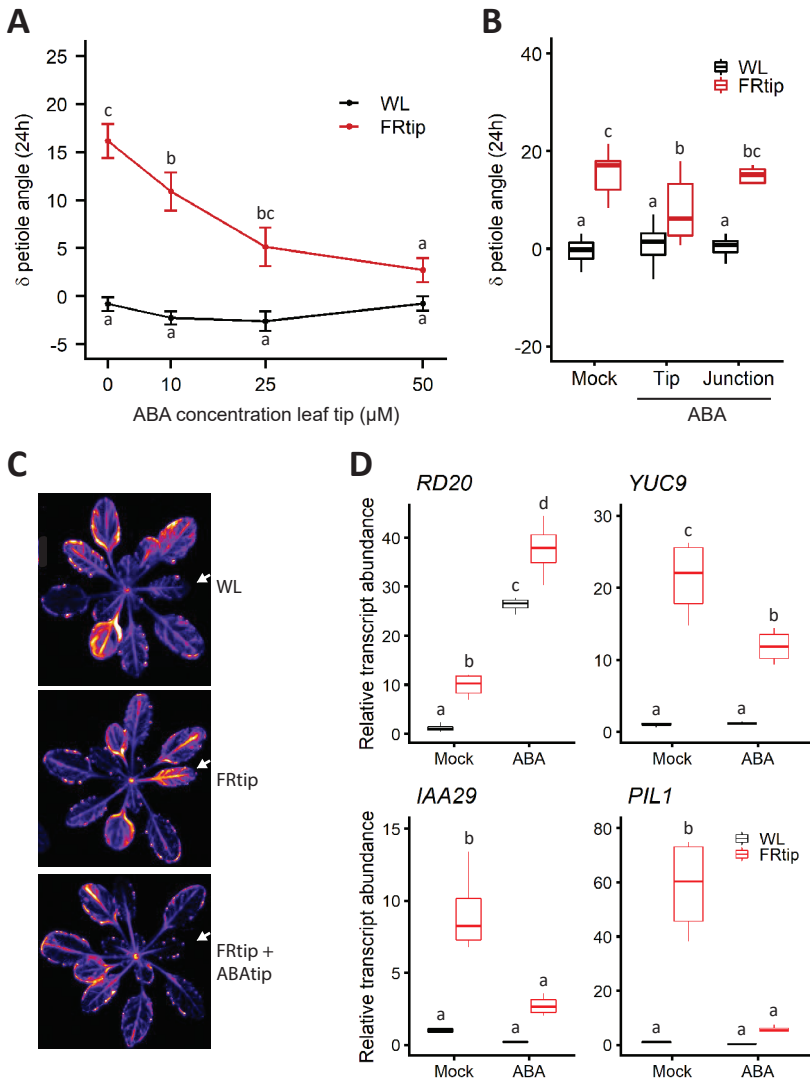


Figure 3.6. Abscisic acid treatment at the leaf tip limits petiole hyponasty and auxin response in FRtip. (A) Quantification of differential petiole angle after 24h in WL and FRtip combined with ABA treatment to the leaf tip at the indicated concentrations. $n = 10-15$, error bars represent SEM, different letters indicate significant difference according to two-way ANOVA + Tukey ($p < 0.05$). (B) Quantification of differential petiole angle after 24h in WL and FRtip combined with 25 μM ABA treatment to the leaf tip and petiole lamina junction. $n = 10$, different letters indicate significant difference according to two-way ANOVA + Tukey ($p < 0.05$). (C) Representative images of the abaxial side of the DR5::LUC rosette after 7 h in the indicated light and ABA treatments. The focal leaf is indicated with the arrowhead. (D) Transcript abundance in the leaf tip after 5h WL and FRtip combined with 25 μM ABA or mock treatment to the leaf tip of the ABA responsive (*RD20*), auxin synthesis (*YUC9*), auxin response (*IAA29*) and shade marker gene (*PIL1*). Transcript abundance was calculated relative to WL + Mock. $n = 4$, leaf material harvested from 10-15 plants per sample, different letters indicate significant difference according to two-way ANOVA + Tukey ($p < 0.05$).

induced petiole hyponasty (Figure 3.6 A). This reduction did not occur when the petiole-lamina junction received ABA treatment (Figure 3.6 B) suggesting that ABA signalling reduced petiole hyponasty by interfering with phytochrome-induced responses in the leaf tip. Indeed, ABA_{tip} treatment reduced FR_{tip} induction of the luciferase signal in DR5::LUC (Figure 3.6 C). Consistently, gene expression analysis revealed that ABA_{tip} induces expression in the leaf tip of the ABA marker gene *RESPONSE TO DESSICATION 20* (*RD20*) but reduces FR-mediated expression of auxin synthesis (*YUC9*) and signalling (*IAA29*) genes as well as the shade marker gene *PIL1* (Figure 3.6 D).

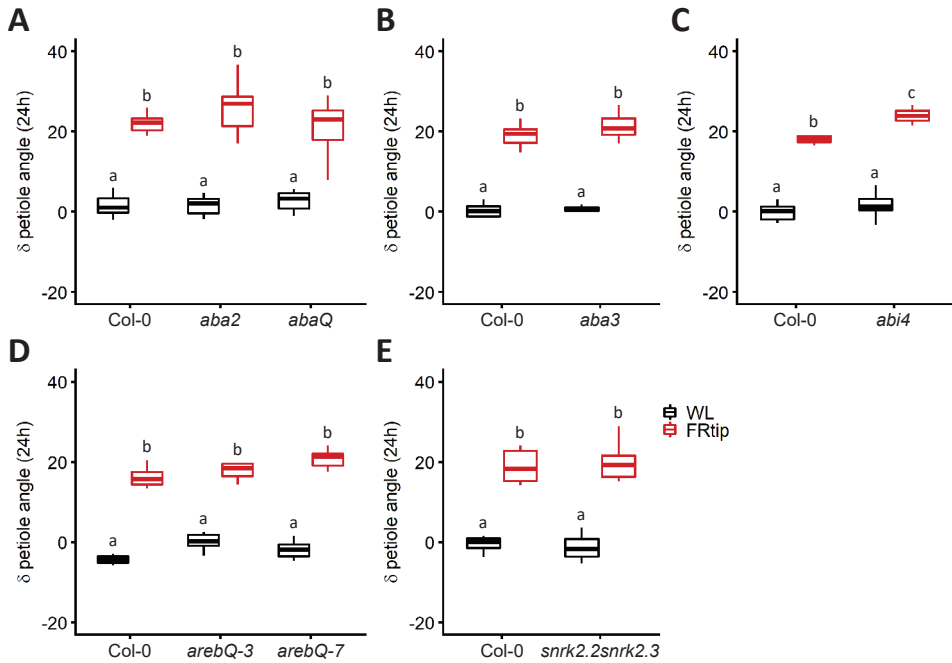


Figure 3.7. Inhibition of ABA signalling has little effect on petiole hyponasty response in FR_{tip}. (A - E) Quantification of differential petiole angle after 24h in the indicated light treatments in Col-0 versus *aba2* and *abaQ* (A, $n = 7$), *aba3* (B, $n = 8$), *abi4* (C, $n = 8$), 2 allelic variants of *arebQ* (D, $n = 7$) and *snrk2.2 snrk2.3* (E, $n = 12$). Different letters indicate significant difference according to two-way ANOVA + Tukey ($p < 0.05$).

To further test the functionality of ABA signalling we analysed the hyponastic response to FR_{tip} in various ABA mutants. The ABA synthesis mutants *aba2* and *aba3* and quadruple ABA receptor mutant *pyr1 pyl1 pyl2 pyl4* (*abaQ*) did not differ from Col-0 in their hyponastic response to FR_{tip} (Figure 3.7 A, B). Mutation in the *ABA INSENSITIVE 4* (*ABI4*) gene resulted

in a slightly increased petiole hyponasty response to FRtip (Figure 3.7 C), while higher order ABA signalling mutants *areb1 areb2 abf1 abf3* (arebQ) and *snrk2.2 snrk2.3* were again undistinguishable from Col-0 (Figure 3.7 D, E).

Discussion

In response to FR light reflected by neighbours plants show adaptive growth responses including petiole elongation and hyponasty (Küpers *et al.*, 2018). Here we found that local FR enrichment elicits different shade avoidance responses depending on the site of perception. Petiole elongation is a local response to FR enrichment in the petiole, while petiole hyponasty is spatially controlled by FR signalling in the leaf tip (Figure 3.1). When a similar amount of FR is supplied to the middle of the lamina, there is no induction of petiole growth responses, confirming the importance of the leaf tip and petiole as sensory regions. This also indicates that putative FR detection in the central region of the lamina in *Arabidopsis* has little function. Moreover, combined FR enrichment to the leaf tip and petiole only leads to petiole elongation, suggesting that the induction of rapid elongation overrides the cue for petiole hyponasty. In whole plant FR, both petiole growth response are induced, which suggests that another part of the lamina may also contribute to generate a stronger hyponasty inducing signal under homogeneous low R/FR conditions. Indeed, when FR was supplied to the serrations around the leaf margin this also led to some petiole hyponasty (Pantazopoulou *et al.*, 2017). Interestingly, IAA application to the leaf margin has been shown in other studies to also induce horizontal relocation of the leaf, suggesting that leaf movement can occur along multiple planes (Michaud *et al.*, 2017). The observation that FR treatment of the leaf margin elicits some degree of hyponasty could also explain that in FRwhole, both petiole elongation and hyponasty are triggered, while FRtip+petiole only results in petiole elongation. Possibly, FR perception in a larger part of the lamina is required to achieve petiole hyponasty at the same time as petiole elongation occurs.

In local treatments, the two different petiole growth responses only occur in the treated leaf, and only when the correct part of the leaf perceives the FR signal (Figure 3.2). Functional structural plant modelling revealed that the spatial control of petiole hyponasty from the leaf tip allows the plant to rapidly respond to early neighbour detection in the outermost part of the plant, without unnecessarily increasing leaf angle when a newly developing leaf causes self-shading of the petiole (Pantazopoulou *et al.*, 2017). Although petiole hyponasty in low R/FR is a transient response that decreases in the morning (Michaud *et al.*, 2017), proper temporal control of leaf angle helps the plant to successfully overtop

their nearby competitors (Woodley of Menie *et al.*, 2019). While upward leaf movement is beneficial to individual success, it hampers weed suppression and competitiveness of the community. Using mutant analysis and FSP modelling, Pantazopoulou *et al.*, 2021 showed that the leaf hyponasty response to neighbour detection results in more light penetrating the canopy, which facilitates weed growth. Rapid closure of the leaf canopy, as occurs in non-hyponastic *pif7* monocultures, optimises communal light harvesting, prevents weed growth and increases plant biomass (Pantazopoulou *et al.*, 2021).

FRtip-induced leaf movement acts through PIFs and auxin

FR-induced petiole hyponasty requires phytochrome inactivation which allows for activation of PIF4, PIF5 and PIF7 (Leivar & Monte, 2014). Our data suggests that PIF7 is the main PIF regulating auxin synthesis in the leaf tip, as *pif7* mutation completely inhibited petiole hyponasty and *YUC* induction without interfering with the response to exogenously applied IAA (Figure 3.3, 3.4). Mutants for the homologues *PIF4* and *PIF5* on the other hand showed wild-type-like induction of *YUC* expression in the leaf tip and reduced, but not completely absent, responses to FR enrichment and exogenous IAA. This suggests specific roles for these two sets of PIFs, with PIF7 being mainly required for the induction of auxin synthesis and PIF4 and PIF5 regulating auxin responsiveness. PIF4 has been shown to stimulate auxin response as a member of the BAP/D module in seedlings. In the BAP/D module the growth promoting transcription factors BRASSINAZOLE RESISTANT 1, AUXIN RESPONSE FACTOR 6 and PIF4 interact and enhance each other's activity while all being repressed by DELLA proteins (Oh *et al.*, 2014; Chaiwanon *et al.*, 2016). Whether this module is also active in the petiole hyponasty response to FR enrichment remains to be studied.

Petiole hyponasty requires differential growth rates between the abaxial and adaxial sides of the petiole (Polko *et al.*, 2012), suggesting that leaf tip-derived auxin has its effect in the abaxial petiole. Whether the stimulation of abaxial growth depends on asymmetric distribution of auxin concentrations or auxin signalling could be studied by improving the spatiotemporal resolution of gene expression and auxin distribution analysis. The auxin transporter PIN3 was previously shown to localise to the outer side of the hypocotyl endodermis in low R/FR and to be required for hypocotyl elongation (Keuskamp *et al.*, 2010). We found that the petiole hyponasty response to tip-derived auxin requires PIN3 as well, but that only a *pin3 pin4 pin7* mutant is completely incapable of inducing hyponasty in response to tip-derived auxin (Figure 3.5). Whether these PINs facilitate long-distance auxin transport from tip to base, or from the petiole vasculature towards

the abaxial petiole is yet unknown. The diversity of PINs required for auxin-induced petiole hyponasty could mean that the regulation of auxin transport by PINs is more complex in petiole hyponasty than in hypocotyl elongation, or that PIN3, PIN4 and PIN7 function is (partially) redundant.

ABA regulation during FR-induced leaf movement

Transcriptome analysis of FR induced genes in the leaf tip suggested activation of ABA signalling (Pantazopoulou *et al.*, 2017). When we applied ABA to the leaf tip we found that this inhibited FR-induced petiole hyponasty, as well as the auxin response in the petiole and PIF-related gene expression in the leaf tip (Figure 3.6). This suggests that ABA could function as a dimmer switch mechanism to control excessive petiole hyponasty. However, when we analysed various ABA mutants, we found that they showed wild-type-like responses to FR enrichment with only *abi4* being slightly more responsive to FRtip (Figure 3.7). This suggests that, despite the strong transcriptional regulation of ABA-related genes, ABA itself may not be a core regulator in FRtip-induced petiole movement under standard growth conditions. However, ABA plays an important signalling role in response to various environmental stresses including drought, cold and salinity (Sah *et al.*, 2016). A recent study revealed that elevated ABA signalling reduces FR-induced hypocotyl elongation in saline soil via the inhibition of BAP/D-induced growth (Hayes *et al.*, 2019). We therefore postulate that ABA may provide a molecular point of interaction at which plants can prioritise the response to environmental stress over FR-induced growth. This could benefit plant survival as it may save essential resources required for stress response.

Conclusion

We conclude that auxin relays phytochrome signals from the leaf tip to growth regulation in the petiole. This mechanism allows plants to sense neighbouring plants as early as possible by using their most remote parts, which are the first to interact with neighbours, and to accurately react with the adaptive response of upward leaf movement.

Materials and Methods

Plant material and growth conditions

Genotypes used in this chapter: *pif4-101 pif5-1* (Lorrain *et al.*, 2008), *pif7-1* (Leivar *et al.*, 2008), *wei8* (Stepanova *et al.*, 2008), *yuc2 yuc5 yuc8 yuc9* (Nozue *et al.*, 2015), *pin3-3* (Friml

et al., 2002a), *pin3-3 pin4 pin7* (Willige *et al.*, 2013), DR5::LUC (Moreno-Risueno *et al.*, 2010), *aba2-1, aba3-1* (Léon-Kloosterziel *et al.*, 1996), *pyr1 pyl1 pyl2 pyl4 - abaQ* (Park *et al.*, 2009), *abi4-101* (Laby *et al.*, 2000), *areb1 areb2 abf1 abf3 - arebQ-3/7* (Yoshida *et al.*, 2015) and *snrk2.2 snrk2.3* (Fujii *et al.*, 2007) were all in Col-0 background; *phyB phyD phyE* (Shalitin *et al.*, 2002) was in Ler background.

Seeds were sown on Primasta soil and cold stratified for three days before transfer to short day white light (WL) conditions light/dark 9 h/15 h, 20 °C, 70 % humidity, 130-150 $\mu\text{M m}^{-2} \text{s}^{-1}$ PAR. Individual seedlings were transplanted to 70mL round pots eight days after germination. For all experiments, 28 day old plants were selected based on homogeneous development and the presence of a ~5 mm petiole on the 5th youngest leaf which would be used in the experiment. All experiments were started at 10:00 A.M. (ZT2). For phenotyping experiments, petiole angle before treatment and after 24 hours was determined in ImageJ using digital images taken from the side.

Light and pharmacological treatments

For light treatments, WL was supplemented with FR using Philips Green-Power FR LEDs for FRwhole, and EPITEX L730-06AU FR LEDs for local FR treatments. These FR LEDs had peak emission at 730nm and locally reduced R/FR from ~2.0 in WL to below 0.1 in FR treatment. For pharmacological treatments at the leaf tip, 5 μL solution was pipetted onto the leaf tip at a standard concentration of 30 μM for IAA and 25 μM for ABA. Pharmacological solutions and mocks for leaf tip application contained DMSO (0.01-0.1 %) and Tween-20 (0.1 %).

RNA isolation and RT-qPCR

For gene expression experiments, leaf tip and petiole material was harvested and snap frozen in liquid nitrogen and stored at -80 °C until further processing. The treatment duration, number of plants per replicate and number of replicates used in RT-qPCR experiments are indicated in the figure legends. RNA was isolated using the Qiagen RNeasy kit with on-column DNase treatment. cDNA was synthesised using SuperScript III Reverse Transcriptase and random hexamer primers (Invitrogen). RT-qPCR was performed on the ViiA7 platform (Thermo Fisher) in 384-well plates using a 5 μL total volume containing SYBR Green (Bio-Rad). Transcript abundance was compared to housekeeping genes *PEX4* and *RHIP1* and made relative to the abundance in a designated control condition (indicated in respective figure legends). RT-qPCR primers can be found in Appendix 1.

Luciferase assay

DR5::LUC plants were exposed to the light or hormone treatments for 7 h. Whole shoots or single leaves were then cut and evenly sprayed with 2 mM D-luciferin potassium salt (BioVision, Inc.) in 0.1% (v/v) Triton X-100. Luciferase luminescence was imaged in a ChemiDoc imager (Bio-Rad) with a 40-min exposure time. The ImageJ lookup table “Fire” was used to convert black and white images into colour scales based on pixel intensity. Relative luciferase intensity in the petiole was analysed by measuring the mean pixel intensity of the petiole in Icy software (de Chaumont *et al.*, 2012).

Statistical analyses and data visualisation

Specific details on statistical analyses can be found in the figure legends. Graphs were prepared in R and finetuned in Adobe Illustrator.



Chapter 4

Far-red light enrichment at the leaf tip induces tissue-specific transcriptomes, hormone signalling and petiole hyponasty

Jesse J. Küpers¹, Basten Snoek², Emilie Reinen^{1,#} & Ronald Pierik¹

¹ *Plant Ecophysiology, Dept. Biology, Utrecht University, 3584CH Utrecht, The Netherlands*

² *Theoretical Biology and Bioinformatics, Dept. Biology, Utrecht University, 3584CH Utrecht, The Netherlands*

[#] *Present address: Gadeta B.V., Yalelaan 62, 3584 CM Utrecht, the Netherlands*

Abstract

Light is an essential resource for plant growth. Hence, plants constantly strive to consolidate light capture while under competition pressure with neighbours. Using the red (R) and far-red (FR) sensitive phytochrome photoreceptors, plants can estimate the competitive status of their environment as R is absorbed by neighbouring plants while FR is reflected, leading to a reduced ratio of R/FR light in dense vegetation. In adult *Arabidopsis thaliana*, the threat to light capture posed by nearby neighbours is first sensed as FR enrichment at the outermost part of the plant, the leaf tip. This FR enrichment at the remote leaf tip (FRtip) leads to adaptive upward leaf movement through differential growth between the abaxial and adaxial sides of the petiole base. The distance between site of light detection and differential growth response implies separation in activation of regulatory modules. Here we study the transcriptional regulation of differential petiole growth by FRtip using sub-organ-specific time-course RNA sequencing. Our analyses show that FRtip-induced synthesis and signalling of various hormones, including auxin, follows tissue- and time-specific patterns.

Introduction

Light competition between plants is an important driver of adaptive growth. The light signal of far-red (FR) light enrichment provides an early neighbour signal, as this wavelength is specifically reflected from neighbouring leaves, while other wavelengths such as red (R) and blue (B) are absorbed (Ballaré *et al.*, 1990). As a result, plants can use horizontal FR reflection to determine the competitive status of their environment, before actual shading occurs. Horizontal FR reflection leads to a reduced R to FR ratio (R/FR) which is sensed by the photoconvertible phytochrome B (phyB) photoreceptor (Legris *et al.*, 2019). A reduction in R/FR is reflected in reduced activity of the pool of phyB protein, which releases the repression of PHYTOCHROME INTERACTING FACTOR (PIF) transcription factors (Legris *et al.*, 2019). Activated PIFs stimulate growth by enhancing expression of target genes, including genes involved in synthesis and signalling of the phytohormone auxin (Hornitschek *et al.*, 2012; Li *et al.*, 2012; Küpers *et al.*, 2020). As a result, in response to FR enrichment, *Arabidopsis* displays shade avoidance growth responses that include hypocotyl elongation in seedlings and petiole elongation and upward leaf movement (hyponasty) in adult plants (Küpers *et al.*, 2018). These responses lift the leaves upwards and reduce the risk of being outcompeted and shaded by neighbours.

In adult *Arabidopsis*, horizontal FR reflection from neighbouring plants is first sensed at the outermost part of the plant, the leaf tip. This FR enrichment at the leaf tip (FRtip) triggers remote petiole hyponasty (Michaud *et al.*, 2017; Pantazopoulou *et al.*, 2017). A similar spatial separation was previously found in seedlings, where FR perception at the cotyledons is required and sufficient for hypocotyl elongation (Procko *et al.*, 2014). The regulatory mechanisms that control these two spatial growth responses both require auxin synthesis and transport from the sensing organ towards the elongating organ (Tanaka *et al.*, 2002; Procko *et al.*, 2014; Kohnen *et al.*, 2016; Michaud *et al.*, 2017; Pantazopoulou *et al.*, 2017). An important difference between FR-induced hypocotyl elongation and petiole hyponasty is that petiole hyponasty requires differential abaxial-adaxial growth (Polko *et al.*, 2012; Rauf *et al.*, 2013), while hypocotyl elongation involves uniform elongation of the organ.

To better understand how FR sensing at the leaf tip specifically induces growth in the abaxial petiole, we performed time-series transcriptome analysis of the leaf tip and separated abaxial and adaxial petiole. This analysis revealed that transcripts related to auxin signalling and gibberellic acid (GA) synthesis are more strongly induced in the abaxial than the adaxial petiole. The presented transcriptome dataset provides a tool

to study the spatial regulation of growth promoting transcripts in response to distal FR enrichment and provides insights into auxin and GA biology that will be investigated in **Chapter 5** and **Chapter 6**.

Results

Neighbour detection through FR light in the leaf tip (FRtip) leads to petiole hyponasty which first becomes visible ~4-5 hours after start of treatment (Figure 4.1 A, B). We measured epidermal cell length in the petiole and found that FRtip specifically enhances epidermal cell elongation in the basal two-thirds of the abaxial petiole (Figure 4.1 C). Considering the previously identified important role of auxin in FRtip induced petiole hyponasty we studied the expression of auxin response genes in the petiole base upon FRtip exposure. Indeed, the *IAA29* and *ACS4* auxin-responsive transcripts were induced in the basal petiole within 100 minutes of FRtip while the shade marker transcript *PIL1* was unaffected in the non-FR-exposed petiole (Figure 4.1 D). In order to get more insight in the spatial regulation of differential gene expression and petiole growth by FR signalling in the leaf tip, we decided to separately harvest the leaf tip and the separated abaxial and adaxial sides of the basal two-thirds of the petiole in white light (WL) and FRtip (Figure 4.1 E). To capture the early transcriptional response, we harvested at twenty-minute intervals ranging from 60 minutes (40 minutes for the leaf tip) to 180 minutes of treatment as well as a 300 minute timepoint (Figure 4.1 F).

Neighbour detection at the leaf tip induces local and remote, tissue-specific transcriptome changes

Reads were annotated to the TAIR10 genome and DEseq2-normalised read counts were used to perform principle coordinate analysis (PCoA). We found clear PCoA separation between samples for timepoint and tissue type (Figure 4.2 A). PCoA per tissue and differentially expressed gene (DEG) analysis per timepoint per tissue showed strong and consistent treatment effects in the leaf tip while in the petiole pronounced treatment effects only became apparent at later timepoints (Figure 4.2 B, C, Supplementary Figure 4.1), consistent with our initial gene expression analyses (Figure 4.1 D).

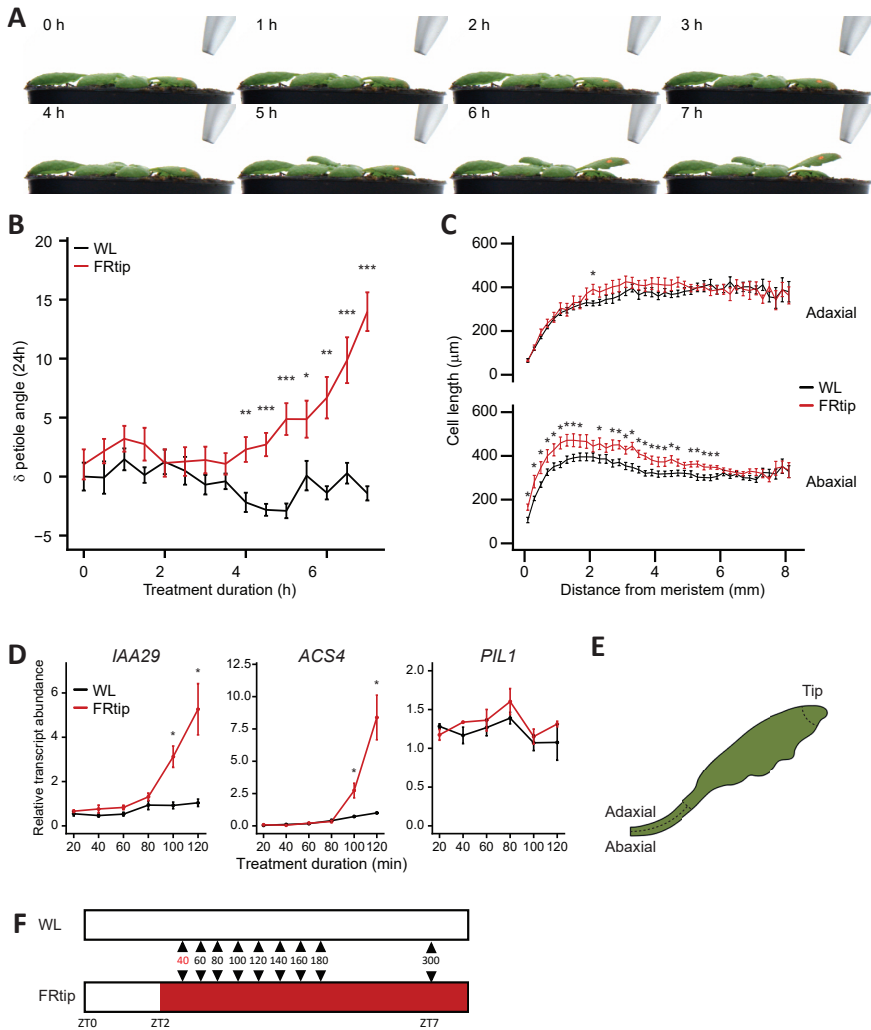


Figure 4.1. Characterizing the dynamics and localisation of FRtip-induced hyponasty and gene expression for RNA sequencing design. (A) Photographs taken approximately 1 hour apart show upward leaf movement in FRtip treatment during the first 7 hours of treatment. (B) Petiole angle dynamics during the first 7 hours of WL and FRtip. Petiole angle change is calculated relative to WL 0 h treatment. ($n = 10$, *: $p < 0.05$, **: $p < 0.01$, ***: $p < 0.001$, two-sided t-test per timepoint). (C) Epidermal cell length measured along the abaxial and adaxial petiole after 24 h in the indicated light treatments ($n = 12-15$, *: $p < 0.05$, two-sided t-test per position along the petiole). (D) Relative transcript abundance of the auxin response marker genes *IAA29* and *ACS4* and the shade marker gene *PIL1* during the first 2h of WL and FRtip. Transcript abundance is calculated relative to 120 min WL. ($n = 2$ (20 & 40 minutes), $n = 4$ (60-120 minutes), material harvested from 7 plants per sample, *: $p < 0.05$, two-sided t-test per timepoint). (E & F) Schematic representations of harvested material (E, dotted lines identify the harvested sections in leaf tip and petiole base) and harvest timepoints (F) for RNA-sequencing. At the 40 minute timepoint, only leaf tip material was analysed. Graphed data represent mean \pm SEM.

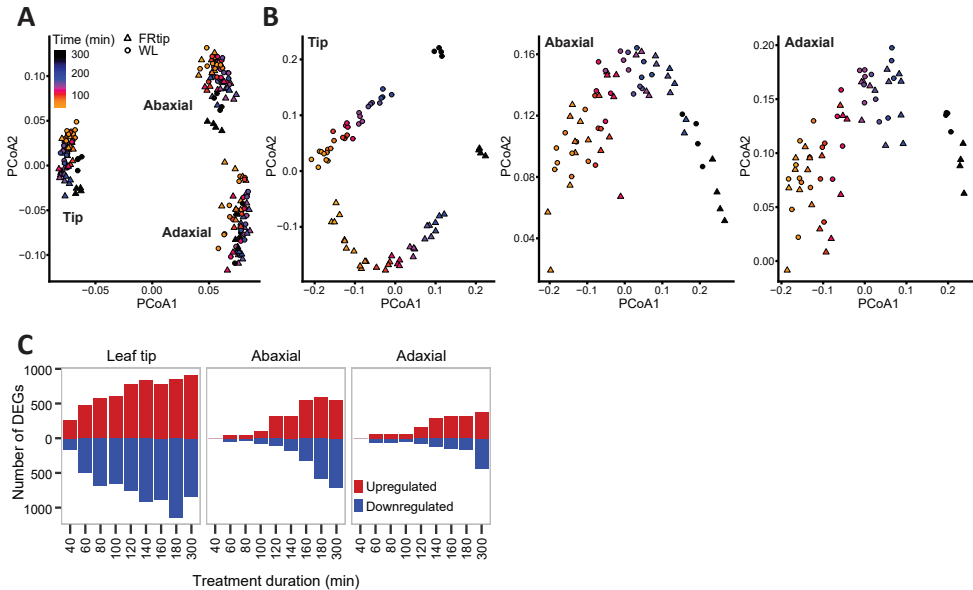


Figure 4.2. RNA-sequencing reveals tissue-specific transcriptional profiles and response to FRtip. (A & B) Principle coordinate analysis (PCoA) on all samples (A) and per tissue (B). (C) Number of differentially expressed genes (DEGs) in FRtip compared to WL, calculated per timepoint and per tissue. DEGs were called when $p < 0.01$ and $\log_2FC > 0.3$ (upregulated; red) or $\log_2FC < -0.3$ (downregulated; blue).

Neighbour detection at the leaf tip induces tissue specific hormone response and synthesis

Gene ontology (GO) analysis for biological processes on upregulated DEGs per tissue per timepoint revealed early enrichment of auxin and light quality-related GO terms in the leaf tip followed by later enrichment of abscisic acid (ABA)-related GO terms (Figure 4.3). As expected, light quality-related GO terms were largely absent from the petiole tissues. In the petiole, we did, however, find enrichment of auxin response terms from 100 to 180 minutes, that dampened towards 300 minutes. This temporal GO enrichment pattern was similar for growth, response to brassinosteroid (BR) and ethylene as well as gibberellin synthesis and response (Figure 4.3). Similar to the leaf tip, there was late enrichment of ABA-related GO terms in the petiole after the auxin response GO terms had passed peak significance. The apparent overrepresentation of auxin signalling in all tissues was confirmed when we analysed expression of all genes that make up the GO category GO:0009733 “response to auxin” (Figure 4.4).

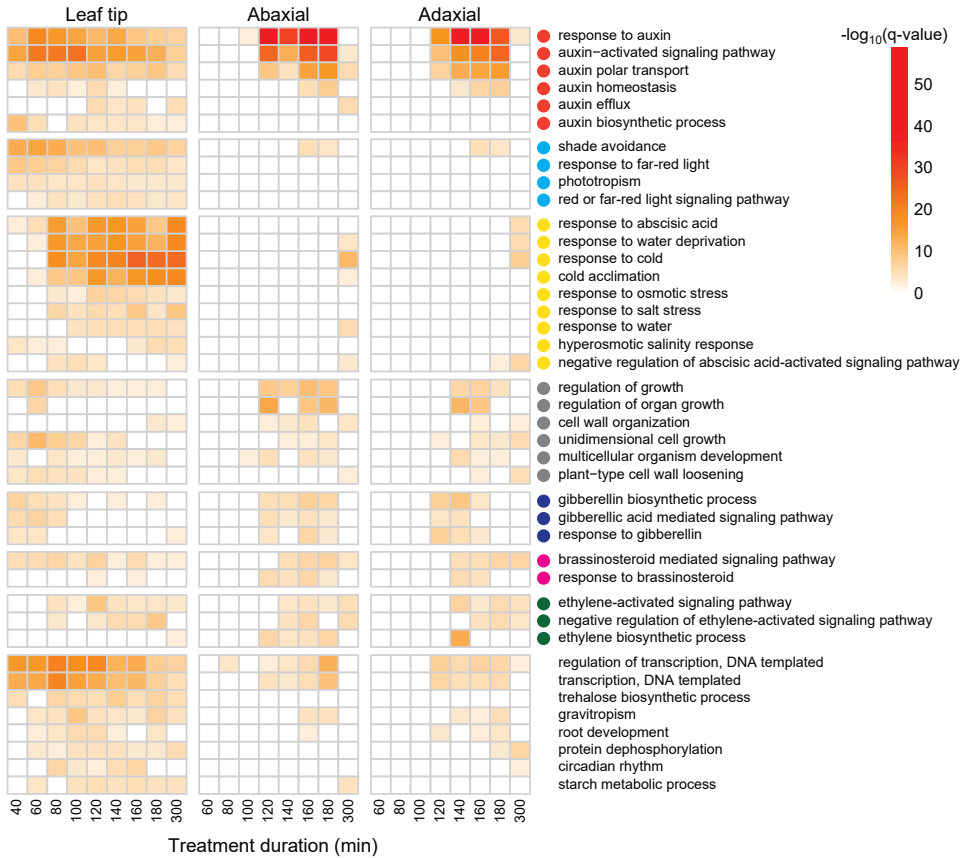


Figure 4.3. Gene ontology analysis on FRtip-induced DEGs per tissue and per timepoint. Heatmap shows the $-\log_{10}(q\text{-value})$ of gene ontology terms identified per timepoint and per tissue based on upregulated DEGs defined in Figure 4.2 C. Coloured circles represent the following defined major biological processes; red – auxin distribution and signalling; cyan – light signalling; yellow – abscisic acid signalling; grey – cell and organ growth; blue – gibberellin synthesis and signalling; magenta – brassinosteroid signalling; green – ethylene synthesis and signalling.

The analysis of these individual genes revealed shared, but also time and tissue-specific expression of many auxin-responsive genes. For example, regarding *SMALL AUXIN UPREGULATED (SAUR)* transcripts, *SAUR19-24* were induced in all tissues, while *SAUR25-29* and *SAUR62-68* were predominantly induced in the petiole (Figure 4.4).

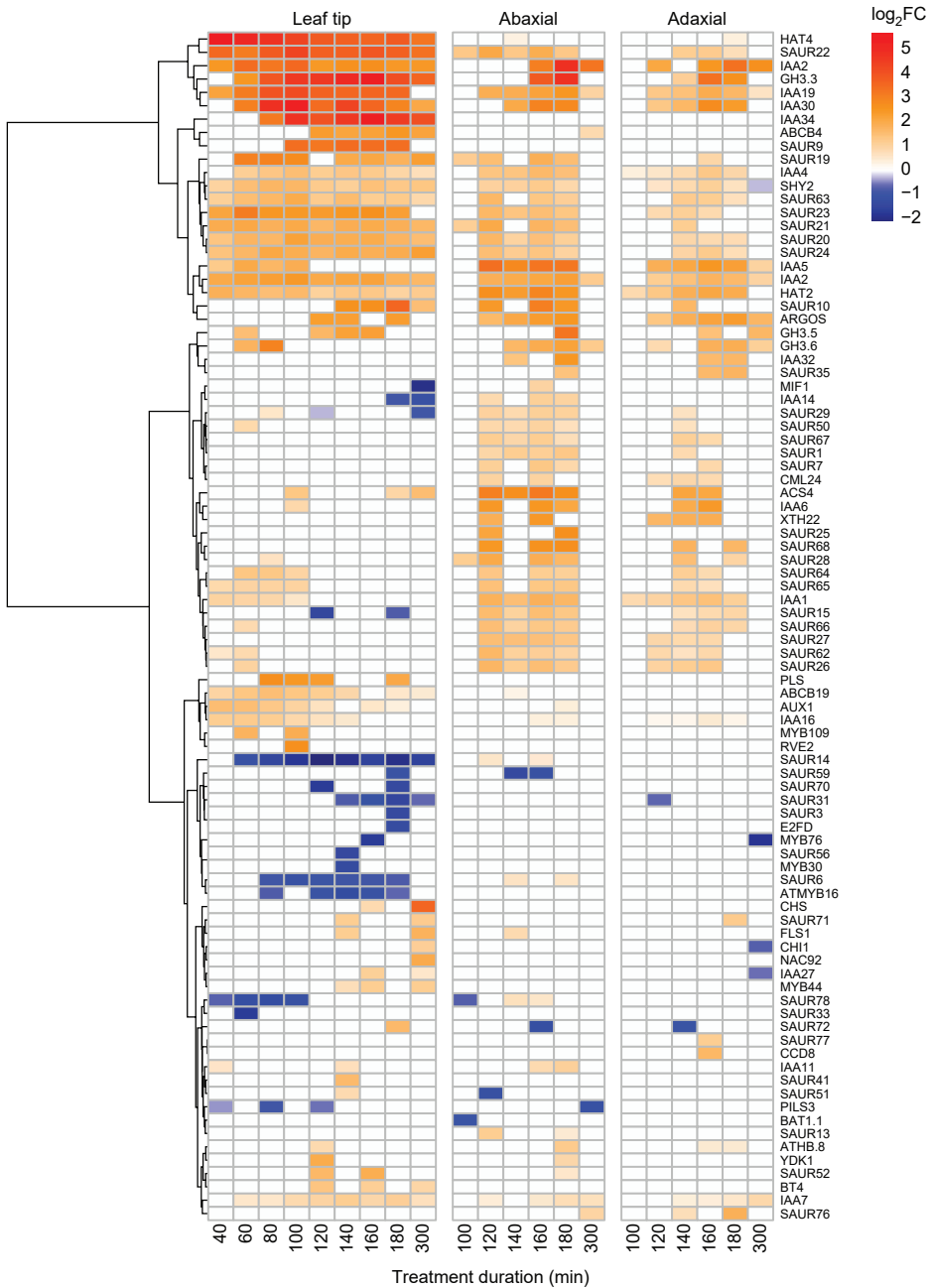


Figure 4.4. FRtip-regulated expression of auxin response genes. Clustered heatmap showing \log_2FC in FRtip compared to WL calculated per timepoint and per tissue of genes in the GO category “GO:0009733 response to auxin”. Only genes that have a significant treatment effect in at least one sample are shown ($p < 0.01$ and $\log_2FC > 1$ or $\log_2FC < -1$).

As we found GO enrichment for several hormone-related processes, we investigated expression of hormone synthesis genes (Figure 4.5). Regarding the main auxin synthesis pathway, expression of *TRYPTOPHAN AMINOTRANSFERASE OF ARABIDOPSIS 1 (TAA1)* and *YUCCA 6 (YUC6)* was repressed in the leaf tip while *YUC2*, *YUC5*, *YUC8* and *YUC9* expression was induced. In contrast, *YUC3* transcription was specifically induced in the petiole. Investigating GA synthesis we found tissue-specific induction of *GA20 OXIDASE 1 (GA20OX1)* and *GA20OX2* in the petiole and *GA20OX3* in the leaf tip. One step downstream of GA20OX proteins in the GA synthesis pathway, *GA3 OXIDASE 1 (GA3OX1)* was induced in both the leaf tip and the petiole. Regarding ABA, we found tissue-specific induction of *NCED3* in the leaf tip while *NCED5* was induced in the petiole. Besides auxin, GA and ABA, we also observed transcriptional regulation of various genes involved in the biosynthesis of BR, ethylene and other hormones (Figure 4.5).

We next identified genes that show differential response to FRtip between the two sides at 100 to 300 minutes of treatment (Figure 4.6). There were no genes with opposite regulation between the two sides but we did observe stronger transcript regulation in the abaxial compared to the adaxial side of the petiole for both up- and downregulated DEGs (Figure 4.6 A). The FRtip-upregulated genes in this subset showed enrichment for biological processes related to auxin and growth as well as to GA, BR and ethylene (Figure 4.6 B). As transcript regulation is strongest in the abaxial side of the petiole in this comparison this suggests that these processes are preferentially activated abaxially. Among the transcripts showing the largest ($-\log_{10}(p) > 5$) significant difference in FRtip-response between the two sides of the petiole were many SAURs and other auxin-induced genes as well as the gibberellin synthesis genes *GA20OX1* and *GA20OX2* (Supplementary Figure 4.2). Abaxial-adaxial transcriptional differences were also found in WL, and included the expression of many genes associated with photosynthesis (Supplementary Tables 4.1, 4.2). Taken together, FR enrichment at the leaf tip induces a transcriptional auxin response throughout the leaf. In the petiole, the leaf tip-derived FR signal triggers a stronger transcriptional response on the abaxial than the adaxial side. Besides auxin signalling, this response includes induction of synthesis and signalling of various other hormones.

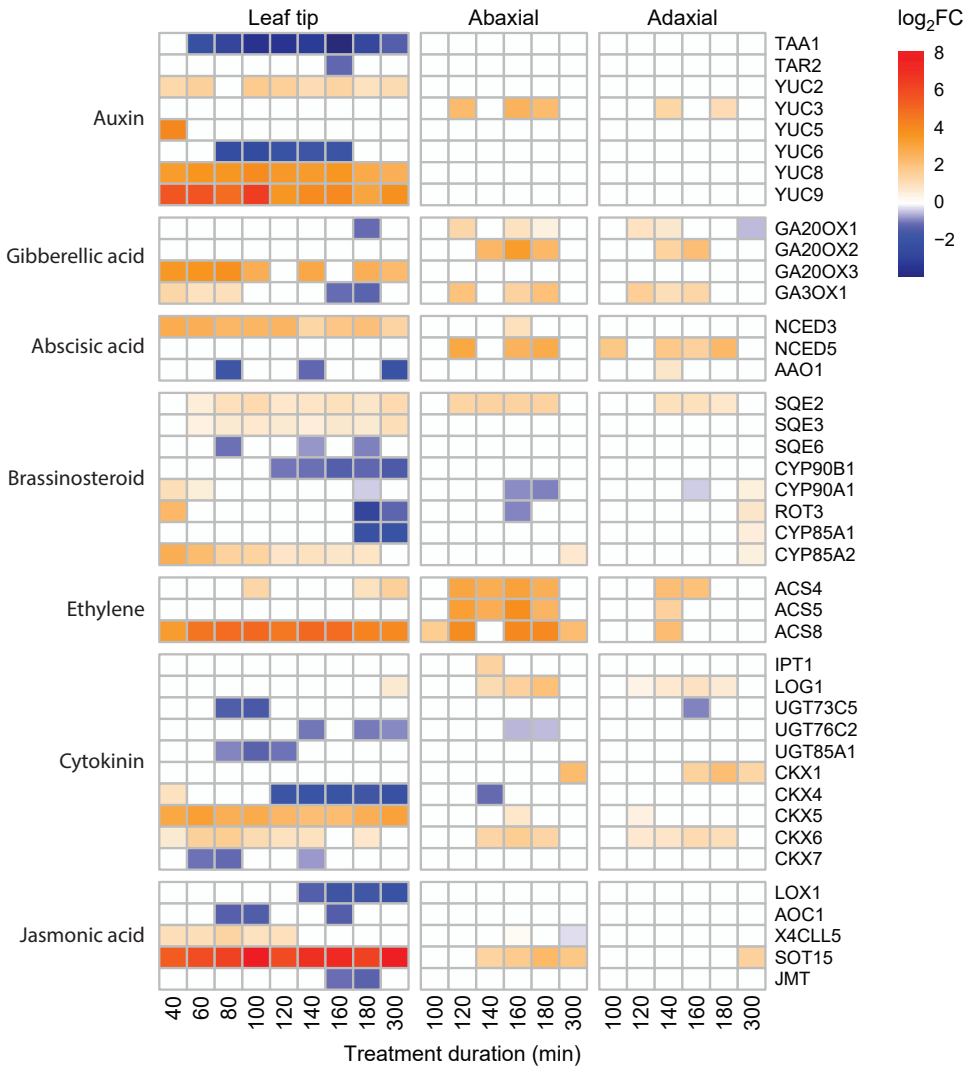


Figure 4.5. FRtip-regulated hormone synthesis gene expression. Heatmap showing log₂FC in FRtip compared to WL calculated per timepoint and per tissue of genes involved in major hormone synthesis pathways. Only genes that have a significant treatment effect in at least one sample are shown (p < 0.01, log₂FC > 1 / < -1).

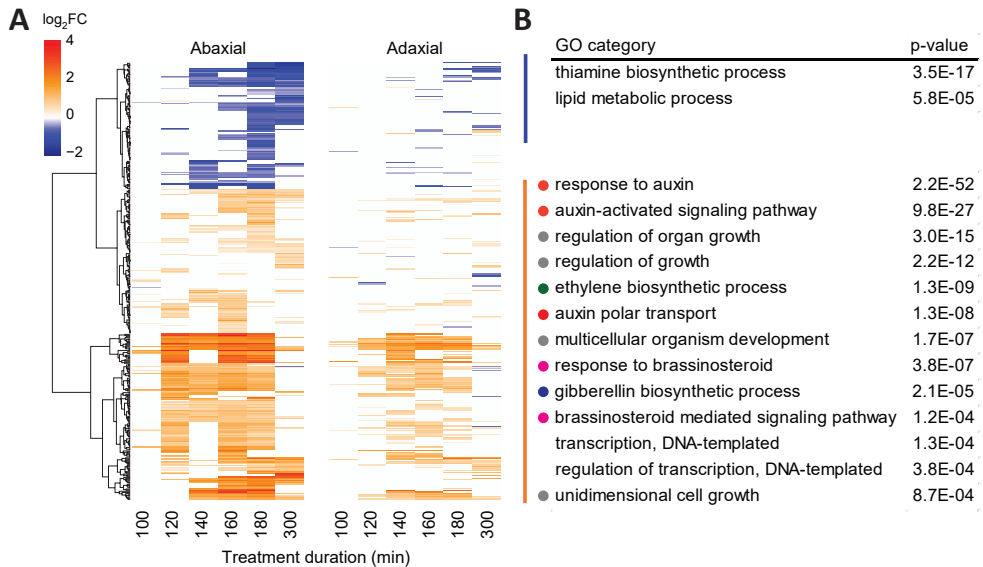


Figure 4.6. Neighbour detection in the leaf tip induces unique abaxial and adaxial transcriptomes. (A) Clustered heatmap showing \log_2FC in FRtip compared to WL of genes that show a different FRtip response between the two sides of the petiole at the indicated timepoints (ANOVA tissue*treatment $p < 0.001$). (B) Separate GO analysis based on the clusters of upregulated (orange-red) and downregulated (blue) genes identified in A. Coloured circles represent the following defined major biological processes; red – auxin distribution and signalling; grey – cell and organ growth; green – ethylene biosynthesis; magenta – brassinosteroid signalling; blue – gibberellin synthesis.

Discussion

We previously showed that FR light enrichment at the leaf tip of adult *Arabidopsis* triggers petiole hyponasty, suggesting long-distance phytochrome-triggered signalling between the two ends of the leaf (Chapter 3). Here we investigated the transcriptional response to FRtip, both locally in the treated leaf tip, as well as in the responding petiole of adult *Arabidopsis*. Using transcriptome analysis we reveal that phytochrome signalling of far-red light in the leaf tip induces a rapid auxin response in the abaxial petiole, that also stimulates expression of *GA20OX* gibberellin synthesis genes. These findings form the basis for our work on characterizing auxin distribution in Chapter 5 and the involvement of gibberellin in FRtip-induced petiole hyponasty in Chapter 6.

Although plants are rooted to their spot, they are capable of moving and reorienting their leaves and stems in response to environmental cues, often through differential growth between two sides of the same organ (Polko *et al.*, 2012; Rauf *et al.*, 2013; Atamian *et al.*, 2016). To achieve petiole hyponasty, the abaxial side of the petiole needs to elongate

faster than the adaxial side. When we analysed cell length along the petiole epidermis, we found that cell length increased along the basal two-thirds of the abaxial side, while on the adaxial side there was little to no cell elongation (Figure 4.1 C). In previous studies, this responding region was limited to approximately the basal quarter of the petiole in ethylene (Polko *et al.*, 2012) and waterlogging (Rauf *et al.*, 2013) exposed plants. An important difference between these studies is total petiole length of the measured leaf, which was around 7 mm in our experiments and 10 mm in Polko *et al.*, 2012 and Rauf *et al.*, 2013. This suggests that the developmental age of a leaf may determine the extent to which abaxial cell elongation occurs. Indeed, when younger leaves with a 5 mm petiole were exposed to ethylene, this resulted in abaxial cell elongation along the entire length of the petiole (Polko *et al.*, 2012).

The transcriptional response to FRtip showed strong enrichment for auxin signalling, both in the sensing leaf tip as well as in the growing petiole (Figure 4.3). In the petiole, GO terms representing auxin signalling, as well as growth, were more strongly enriched in the abaxial than the adaxial side (Figure 4.6), suggesting a functional role of auxin in stimulating abaxial cell growth. Auxin signalling was enriched from the first timepoint onwards in the leaf tip, while in the petiole auxin signalling first occurred after 100-120 minutes, suggesting that this is approximately the time window required for long-distance auxin transport from tip to base. Meta-analysis of auxin transport velocities suggests that in *Arabidopsis* inflorescence stems, auxin transport occurs at a rate of around 9 mm/h (Kramer *et al.*, 2011). Assuming transport velocities to be similar in the leaf, this would mean that in just over an hour, leaf tip-generated auxin can move towards the petiole base of the 1 cm long leaves used in our experiments. The time between first induction of auxin signalling in the petiole after around 2 hours and the onset of hyponasty after around 4 hours of FRtip (Figure 4.1 A, B) leaves a two-hour time window in which auxin-induced abaxial cell growth can occur. In hypocotyls, exogenous auxin application can induce apoplast acidification and cell elongation in just 20 minutes (Fendrych *et al.*, 2016). Compared to this, the relatively slow induction of hyponasty could be due to the requirement of auxin accumulation to sufficient levels in the appropriate cell layers. In hypocotyl elongation, the rigid epidermis controls elongation of the entire organ (Procko *et al.*, 2016). Assuming tip-to-base auxin transport to occur through the vasculature, auxin transport across cell layers from the vasculature to the abaxial epidermis may delay the onset of hyponasty. Additionally, auxin may need to activate downstream signalling in the petiole to stimulate abaxial cell elongation and petiole hyponasty.

Besides auxin, we observed GO enrichment in the petiole for several other growth-promoting hormones including gibberellin, brassinosteroid and ethylene (Figure 4.3). Between the abaxial and adaxial petiole, we found that gibberellin and ethylene synthesis as well as brassinosteroid signalling were most strongly induced in the abaxial petiole (Figure 4.6). Regarding gibberellin, the gibberellin synthesis genes *GA20OX1* and *GA20OX2* were induced by FRtip in both sides of the petiole, but more strongly in the abaxial side (Figure 4.5, Supplementary Figure 4.2). Previous work has shown that *GA20OX1* and *GA20OX2* expression is induced in auxin-treated seedlings, as well as in the petioles in whole plant FR treatment (Hisamatsu *et al.*, 2005; Frigerio *et al.*, 2006). Whether the induction of *GA20OX* expression in the abaxial petiole is a downstream response to tip-derived auxin, and whether gibberellin synthesis and signalling are required for FRtip-induced petiole hyponasty will be investigated in **Chapter 6**.

The strong induction of the ethylene synthesis genes *1-AMINO-CYCLOPROPANE-1-CARBOXYLATE SYNTHASE 4 (ACS4)*, *ACS5* and *ACS8* could indicate locally increased ethylene synthesis during FRtip-induced petiole hyponasty. Indeed, elevated ethylene production has been documented for low R/FR-exposed *Arabidopsis* (Kegge *et al.*, 2013). While *ACS4* and *ACS5* are primarily induced in the petiole, *ACS8* is also strongly upregulated in the leaf tip (Figure 4.5). The predominantly abaxial expression of these ethylene synthesis genes in the petiole suggests that, like gibberellin synthesis, ethylene synthesis may be a response to abaxial auxin (Figure 4.5, 4.6, Supplementary Figure 4.2). Ethylene can induce hypocotyl growth via a, partially, similar pathway as shade in hypocotyls (Das *et al.*, 2016). Moreover, petiole hyponasty is also triggered by ethylene treatment (Polko *et al.*, 2012). Activation of ethylene synthesis in the petiole by leaf tip-derived auxin could therefore also be involved in stimulating petiole hyponasty.

In our analysis of hormone synthesis gene expression the most strongly induced gene was *CYTOSOLIC SULFOTRANSFERASE 15/SULFOTRANSFERASE 2 α* (*SOT15/ST2 α*), which was mainly induced in the leaf tip but also in the abaxial petiole (Figure 4.5). A recent study found that the induction of *SOT15* expression by FR enrichment leads to a reduction in the pool of active jasmonate precursors (Fernández-Milmanda *et al.*, 2020). This reduces jasmonate-related repression of FR-induced growth, but also reduces defense against pests and pathogens through the same jasmonate signalling. Our observation that *SOT15* expression also occurs in the non-FR-treated abaxial petiole suggests that this repression of jasmonate activity could be mediated by an intermediary signal (e.g. auxin) and may be important for FRtip-induced petiole hyponasty.

The enrichment of auxin signalling in the petiole was largely lost 5 hours after the start of treatment, implying a transient increase in auxin signalling that is lost when FRtip-induced petiole hyponasty becomes clearly visible (Figure 4.1 A, B). Similarly, in the leaf tip, the enrichment of auxin signalling dampened towards the later timepoints. Interestingly, we found a contrasting enrichment pattern of ABA signalling, which was most strongly enriched towards the later timepoints in both the leaf tip and petiole (Figure 4.3). In **Chapter 3**, we showed that ABA treatment of the leaf tip reduces the hyponastic response and induction of auxin synthesis and response genes in FRtip. We hypothesised that ABA signalling may provide a molecular point of interaction between growth repression by environmental stresses such as soil salinity (Hayes *et al.*, 2019) and growth induction by FR enrichment. The negative temporal correlation between ABA and auxin signalling found in our current transcriptome analysis suggests that ABA might also function to inhibit excessive auxin signalling and petiole hyponasty in FRtip treatment. As strong ABA mutants often have severe phenotypes, creating inducible expression lines or targeting specific binding sites in the promoter regions of ABA synthesis or signalling genes could help study this interaction further.

By carefully designing our transcriptomics experiment based on spatiotemporal analysis of the growth response, we observed quick, slow and transient gene expression patterns, as well as gene expression differences between organs. As a next step in generating even more detailed knowledge on expression patterns, a tissue-specific RNA sequencing approach may prove valuable (Zanetti *et al.*, 2005; Mustrup *et al.*, 2009; Deal & Henikoff, 2011). Although sufficiently precise to ensure abaxial or adaxial enrichment, the manual separation of the two petiole halves is likely to have caused a degree of noise that could be reduced by such more precise analyses. In addition, analysing the transcriptome between three and five hours after start of treatment will give further insight in the temporal regulation of auxin and other hormone signalling.

Spatial separation of light signalling and shoot growth response has been carefully studied in seedlings in the past (Procko *et al.*, 2014; Das *et al.*, 2016; Kohnen *et al.*, 2016). However, our study system provides an opportunity to study the effects of FR enrichment on distal growth without local light treatment of the responding organ. The transcriptome analysis presented here is the starting point for further investigation of FRtip-induced auxin distribution and gibberellin signalling in this thesis, and may be used for future studies on long-distance phytochrome signalling.

Acknowledgements

We would like to thank the whole Plant Ecophysiology research group for their help with harvesting leaf material for RNA sequencing.

Materials and Methods

Plant material and growth conditions

All experiments described in this chapter were performed using Col-0 wild type. Seeds were sown on Primasta soil and cold stratified for three days before transfer to short day white light (WL) conditions light/dark 9 h/15 h, 20 °C, 70 % humidity, 130-150 $\mu\text{M m}^{-2} \text{s}^{-1}$ PAR. Individual seedlings were transplanted to 70mL round pots eight days after germination.

For all experiments, 28 day old plants were selected based on homogeneous development and the presence of a ~5 mm petiole on the 5th youngest leaf which would be used in the experiment. All experiments were started at 10:00 A.M. (ZT2). For phenotyping experiments, petiole angle before treatment and after 24 hours was determined in ImageJ using digital images taken from the side.

Light treatment

For FRtip light treatment, WL was supplemented with FR using EPITEX L730-06AU FR LEDs. These FR LEDs had peak emission at 730nm and locally reduced R/FR from ~2.0 in WL to below 0.1 in FRtip.

Epidermal imprints and cell size measurements

Leaf material for epidermal imprints was harvested after 24 hours treatment. Dissected petioles were gently pressed into dental paste mixture (Coltene) to produce a leaf mold. After a few minutes of drying, a thin layer of transparent nail polish was applied onto the partially hardened dental paste before application of a second layer of dental paste on the adaxial side of the petiole. After solidification, the petiole sample was removed from the dental paste and a thin layer of transparent nail polish was brushed onto the imprint. The nail polish film was mounted on a microscopy slide and imaged at 40x magnification. Images were digitally stitched together and abaxial and adaxial cell lengths were measured along the petiole in ICY software (de Chaumont *et al.*, 2012). Data was smoothed using a rolling average combining cell length data from up to 5 x-axis positions, depending on whether neighbouring datapoints were available.

RT-qPCR and RNA-sequencing

RNA isolation and RT-qPCR were performed as described in **Chapter 3**. A total of 4 biological replicates were harvested from 7 plants per replicate. RT-qPCR primers can be found in Appendix 1.

For RNA-sequencing, material was harvested from 13 leaves per sample, for a total of 4 biological replicates. Poly-A mRNA was isolated and used for the preparation of barcoded cDNA libraries according to the BrAD-seq protocol (Townsend *et al.*, 2015). Libraries were sequenced on an Illumina NextSeq 500 platform at 1*75bp read length yielding around 13 million reads per sample.

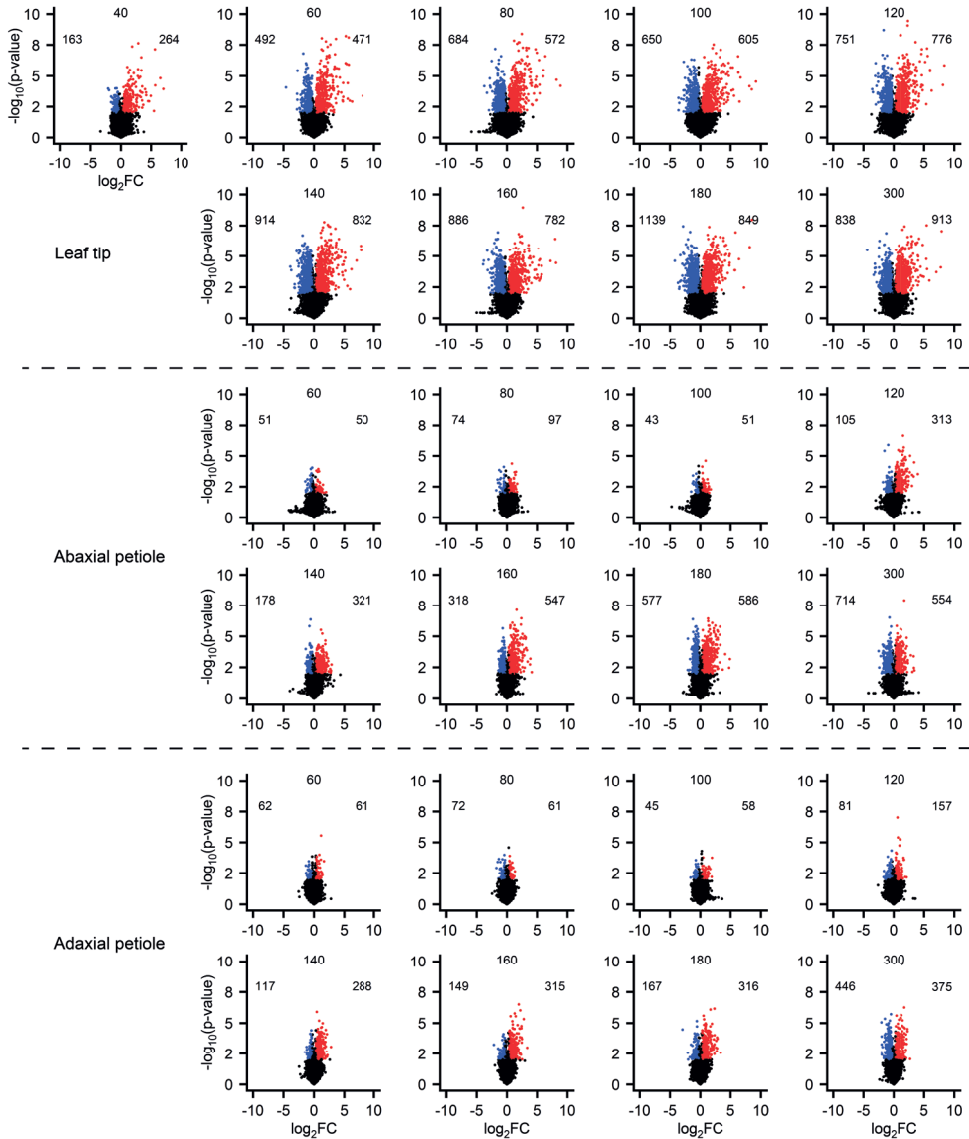
RNA-sequencing data analysis

Reads were annotated to the TAIR10 genome and read counts were normalised using DESeq2. Genes that had an average of less than 1 annotated read per sample were removed. For the remaining 19663 genes, we calculated the mean read count in WL and FRtip as well as \log_2FC and p-value between treatments. Treatment-induced differentially expressed genes (DEGs) were identified per timepoint and per tissue according to p-value and \log_2FC criteria indicated in the figure legends. For Figure 4.6, we used an ANOVA approach to find genes with a significant ($p < 0.001$) two-way interaction Treatment*Tissue between the two petiole halves at timepoints 100-300 minutes. Principle Coordinate Analysis (PCoA) was performed on \log_2 transformed relative transcript abundance. Gene ontology (GO) enrichment analyses were performed using the hypergeometric test available in R. GO terms are only shown when highly significantly enriched in one sample ($-\log_{10}(q\text{-value}) > 25$) or consistently significantly enriched in five or more samples ($-\log_{10}(q\text{-value}) > 5$).

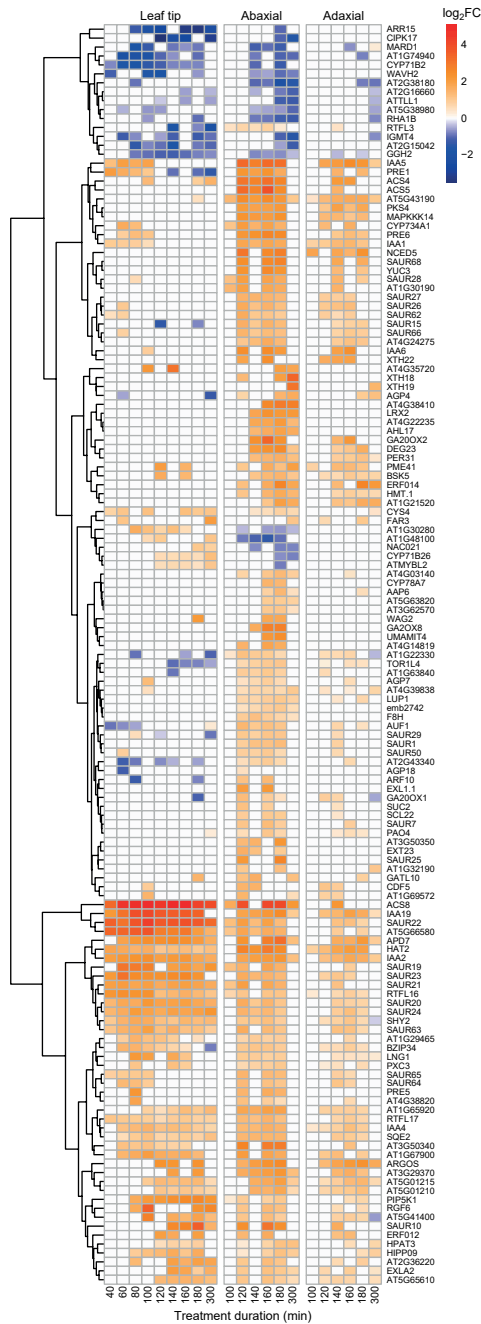
Statistical analyses and data visualisation

Specific details on statistical analyses can be found in the figure legends. Graphs and heatmaps were prepared in R and finetuned in Adobe Illustrator.

Supplementary Figures



Supplementary Figure 4.1. Volcano plots showing \log_2FC and $-\log_{10}(p\text{-value})$ in FRtip compared to WL for all genes per timepoint and tissue. Inset numbers represent DEG number for downregulated genes (left) and upregulated genes (right). Treatment duration (min) indicated above each plot. Coloured dots represent genes that pass the thresholds for $p\text{-value} < 0.01$ and $\log_2FC > 0.3$ (upregulated, red) or $\log_2FC < -0.3$ (downregulated, blue).



Supplementary Figure 4.2. Heatmap showing log₂FC in FRtip compared to WL calculated per timepoint and per tissue of genes that show the most strongly different FRtip response between the two sides of the petiole at the indicated timepoints (ANOVA tissue*treatment $p < 10^{-5}$). Only samples that have a significant treatment effect received colour ($p < 0.01$, $\log_2FC > 1 / < -1$).

Supplementary Tables

Supplementary Table 4.1. ANOVA p-value results for the top 100 genes that show the largest Tissue effect in a two-way interaction analysis for Tissue * Timepoint. Analysis was performed to compare samples of the abaxial versus the adaxial petiole using all timepoints, but only WL treatment. AGI = *Arabidopsis* Gene Identifier.

AGI	Gene	Tissue	Time	Interaction	AGI	Gene	Tissue	Time	Interaction
AT1G01320	REC1	3.6E-28	3.6E-09		AT3G26060	PRXQ	8.3E-28		
AT1G03130	PSAD-2	9.5E-26			AT3G27690	LHCB2.3	3.1E-28	4.9E-10	6.7E-03
AT1G04800	AT1G04800	5.0E-28			AT3G44890	RPL9	7.9E-26		
AT1G07180	NDA1	1.4E-31	6.8E-13	1.3E-09	AT3G46780	PTAC16	1.8E-27	9.5E-04	
AT1G09340	CRB	1.4E-27	4.9E-07		AT3G47650	BSD2	2.3E-25		
AT1G10960	FD1	3.2E-25	1.8E-15	2.7E-03	AT3G49140	AT3G49140	1.2E-26	9.6E-08	
AT1G11545	XTH8	2.2E-27			AT3G50820	PSBO2	1.5E-30		
AT1G11860	GLDT	1.0E-27	7.3E-06		AT3G53460	CP29	1.2E-25	2.7E-27	1.0E-06
AT1G12800	SDP	2.9E-26			AT3G54050	HCEF1	7.9E-30	3.2E-02	
AT1G14150	PnsL2	1.1E-26			AT3G54210	PRPL17	1.5E-29		
AT1G14670	AT1G14670	1.7E-25			AT3G55800	SBPASE	3.6E-32	3.9E-09	
AT1G15980	PnsB1	5.4E-27			AT3G56290	AT3G56290	2.2E-25	6.5E-16	3.2E-02
AT1G20340	DRT112	2.1E-31	9.1E-06		AT3G56910	PSRP5	3.7E-31		
AT1G21460	SWEET1	1.0E-25			AT3G60750	TKL1	2.8E-26		
AT1G27030	AT1G27030	9.0E-27	2.3E-07		AT3G62030	ROC4	4.1E-28		
AT1G29920	CAB2	6.2E-27	2.3E-02		AT3G62410	CP12-2	5.8E-26		
AT1G32060	PRK	2.5E-30	7.1E-08		AT3G63160	OEP6	1.1E-25	8.7E-15	2.3E-06
AT1G32470	GDC-H1	2.3E-25	6.6E-06		AT3G63190	RRF	1.2E-28		
AT1G43670	FBP	4.3E-27			AT4G01460	AT4G01460	6.7E-30		
AT1G55480	ZKT	2.9E-29	5.0E-10		AT4G02770	PSAD-1	3.9E-26		
AT1G55490	CPN60B	6.9E-29			AT4G03280	PETC	4.7E-26	6.6E-04	
AT1G58290	HEMA1	1.9E-30	4.5E-12	3.3E-02	AT4G11175	AT4G11175	2.7E-26		
AT1G60590	AT1G60590	3.2E-26	1.3E-07		AT4G12830	AT4G12830	2.0E-27		
AT1G62780	AT1G62780	1.4E-28			AT4G23400	PIP1;5	1.5E-29		
AT1G64650	AT1G64650	6.4E-26			AT4G24770	RBP31	5.7E-26		
AT1G64770	PnsB2	1.3E-30			AT4G28080	REC2	2.1E-29	1.5E-09	
AT1G67700	HHL1	5.9E-27			AT4G32260	PDE334	1.4E-25	3.7E-02	
AT1G70830	MPL28	4.5E-36			AT4G35090	CAT2	4.0E-27	9.6E-13	3.7E-03
AT1G74470	AT1G74470	4.2E-27	4.3E-02		AT4G35250	HCF244	8.1E-28	1.7E-11	
AT1G74730	RIQ2	4.9E-26	3.3E-05		AT4G37930	SHM1	2.2E-28	4.3E-06	
AT1G74880	NdhO	1.6E-28	1.1E-02		AT4G38970	FBA2	6.0E-26	3.7E-12	
AT1G77760	NIA1	3.2E-25	4.3E-18	1.4E-02	AT4G39710	PnsL4	1.4E-26		
AT2G21330	FBA1	1.5E-26	2.7E-16		AT5G03150	JKD	6.1E-26		
AT2G24090	PRPL35	2.0E-27			AT5G09660	PMDH2	1.6E-25	6.4E-10	
AT2G28190	CSD2	1.7E-26			AT5G13630	GUN5	2.2E-26	2.0E-17	
AT2G33450	PRPL28	1.1E-29			AT5G14740	CA2	3.1E-34	1.1E-05	
AT2G35370	GDCH	5.7E-27			AT5G15160	BNQ2	1.9E-26	2.3E-03	
AT2G39470	PnsL1	2.4E-26			AT5G17230	PSY	4.5E-28	8.8E-13	
AT2G40100	LHCB4.3	1.4E-26	1.7E-06		AT5G19220	APL1	4.2E-26	1.9E-03	
AT2G41680	NTRC	1.3E-26			AT5G20720	CPN20	1.1E-25		
AT2G46820	PSI-P	9.6E-28			AT5G23060	CaS	3.6E-27	7.7E-15	
AT3G01500	CA1	2.2E-35			AT5G38420	RBCS2B	1.3E-34	6.9E-08	3.5E-02
AT3G06980	AT3G06980	4.9E-27			AT5G48490	DIR1-LIKE	2.7E-29	4.7E-08	2.9E-04
AT3G10450	SCPL7	1.7E-25			AT5G49910	cpHsc70-2	4.3E-26	9.0E-07	
AT3G12780	PGK1	2.2E-26			AT5G54600	RPL24	2.1E-26		
AT3G13470	CPN60BETA2	3.0E-26	1.3E-06		AT5G55220	TIG1	8.5E-26		
AT3G14415	GOX2	9.4E-26	1.4E-06		AT5G57180	CIA2	3.7E-28		
AT3G14420	GOX1	1.4E-26	7.2E-11		AT5G61410	RPE	1.7E-25		
AT3G17170	RFC3	4.2E-27			AT5G64840	ABCF5	9.2E-26	8.4E-22	3.9E-02
AT3G24140	FMA	1.5E-26			AT5G66570	PSBO1	5.6E-30		

Supplementary Table 4.2. GO enrichment analysis result showing the 10 most strongly enriched biological process GO categories using the 100 genes with the strongest tissue effect shown in Supplementary Table 4.1.

GO category	p-value
reductive pentose-phosphate cycle	1.2E-17
photosynthesis	1.8E-15
fructose metabolic process	6.1E-12
plastid translation	2.3E-11
response to cold	5.6E-11
glycine decarboxylation via glycine cleavage system	5.9E-11
photosynthetic electron transport in photosystem I	5.0E-10
gluconeogenesis	9.5E-10
carbon utilization	2.2E-09
response to light stimulus	2.3E-08



Chapter 5

PIN-dependent transport facilitates tissue-specific auxin accumulation in the petiole to regulate hyponasty upon remote far-red light enrichment

Jesse J. Küpers¹, Lisa Oskam¹, Sanne Matton¹, Harold Weekamp¹, Basten L. Snoek², Che-Yang Liao³, Wouter Kohlen⁴, Dolf Weijers³ & Ronald Pierik¹

¹ *Plant Ecophysiology, Dept. Biology, Utrecht University, 3584CH Utrecht, The Netherlands*

² *Theoretical Biology and Bioinformatics, Dept. Biology, Utrecht University, 3584CH Utrecht, The Netherlands*

³ *Laboratory of Biochemistry, Wageningen University, Stippeneng 4, 6708WE Wageningen, The Netherlands*

⁴ *Laboratory for Molecular Biology, Wageningen University, Droevendaalsesteeg 1, 6708PB Wageningen, The Netherlands*

Abstract

The plant hormone auxin plays an important regulatory role in various adaptive plant growth responses. Closely controlled long-distance auxin transport has been documented to regulate growth in target cells across cell-layers and organs. In **Chapter 4**, we revealed that detection of nearby neighbours through far-red (FR) light reflection, sensed as FR enrichment in the leaf tip triggers a transcriptional auxin response in the abaxial petiole base that is related to upward leaf movement. Here, we study how leaf tip-derived auxin that is produced upon FR enrichment in the leaf tip induces such specific abaxial auxin signalling in the petiole. Combining various recent developments in microscopy and optical clearing methods, we developed a protocol to visually describe auxin concentration at a cellular level in the petiole. We reveal that auxin rapidly accumulates in the abaxial petiole, and that this auxin asymmetry in the petiole is required for upward leaf movement. This asymmetrical auxin distribution requires PIN-FORMED (PIN) auxin transport proteins, of which we show that PIN3 is more abundant on the abaxial than the adaxial petiole endodermis.

Introduction

Plants require light to power photosynthesis. With the exception of shade tolerant species, most plants will therefore adjust their growth when they detect a threat to light capture (Gommers *et al.*, 2013). To drive photosynthesis, plants absorb blue (B) and red (R) light while FR is mostly reflected or transmitted through the leaf. The reflection of FR reduces the ratio of red (R) to far-red (FR) light (R/FR) which provides an important signal that indicates neighbour proximity, even before actual light deprivation occurs (Ballaré *et al.*, 1990). In response to low B and low R/FR cues, plants display various adaptive growth responses including hypocotyl elongation and bending towards light in seedlings and petiole elongation and hyponasty in adult plants (Küpers *et al.*, 2018). These responses serve to actively forage for light and avoid shading by neighbours.

The growth-promoting phytohormone auxin plays an important role in these adaptive growth responses (Fernández-Milmanda & Ballaré, 2021). During hypocotyl bending in response to unilateral B (i.e. phototropism) auxin is transported from the light-exposed towards the shaded side of the hypocotyl, where it triggers cell elongation driving the bending of the hypocotyl towards the light (Legris & Boccaccini, 2020). Hypocotyl elongation in low B or low R/FR occurs through inactivation of the cryptochrome and phytochrome photoreceptors respectively, which releases photoreceptor repression of the growth-promoting bHLH transcription factors PHYTOCHROME INTERACTING FACTORS (PIFs) (Fernández-Milmanda & Ballaré, 2021). Active PIFs stimulate growth in part by enhancing auxin biosynthesis via activation of *YUCCA* gene expression (reviewed in Küpers *et al.*, 2020). To initiate specific growth responses, auxin is transported towards target tissues via auxin transporters such as AUXIN1/LIKE AUX1 (AUX/LAX), ATP-BINDING CASSETTE TRANSPORTERS OF THE B SUBFAMILY (ABCB), PIN-LIKES (PILS) and most importantly PIN-FORMED (PIN) proteins (Adamowski & Friml, 2015; Geisler *et al.*, 2017; Singh *et al.*, 2018; Sauer & Kleine-Vehn, 2019). In seedlings, the rigid outermost epidermal cell layer controls the auxin-mediated hypocotyl elongation response to low R/FR and high temperature cues (Procko *et al.*, 2016; Kim *et al.*, 2020). In low R/FR, auxin synthesis takes place in the cotyledons from where it is directed towards the hypocotyl (Procko *et al.*, 2014; Kohnen *et al.*, 2016). In the hypocotyl, PIN3 mediates auxin transport from the endodermis towards the rigid epidermis, which results in hypocotyl elongation (Keuskamp *et al.*, 2010).

We previously showed that neighbour detection at the leaf tip (FRtip) of adult *Arabidopsis* leaves results in adaptive upward leaf movement through auxin-mediated cell elongation in the abaxial petiole (**Chapters 3 and 4**). The preferential induction of auxin signalling

in the abaxial petiole suggests that leaf tip-derived auxin specifically accumulates in the abaxial petiole. Alternatively, differences in auxin responsiveness between the abaxial and adaxial petiole could also explain the observed abaxial-adaxial asymmetry. In this chapter, we set out to unravel the distribution dynamics of auxin in the petiole in response to FRtip exposure. We combined recent developments in fluorescent protein fixation and optical clearing methods to visualise auxin distribution in the petiole. We show that leaf tip-derived auxin is indeed transported towards the abaxial petiole in a process that requires PIN proteins.

Results

Neighbour detection in the leaf tip leads to directed auxin transport towards the abaxial petiole

In **Chapter 4**, FR enrichment at the leaf tip was shown to activate auxin signalling, both locally in the leaf tip as well as in the upwardly bending petiole. In the petiole, the auxin signalling was strongest on the abaxial side, where cell elongation occurred. This prompted us to investigate the effect of FRtip on the distribution of auxin in the leaf. We found that FRtip increased auxin concentrations in the leaf tip and the abaxial petiole, but not in the adaxial petiole (Figure 5.1 A). To study whether such differential auxin concentrations are required for petiole hyponasty, we exogenously applied indole-3-acetic acid (IAA) to the abaxial or adaxial petiole. We found that abaxial IAA application results in strong hyponasty regardless of R/FR, while adaxial IAA application inhibits the hyponastic response to FRtip (Figure 5.1 B, C). These observations indicate that an auxin gradient, either installed endogenously upon FRtip exposure, or through directional external application, is both sufficient and required for hyponastic leaf movement.

To achieve further spatiotemporal resolution of auxin distribution, we visualised auxin distribution using a newly made C3PO fluorescent auxin reporter. C3PO conveniently combines the previously described R2D2 reporter for auxin concentration quantification and the DR5v2 reporter that reports auxin response (Liao *et al.*, 2015) into a single construct (Supplementary Figure 5.1). We developed a method to image transverse cross-sections of fixated and optically cleared (Kurihara *et al.*, 2015) petiole material in which we could measure nuclear fluorescence in individual cells and cell layers (Figure 5.2 A, B, Supplementary Figure 5.2).

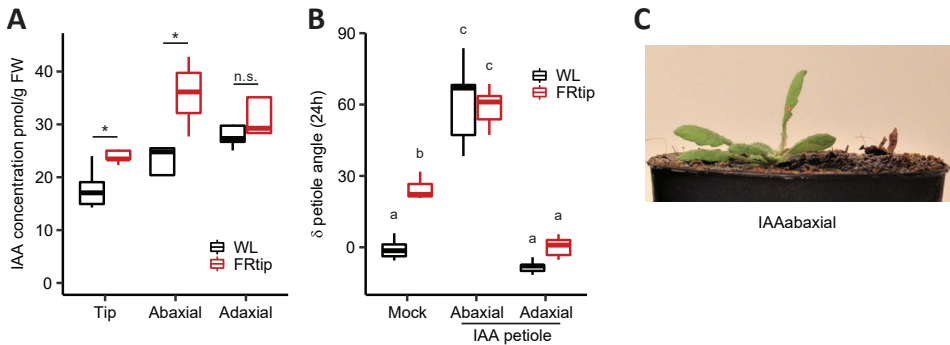


Figure 5.1. Asymmetric accumulation of IAA in the abaxial petiole is required for FRtip-induced hyponasty. (A) Free IAA concentration (nmol/g FW) in the leaf tip and abaxial/adaxial split petiole after 5h light treatment. ($n = 5$ biological replicates from 20 plants each, *: $p < 0.05$, two-sided t-test). (B) Petiole angle change after 24h light treatment combined with $30 \mu\text{M}$ IAA or mock application to the petiole. When IAA was applied to one side of the petiole, the other side was mock treated. ($n = 7$ biological replicates per treatment group, different letters indicate significant differences, Tukey HSD $p < 0.05$). (C) Photograph of petiole hyponasty in FRtip + IAAabaxial treated plant showing extreme petiole hyponasty.

We found that the auxin concentration, as determined by the mD2-tdTomato/D2-Venus (mD2/D2) intensity ratio, increased in all cell layers on the abaxial side within 3 hours of FRtip and remained higher than WL throughout the 7 hour interval that we measured, while there was little increase on the adaxial side (Figure 5.2 C, D). When substituting FRtip with local IAA application on the leaf tip (IAAtip) we found increased auxin concentrations after three hours in both sides of the petiole. At later timepoints, the adaxial increase was lost and even changed into decreased auxin concentrations in the adaxial endodermis and cortex, whereas the abaxial tissues continued to have elevated auxin (Figure 5.2 C, D). In contrast with the induction of mD2/D2 by FRtip and IAAtip, we did not find clear and consistent induction of DR5v2::mTurquoise2 intensity by these treatments (Figure 5.2 E, F). Since our transcriptome analysis shows very clear induction of auxin response in the petiole upon FRtip (**Chapter 4**), the lack of DR5V2 response suggests that this reporter lacks sensitivity in the petiole.

Similar to local FR enrichment at the leaf tip, direct IAA application to the abaxial petiole (IAAabaxial) induces a strong petiole hyponasty response (Figure 5.1 B). When we measured the mD2/D2 ratio in this treatment we found that it results in a clear induction of the reported auxin concentration in the outermost parts of the abaxial petiole, as well as a minor induction in the adaxial endodermis (Figure 5.3 A, B). Interestingly, unlike FRtip and IAAtip, IAAabaxial induced an increase in DR5v2::mTurquoise2 fluorescence in the

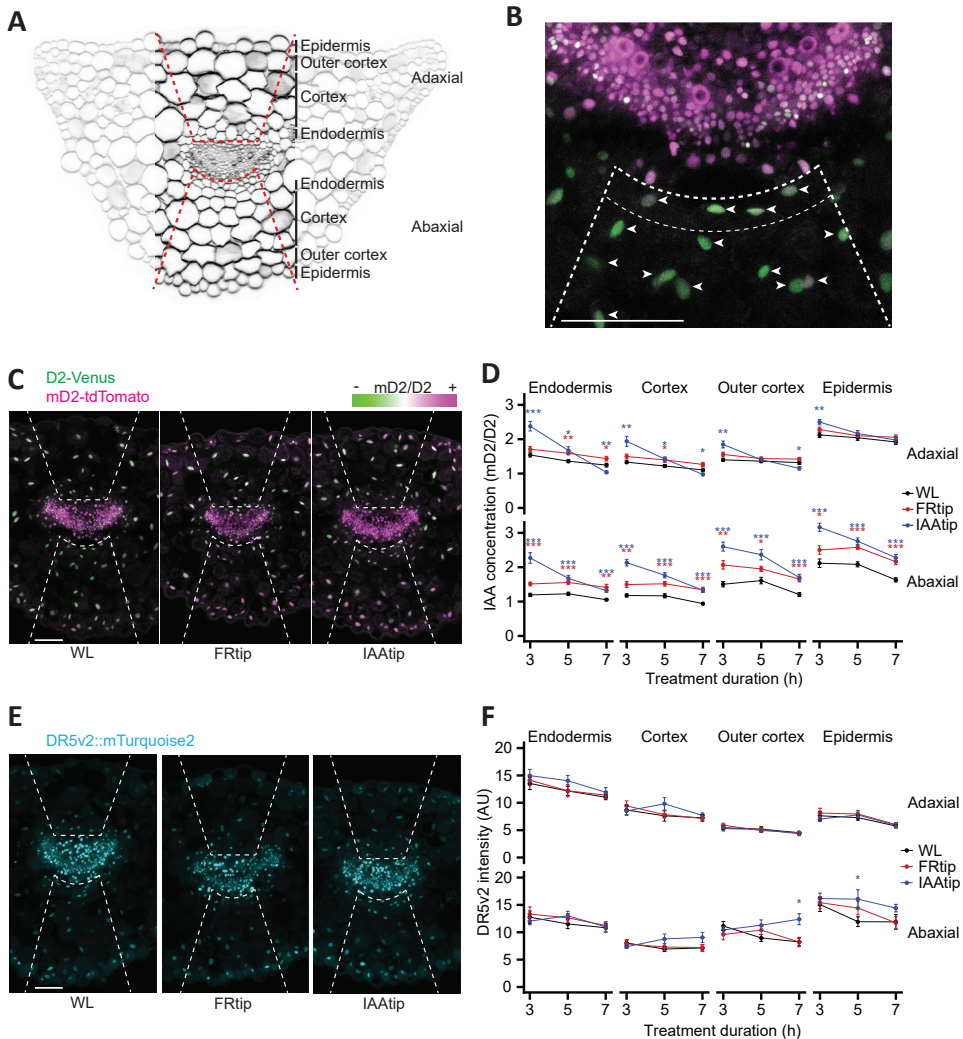


Figure 5.2. Leaf tip-derived auxin accumulates throughout the abaxial petiole. (A & B) Petiole base cross-section indicating cell layers and region of the petiole (A) and nuclei (B) that were used to measure nuclear fluorescence in petiole cross-sections. Dashed lines indicate the region, and arrowheads indicate the nuclei in which fluorescence was measured. (C & D) Representative images after 5 h (C) and quantification at indicated timepoints (D) of the mD2/D2 ratio that reports IAA concentration in the petiole base. (E & F) Representative images after 5 h (E) and quantification at indicated timepoints (F) of DR5v2::mTurquoise2 fluorescence in the petiole base. Plants were treated with mock, FRtip or IAAtip. ($n = 11-12$ samples per treatment, coloured asterisks represent significant treatment effect compared to WL, *: $p < 0.05$, **: $p < 0.01$, ***: $p < 0.001$, two-sided t-test, data represent mean \pm SEM, scale bars in microscopy images represent 100 μm).

outermost cell layers of the abaxial petiole (Figure 5.3 C, D). It is important to note that the change in petiole angle induced by IAAabaxial strongly exceeded what was observed in any of the other treatments (Figure 5.1 B, C).

PIN auxin transporters mediate auxin accumulation in the abaxial petiole

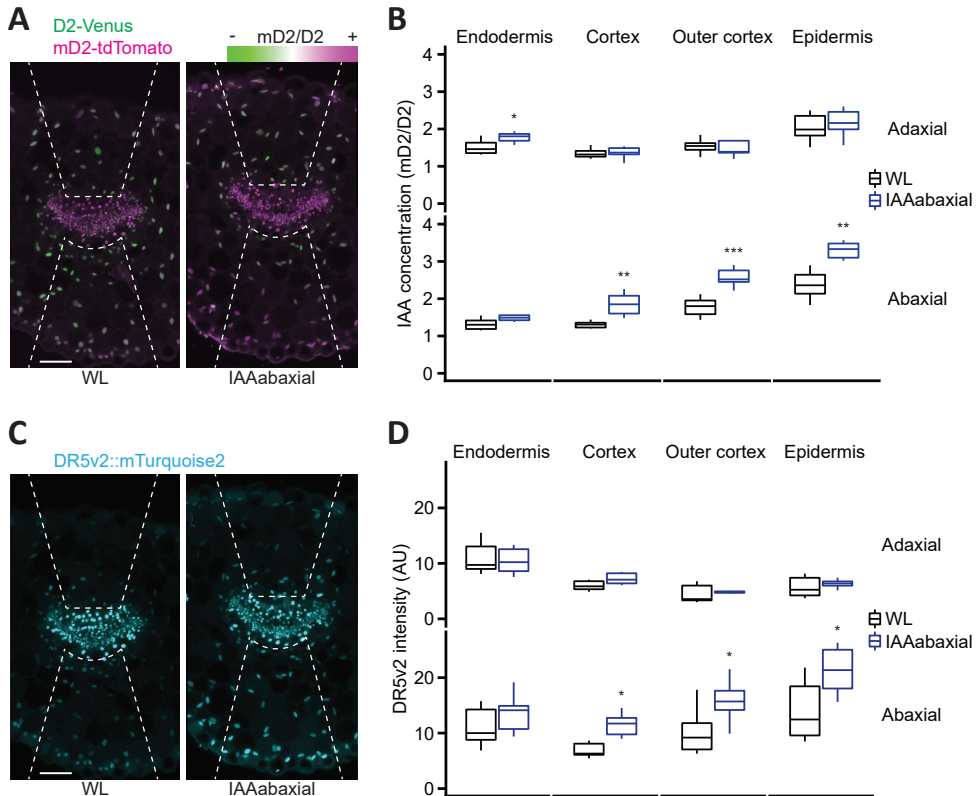


Figure 5.3. Abaxial IAA treatment increases auxin concentration and response in the abaxial petiole. (A & B) Representative images (A) and quantification (B) of the mD2/D2 ratio that reports IAA concentration in the petiole base. (C & D) Representative images (C) and quantification (D) of DR5v2::mTurquoise2 fluorescence in the petiole base. Plants were treated for 5 hours with mock or IAAabaxial. ($n = 6$ samples per treatment, asterisks represent significant treatment effect compared to WL, *: $p < 0.05$, **: $p < 0.01$, ***: $p < 0.001$, two-sided t-test, data represent mean \pm SEM, scale bars in microscopy images represent $100 \mu\text{m}$, dashed lines indicate the region in which fluorescence was measured).

The petiole hyponasty response to FRtip requires intact auxin transport and is, therefore, reduced in the *pin3* single mutant and absent in the *pin3 pin4 pin7* triple mutant (Michaud *et al.*, 2017; Pantazopoulou *et al.*, 2017). Similarly, in **Chapter 3**, we showed that auxin application to the leaf tip resulted in reduced and absent hyponasty in *pin3* and *pin3 pin4 pin7* respectively.

Analysis of auxin transport gene expression revealed that *AUX1*, *ABCB4* and *ABCB19* were primarily induced by FRtip in the leaf tip, while *PIN1*, *PIN3*, *PIN4* and *PIN7* were also upregulated in the petiole (Figure 5.4 A). When we analysed auxin distribution using the mD2/D2 ratio from C3PO crossed to the *pin3 pin4 pin7* mutant background we found that these mutations inhibited FRtip and IAAtip-induced abaxial auxin accumulation (Figure 5.4 B, C). The mD2/D2 ratio in WL was also different from wild-type in *pin3 pin4 pin7* with relatively increased mD2/D2 in the inner cell layers and reduced mD2/D2 in the abaxial outer cortex and epidermis in *pin3 pin4 pin7* compared to wild-type. Regarding the auxin response in *pin3 pin4 pin7*, visualised by the DR5v2::mTurquoise2 intensity, we again observed no clear treatment effect (Figure 5.4 D, E). However, we observed a similar pattern of difference from wild-type for DR5v2::mTurquoise2 as for the mD2/D2 ratio with decreased relative DR5v2::mTurquoise2 intensity in the outer cell layers in *pin3 pin4 pin7*. This suggests that very large differences in auxin signalling induced by strong IAAabaxial treatment (Figure 5.3 C, D) or genetic mutation of multiple auxin transporters (Figure 5.4 D, E) do affect DR5v2::mTurquoise2 signal in petiole tissue.

Given the prominent effect of *pin* mutations on hyponasty and abaxial auxin accumulation in response to auxin and supplemental FR, and the established regulation of PIN3 localisation by supplemental FR in seedlings (Keuskamp *et al.*, 2010) we studied PIN3 localisation and abundance in petioles using *pPIN3::PIN3-GFP*. We first tried to use the same fixation and clearing technique as used for the C3PO reporter, but we could not retain stable signal of the membrane-localised PIN3-GFP protein.

We therefore decided to use fresh petiole material that was cut longitudinally through the midvein. We found that in the petiole endodermis, PIN3-GFP is slightly more abundant on the abaxial compared to the adaxial side and that this asymmetry is reinforced by IAAtip treatment (Figure 5.5). Taken together, PIN-dependent auxin transport directs leaf tip-derived auxin towards the abaxial petiole to stimulate abaxial cell elongation and petiole hyponasty upon neighbour detection.

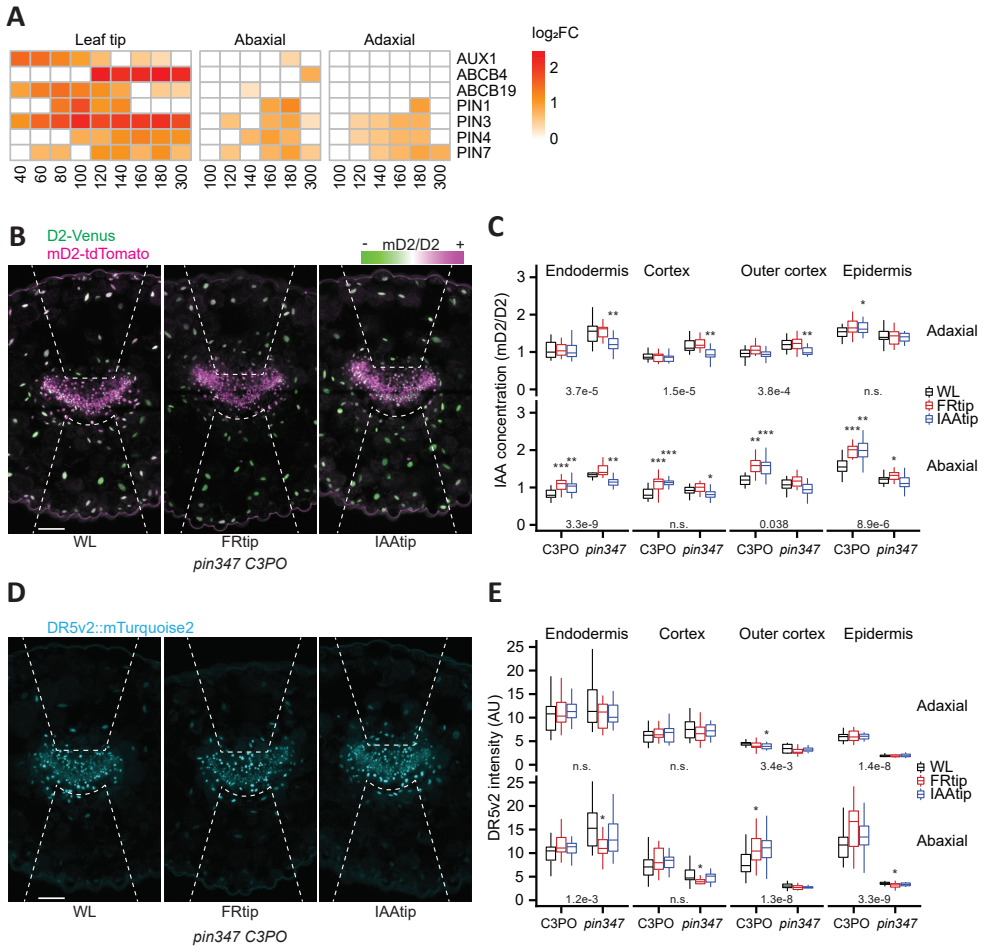


Figure 5.4. PIN transporters are required for abaxial accumulation of leaf tip-derived auxin. (A) Heatmap showing log₂FC in FRtip relative to WL, calculated per timepoint for auxin transport genes. Only genes that have a significant treatment effect in at least one sample are shown ($p < 0.01$, log₂FC > 1 / < -1). (B & C) Representative images in *pin3 pin4 pin7* C3PO (B) and quantification in C3PO and *pin3 pin4 pin7* C3PO (C) of the mD2/D2 ratio that reports IAA concentration in the petiole base. (D & E) Representative images in *pin3 pin4 pin7* C3PO (D) and quantification in C3PO and *pin3 pin4 pin7* C3PO (E) of DR5v2::mTurquoise2 fluorescence in the petiole base. Plants were treated for 7 hours with mock, FRtip or IAAtip. ($n = 13$ -16 samples per treatment, asterisks represent significant treatment effect compared to WL, *: $p < 0.05$, **: $p < 0.01$, ***: $p < 0.001$, two-sided t-test, inset values represent p-value for genotype difference in WL calculated per cell layer, two-sided t-test, data represent mean \pm SEM, scale bars in microscopy images represent 100 μ m, dashed lines indicate the region in which fluorescence was measured, *pin347* = *pin3 pin4 pin7*).

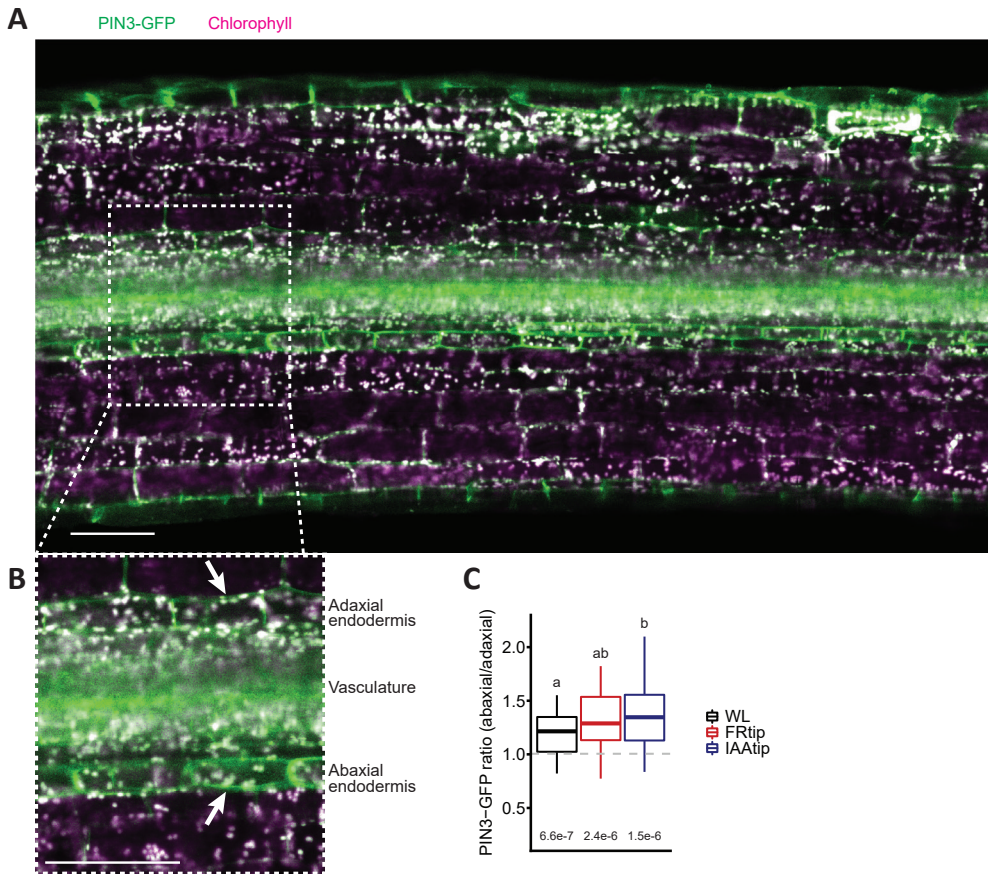


Figure 5.5. Abaxial localisation of endodermal PIN3-GFP is reinforced by leaf tip-derived auxin. (A & B) Representative overview image (A) and closeup around the vasculature (B) of *pPIN3::PIN3-GFP* in a longitudinal petiole cross-section. (Arrows indicate the endodermal cells in which PIN3-GFP intensity in the membranes was quantified for C). (C) Ratio of PIN3 intensity in the abaxial/adaxial endodermis after 2.5-4 h in WL, FRtip or IAAtip. ($n = 46$ - WL, 28 - FRtip, 30 - IAAtip biological replicates per treatment group, different letters indicate significant differences, Tukey HSD $p < 0.05$, inset values represent p-value for difference from ratio 1, one-sample t-tests, scale bars in microscopy images represent $100 \mu\text{m}$).

Discussion

In **Chapter 4**, we showed that FRtip induces abaxial cell elongation and petiole hyponasty through differential transcriptome regulation, including auxin signalling, between the abaxial and adaxial petiole. Here we showed that this asymmetric auxin signalling corresponds with increased auxin concentrations in the abaxial but not the adaxial petiole in response to FRtip. In addition, we showed that this auxin distribution asymmetry requires PIN auxin transporter action and that it the auxin asymmetry is required and sufficient to induce petiole hyponasty.

To increase the resolution of our auxin distribution measurements from the sub-organ level to cellular level, we made use of the fluorescent auxin reporter C3PO. C3PO reports auxin concentration via the ratio of non-auxin-degradable mD2-tdTomato to auxin-degradable D2-Venus fluorescence as well as auxin response via DR5v2::mTurquoise2 (Liao *et al.*, 2015). The ratiometric analysis of auxin concentration by mD2/D2 greatly improves the accuracy of auxin concentration analysis compared to just D2-Venus, as tissue-specific differences in transgene expression are corrected for by the internal mD2-tdTomato control (Bhatia *et al.*, 2019). Nevertheless, the auxin-induced degradation of D2-Venus still requires a functional endogenous auxin receptor complex and so using the new direct auxin sensor AuxSen (Herud-Sikimić *et al.*, 2021) may provide resolution that cannot be achieved using mD2/D2.

Using the mD2/D2 ratio to analyse auxin distribution, we confirmed that auxin levels were persistently increased in the abaxial petiole from 3 to 7 hours after the start of either FR enrichment or direct auxin application to the leaf tip (Figure 5.2 C, D). In the adaxial side of the petiole, leaf tip-derived auxin also led to increased auxin concentrations, but mainly on the inner cell layers or at the early timepoints. The petiole epidermis likely controls auxin-induced organ growth, as it does in the hypocotyl (Procko *et al.*, 2016; Kim *et al.*, 2020). Therefore, a lack of sustained epidermal auxin increases on the adaxial side, would limit growth of the adaxial petiole, causing the growth response to increased auxin in the abaxial epidermis to result in petiole hyponasty, rather than petiole elongation. In particular, IAAtip treatment caused a strong early spike in adaxial auxin, which later turned into a reduction in most of the adaxial petiole relative to the white light control. This may indicate a mechanism that removes excess tip-derived auxin from the adaxial petiole by redirecting that auxin towards the vasculature or abaxial petiole. Alternatively excess auxin could be inactivated or degraded through conjugation to amino acids (Staswick *et al.*, 2005; Zheng *et al.*, 2016).

The auxin transport towards the abaxial petiole requires functional PIN auxin efflux proteins (Figure 5.4 B, C). We show that in the petiole endodermis PIN3 is mainly present on the abaxial side and that this PIN3 asymmetry is enhanced in response to auxin application to the leaf tip (Figure 5.5). The PIN3 asymmetry likely directs tip-derived auxin flow from the vasculature towards the abaxial petiole, thereby stimulating asymmetric cell growth and hyponasty. Comparable endodermal PIN3 redistribution also occurs during FR light-induced hypocotyl elongation and during phototropism (Keuskamp *et al.*, 2010; Ding *et al.*, 2011 respectively). Moreover, the hyponastic petiole response to elevated temperatures also involves PIN3 accumulation in the abaxial endodermis (Park *et al.*, 2019). However, these examples involve direct light or temperature treatment exposure of the tissues where PIN3 redistributes. Our observation that IAA_{tip} triggers similar endodermal PIN3 redistribution in the distal petiole, that is not exposed to treatment, implies that auxin itself reinforces the endodermal PIN3 asymmetry such that IAA is predominantly directed towards the abaxial side of the petiole. In support of this hypothesis, Keuskamp *et al.*, 2010 showed that the FR-induced changes in PIN3 abundance and localisation in elongating hypocotyls indeed relied on signalling of auxin itself, as evidenced by their use of an auxin signalling inhibitor. How the endodermal PIN3 asymmetry in WL conditions is installed remains to be studied. It could follow from the basic levels of auxin distribution under control conditions, but other possible explanations include signalling via leaf-polarity factors (Bou-torrent *et al.*, 2012; Merelo *et al.*, 2017; Park *et al.*, 2019), asymmetric leaf and vasculature structure (Figure 5.2 A, B, Bou-torrent *et al.*, 2012), gravity (Rakusová *et al.*, 2011) and even a light signalling gradient within the tissue (Legris *et al.*, 2021). These possible scenarios are discussed in greater detail in the general discussion of this thesis (**Chapter 8**).

In addition to studying PIN3 in more detail, improving our understanding of auxin transport via the partially redundant PIN4 and PIN7 would yield even more insight in the regulation of directed long-distance auxin transport. In the root tip, the distribution of auxin follows a “reverse fountain” pattern, that is directed by distinct expression and localisation patterns of multiple PINs (Ruiz Rosquete *et al.*, 2012). Perhaps also in the leaf, specific PINs would regulate long-distance tip-to-base auxin transport and other PINs might regulate lateral auxin distribution between petiole cell layers. Moreover, it is possible that still other auxin transporters, such as AUX/LAX, ABCB and PILS proteins and even auxin transport through plasmodesmata may contribute to the control of auxin distribution in the leaf (Geisler *et al.*, 2017; Singh *et al.*, 2018; Sauer & Kleine-Vehn, 2019; Gao *et al.*, 2020).

The transcriptome analysis (**Chapter 4**) revealed strong induction of auxin signalling in the petiole upon FR enrichment at the leaf tip. While our microscopy approach revealed that FRtip triggered abaxial auxin accumulation in the petiole, this did not increase the auxin signalling output visualised by DR5v2::mTurquoise2 (Figure 5.2 E, F). We did see induction of DR5v2::mTurquoise2 by direct auxin application to the abaxial petiole (Figure 5.3 C, D), a treatment that triggers exaggerated hyponasty (Figure 5.1 B, C), and a reduction of DR5v2::mTurquoise2 intensity compared to wild-type in *pin3 pin4 pin7* (Figure 5.4 D, E). This suggests that DR5v2::mTurquoise2 lacks the sensitivity to report the relatively mild treatment-induced changes in auxin signalling in the petiole that were recorded using DR5::GUS and DR5::LUC (Michaud *et al.*, 2017; Pantazopoulou *et al.*, 2017, **Chapter 3**) and that also stand out from the RNAseq analyses (**Chapter 4**).

So, although DR5v2 does sensitively report auxin signalling in the roots (Liao *et al.*, 2015, Supplementary Figure 4.1) it does not seem to have the same sensitivity window in petioles of adult plants. These observations highlight the importance of combining experimental approaches before drawing conclusions based on individual observations. We conclude that upon neighbour detection, plants use carefully controlled long-distance auxin transport from the leaf tip to the abaxial petiole epidermis to adaptively raise their leaves.

Materials and Methods

Plant material and growth conditions

Genotypes used in this chapter: *pin3-3 pPIN3::PIN3-GFP* (Žádníková *et al.*, 2010), C3PO and *pin3 pin4 pin7* C3PO were all in Col-0 background. Seeds were sown on Primasta soil or agarose plates for germination and cold stratified for three days before transfer to short day white light (WL) conditions light/dark 9 h/15 h, 20 °C, 70 % humidity, 130-150 $\mu\text{M m}^{-2} \text{s}^{-1}$ PAR. Individual seedlings were transplanted to 70mL round pots eight days after germination.

For all experiments, 28 day old plants were selected based on homogeneous development and the presence of a ~5 mm petiole on the 5th youngest leaf which would be used in the experiment. All experiments were started at 10:00 A.M. (ZT2). For phenotyping experiments, petiole angle before treatment and after 24 hours was determined in ImageJ using digital images taken from the side.

For microscopic screening of C3PO fluorescence in the root, seeds were surface sterilised, sown on half-strength Murashige and Skoog medium with 0.8% Daichin agar (Duchefa)

(1/2 MS plate) and vernalised at 4 °C for 2 d. Afterwards, the seedlings were grown in climate room conditions at 22 °C in 16 h/8 h light/dark cycles.

Construction of the C3PO auxin reporter

The C3PO construct (pGIIM/DR5v2::n3mTurquoise2-pRPS5A::mD2:ntdTomato-pRPS5A::D2:n3Venus) was generated via inserting DR5v2::n3mTurquoise2 into R2D2 (Liao *et al.*, 2015). n3mTurquoise2 was generated by sequentially cloning the following three constructs, that were generated via PCR from plasmid template “pmTurquoise2-C1100”, into pGIIK/LIC_SwaI-LIC_HpaIv2-tNOS: mTurquoise2 coding sequence (CDS) with a stop codon, mTurquoise2 CDS without stop codon and NLS: mTurquoise2 without stop codon. The n3mTurquoise2-tNOS cassette was then excised via BamHI-XbaI double-digestion and inserted via conventional cloning into pGIIK/DR5v2::ntdTomato-tNOS, after the ntdTomato-tNOS cassette had first been removed via BamHI-XbaI double-digestion, to generate pGIIK/DR5v2::n3mTurquoise2-tNOS. An Ascl restriction site was inserted into XbaI-digested pGIIK/DR5v2::n3mTurquoise2-tNOS via conventional cloning before ligating DR5v2::n3mTurquoise2-tNOS, that was excised by Bsp120I-Ascl double-digestion, with Bsp120I-Ascl double-digested pGIIM/pRPS5A::mD2:ntdTomato-pRPS5A::D2:n3Venus to generate pGIIM/DR5v2::n3mTurquoise2-pRPS5A::mD2:ntdTomato-pRPS5A::D2:n3Venus that we named C3PO. C3PO was then introduced into *Arabidopsis* via floral dip and selected using methotrexate. *pin3 pin4 pin7* C3PO was generated by crossing C3PO to *pin3-3 pin4 pin7*. Primer sequences used for cloning are shown in Appendix 1.

Light and pharmacological treatments

For FRtip treatments, WL was supplemented with FR using EPITEX L730-06AU FR LEDs. These FR LEDs had peak emission at 730nm and locally reduced R/FR from ~2.0 in WL to below 0.1 in FRtip. For IAA treatment at the leaf tip, 5 µL 30 µM IAA (0.03% DMSO, 0.1% Tween-20) solution was pipetted onto the leaf tip. For IAA application to the petiole, concentrated stocks were diluted to 30 µM IAA in 97 % lanolin (0.03 % DMSO). The lanolin containing solutions were carefully applied to the petiole using a tooth pick.

IAA extraction and quantification by liquid chromatography-tandem mass spectrometry

For the extraction of IAA from *A. thaliana*, ~40 mg of snap-frozen leaf material was used per sample. Tissue was ground to a fine powder at -80 °C using 3-mm stainless steel

beads at 50 Hz for 2*30 seconds in a TissueLyser LT (Qiagen, Germantown, USA). Ground samples were extracted with 1 mL of cold methanol containing [phenyl 13C6]-IAA (0.1 nmol/mL) as an internal standard as previously described (Schiessl *et al.*, 2019). Samples were filtered through a 0.45 µm Minisart SRP4 filter (Sartorius, Goettingen, Germany) and measured on the same day. Auxin was analysed on a Waters Xevo TQs tandem quadruple mass spectrometer as previously described (Ruyter-Spira *et al.*, 2011; Gühl *et al.*, 2021).

Confocal microscopy

For confocal microscopy in transverse petiole cross-sections we harvested leaves into 24-well plates containing 4 % paraformaldehyde in PBS (pH 6.8) with Tween-20 (0.05 %). After vacuum incubation for one hour, leaves were washed three times for two minutes in PBS and stored for up to 24 h in PBS. Next, leaves were dried and placed in an Eppendorf tube containing warm agarose (3.5 %) and transferred to ice to solidify the agarose. Solid agarose plugs were sectioned to 250 µm slices using a Leica VT1000S vibratome. The first two slices from the petiole base (~0-500 µm) were discarded, and the next two (~500-1000 µm) were moved to 24-well plates containing ClearSee medium (Kurihara *et al.*, 2015) and incubated for at least 7 days before microscopy. For Figure 5.2 A, after the initial clearing, ClearSee was supplemented with Calcofluor white (0.01 %, 5 h), and rinsed afterwards with ClearSee. Longitudinal cross-sections for pPIN3::PIN3-GFP were made by hand, without prior fixation or clearing. Samples were directly placed with the cut edge onto a coverslip container (Lab-Tek) and immediately imaged. Sample drying was prevented by adding some wet filter paper around the sample and covering the combination with a coverslip.

Confocal microscopy was largely performed on a Zeiss LSM880 system using a 25x glycerol objective. For C3PO we used the following laser and filters; mTurquoise2 – 458 nm laser, 467-500 nm filter, Venus – 514 nm laser, 525-550 nm filter, tdTomato – 561 nm laser, 571-629 nm filter. For PIN3-GFP we used; GFP – 488 nm laser, 501-548 nm filter, chlorophyll – 561 nm laser, 651-704 nm filter Z-stacks were generated and combined into maximum intensity projections for nuclear fluorescence intensity measurements in ICY software (de Chaumont *et al.*, 2012). For PIN3-GFP, mean fluorescence intensity was measured in ICY on all sides of the visible endodermal cells in a single representative Z-layer. ICY was also used to select representative microscopy images and adjust brightness and contrast for improved clarity. Image adjustments were performed the same way between treatments.

For the development of C3PO, confocal microscopy was performed on a Leica SP5II system using a 20x water-immersion objective with the following laser and filters; mTurquoise2 – 458 nm laser, 468-495 nm filter, Venus – 514 nm laser, 524-540 nm filter, tdTomato – 561 nm laser, 571-630 nm filter.

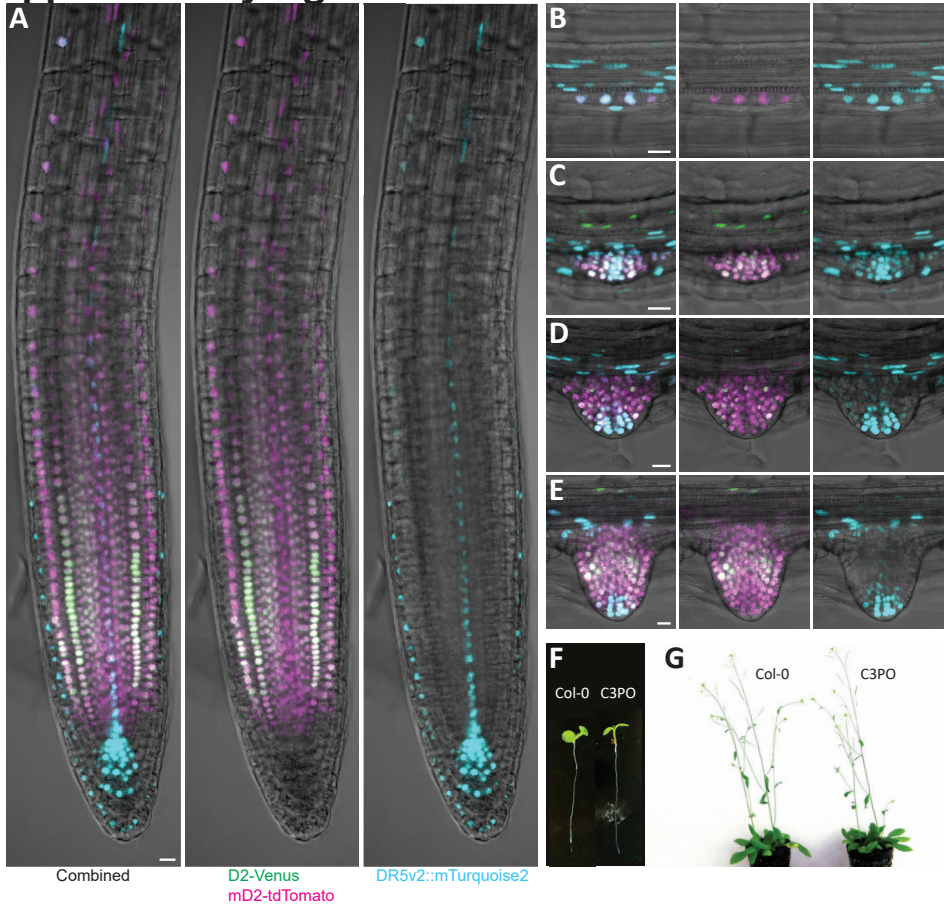
RNA sequencing data analysis

RNA sequencing data analysis was done as described in **Chapter 4**. Only genes with a significant treatment effect in at least one sample were shown ($p < 0.01$, $\log_2FC > 1 / < -1$).

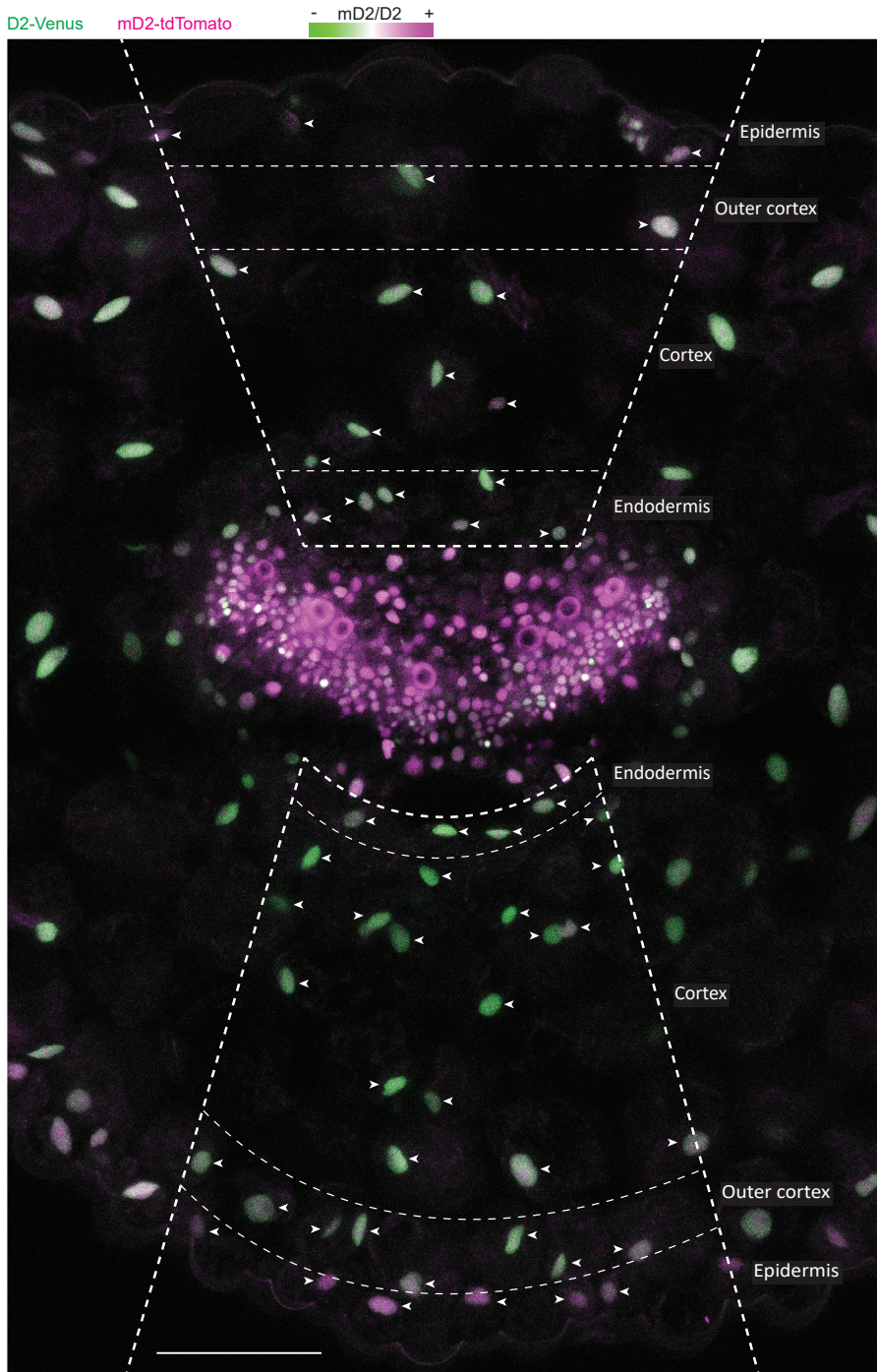
Statistical analyses and data visualisation

Specific details on statistical analyses can be found in the figure legends. In multi-comparison analyses, we performed multi-factorial ANOVA with Tukey's HSD post hoc correction. Elsewhere, we used two-sided t-test with $p < 0.05$ cut-off. Graphs and heatmaps were prepared in R and finetuned in Adobe Illustrator.

Supplementary Figures



Supplementary Figure 5.1. Root fluorescence patterns and plant development in C3PO. (A - E) C3PO fluorescence patterns in the root tip (A), and lateral root primordium at stage I (B), stage IV (C), stage VI (D) and stage VIII (E) of 5 day old seedlings. For each panel, the three images show all fluorophores (left), D2-Venus and mD2-tdTomato (middle) and DR5v2::mTurquoise2 (right). Scale bars represent 10 μ m. (F & G) Plant phenotype of 6 day old seedling (F) and 35 day old flowering plant (G) of Col-0 and C3PO grown in 16 h/8 h light/dark conditions.



◀Supplementary Figure 5.2. Regions used in quantification of C3PO fluorescence in petiole cross-sections. Close-up image of the transverse petiole cross-section of C3PO in WL (Figure 5.2 C), showing D2-Venus and mD2-tdTomato fluorescence. Dashed lines indicate the region and cell types where C3PO fluorescence was imaged. Arrowheads indicate individual nuclei in which fluorescence was measured using Icy image analysis software. Note that in the adaxial epidermis, stomatal fluorescence was not measured. Scale bar represents 100 μm .



Chapter 6

Gibberellin action and BAP/D
module activation are required for
the petiole hyponasty response to
leaf tip-derived auxin

Jesse J. Küpers, Eline Eggermont & Ronald Pierik

*Plant Ecophysiology, Dept. Biology, Utrecht University, 3584CH Utrecht, The
Netherlands*

Abstract

An early response of plants to detection of nearby competitors is adaptive upward leaf movement (hyponasty) that occurs when a plant perceives the neighbour proximity signal of far-red (FR) light enrichment at the leaf tip (FRtip). This growth response requires auxin synthesis in the leaf tip and subsequent auxin transport towards the abaxial petiole base, where cell growth is induced, leading to the differential petiole growth that is required for hyponasty. Transcriptome analysis of plants exposed to FRtip suggested that besides auxin response, synthesis of the growth promoting hormone gibberellin (GA) is also induced in the abaxial petiole. GA signalling occurs through breakdown of DELLA proteins that inhibit the growth-promoting transcription factors BRASSINAZOLE RESISTANT 1 (BZR1), AUXIN RESPONSE FACTOR 6 (ARF6) and PHYTOCHROME INTERACTING FACTOR 4 (PIF4) in the BZR1, ARF6, PIF4 / DELLA (BAP/D) module. Here, we show that GA is required for petiole hyponasty and that GA synthesis genes are induced in the petiole in response to leaf tip-derived auxin. We hypothesise that GA synthesis in the petiole in response to tip-derived auxin allows for the induction of abaxial cell growth by releasing the BAP/D module from their DELLA repressor.

Introduction

To optimise light capture to fuel photosynthesis, plants use the red (R) and far-red (FR)-sensing phytochrome photoreceptors to estimate the severity of light competition with neighbours as well as predict when and where future light competition may occur (Legris *et al.*, 2019). In full sunlight the ratio of R to FR light (R/FR) is high, but this ratio reduces in vegetational shade through specific absorption of R light for photosynthesis and reflection or transmission of non-photosynthetic FR light (Legris *et al.*, 2019). The R/FR is mirrored by phytochrome activity, which is high in full sunlight and decreases with decreasing R/FR. Phytochrome inactivation results in adaptive shade avoidance growth responses that improve the plant's competitive ability by raising the leaves to capture more light (Fraser *et al.*, 2016). In *Arabidopsis*, these shade avoidance growth responses include hypocotyl elongation in seedlings, and petiole elongation and hyponasty in adult plants. It was recently found that FR enrichment at the leaf tip, which simulates neighbour proximity, induces adaptive petiole hyponasty in the FR-sensing leaf (Michaud *et al.*, 2017; Pantazopoulou *et al.*, 2017). The spatial separation between the leaf tip and the bending petiole base suggests long-distance transduction of phytochrome signalling that results in differential growth between the abaxial and adaxial sides of the petiole.

We previously showed that phytochrome inactivation in the leaf tip locally induces auxin synthesis via activation of PHYTOCHROME INTERACTING FACTORS (PIFs) and YUCCAs (Michaud *et al.*, 2017; Pantazopoulou *et al.*, 2017, **Chapter 3**). This auxin is transported to the petiole to induce petiole hyponasty. How non-differential auxin, coming from the leaf tip, could so specifically induce petiole hyponasty through enhanced abaxial cell elongation was investigated in later chapters. In **Chapter 4**, using RNA sequencing, we showed that FR enrichment at the leaf tip induces a strong auxin signal that is primarily activated in the elongating abaxial side of the petiole. In **Chapter 5**, we revealed that leaf tip-derived auxin preferentially accumulates in the abaxial petiole through directed transport via PIN-FORMED 3 (PIN3), PIN4 and PIN7. What remained unknown was how the abaxial auxin signal is translated into the cell elongation required for petiole hyponasty.

In the canonical auxin signalling pathway, auxin stimulates growth by activating target gene expression via stabilisation of AUXIN RESPONSE FACTORS (ARFs, Weijers & Wagner, 2016). To reinforce growth, ARF6 forms a trans-activating transcription factor network together with PIF4 and the brassinosteroid-induced BRASSINAZOLE RESISTANT 1 (BZR1) (Oh *et al.*, 2014). These growth-promoting transcription factors are all repressed by DELLA proteins in what is collectively called the BZR1, ARF6, PIF4 / DELLA (BAP/D) module. The growth-repressing DELLAs are degraded through gibberellin (GA) signalling (Sun, 2010)

and GA has been long known to be important for shade avoidance elongation responses. Its involvement has been particularly well-studied in shade avoidance responses of internode-forming plants such as tobacco (Pierik *et al.*, 2004a), bean (Beall *et al.*, 1996) and cucumber (López-Juez *et al.*, 1995). Gibberellins are also known to regulate shade avoidance responses in *Arabidopsis*, both in seedling hypocotyls and in petioles of adult plants (Hisamatsu *et al.*, 2005; Djakovic-Petrovic *et al.*, 2007; Pierik *et al.*, 2009). These studies showed that some of the *GA20 OXIDASE* GA biosynthesis genes are induced in low R/FR (Hisamatsu *et al.*, 2005) and are associated with degradation of the DELLA protein REPRESSOR OF GA (RGA) (Djakovic-Petrovic *et al.*, 2007; Pierik *et al.*, 2009). However, we are not aware of studies investigating if and how GA would contribute to plant movements in general, or during low R/FR exposure in particular. In our transcriptome survey (**Chapter 4**) we identified an enrichment signature of GA synthesis genes, particularly in the abaxial petiole in response to FR light enrichment of the leaf tip. This prompted us to investigate if and how GA is involved in hyponastic leaf movement in response to localised FR treatment. We reveal that auxin induces GA synthesis-associated genes in the petiole, that DELLA proteins are degraded in the petiole as well, and that GA, together with activity of ARFs and PIFs, is required for petiole hyponasty in response to leaf tip-derived auxin.

Results

Leaf tip-derived auxin requires members of the BAP/D module in the abaxial petiole for hyponasty

As ARFs are the main transcription factors that regulate auxin responsive gene expression and growth (Weijers & Wagner, 2016), we tested their involvement in the petiole hyponasty response to leaf tip-derived auxin. We found that higher order mutant combinations of *ARF6*, *ARF7* (*NON-PHOTOTROPIC HYPOCOTYL 4*, *NPH4*) and *ARF8*, which were previously described to collectively regulate hypocotyl elongation responses (Reed *et al.*, 2018), reduce the hyponastic response to FR enrichment (FRtip) or auxin application to the leaf tip (IAAtip) (Figure 6.1 A). As *ARF6* is one of the growth-promoting members of the BAP/D module, together with *BZR1* and *PIF4* (Oh *et al.*, 2014), we next tested the involvement of PIFs and confirmed our previous finding (**Chapter 3**) that mutation of *PIF4* and *PIF5* reduced the petiole hyponasty response to leaf tip IAA application (IAAtip) (Figure 6.1 B). Mutation of *PIF7*, in wild-type or *pif4 pif5* background, had little to no effect on the responsiveness to IAAtip. To circumvent a putative interaction of *PIF4* and *PIF5*-mutation with auxin transport (Park *et al.*, 2019), we also applied IAA directly to the abaxial petiole of these *pif* mutants and found a similar pattern as when applied remotely on the leaf tip

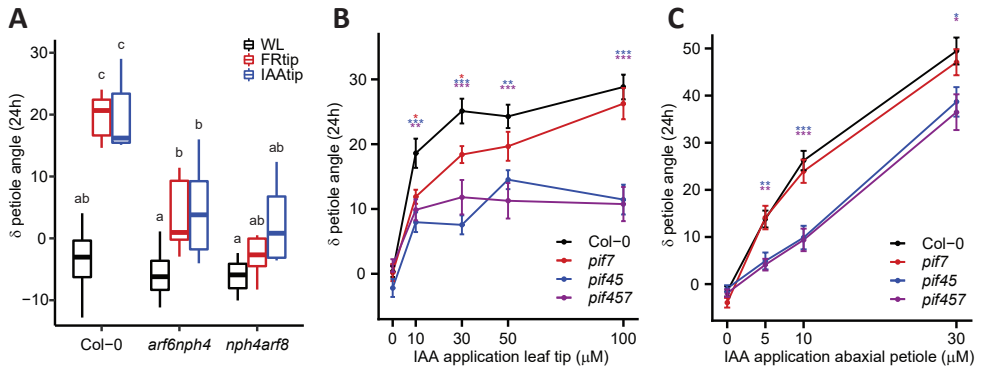


Figure 6.1. Leaf tip-derived auxin stimulates petiole hyponasty through PIFs and ARFs. (A) Petiole angle change after 24h WL, FRtip or IAAtip treatment in Col-0, *arf6 nph4* and *nph4 arf8*. ($n = 7$ biological replicates per treatment group, different letters indicate significant differences, Tukey HSD $p < 0.05$). **(B & C)** Petiole angle change after 24h in Col-0, *pif7*, *pif4 pif5* (*pif45*) and *pif4 pif5 pif7* (*pif457*) treated with different concentrations of IAA or mock to the leaf tip **(B)** and abaxial petiole **(C)**. ($n = 14$ biological replicates per treatment group, coloured asterisks represent significant genotype effect compared to Col-0, *: $p < 0.05$, **: $p < 0.01$, ***: $p < 0.001$, two-sided t-test, data represent mean \pm SEM).

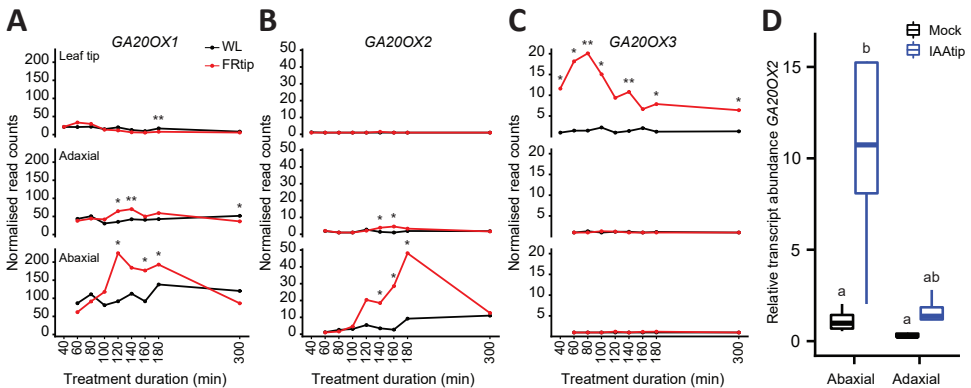


Figure 6.2. Expression of *GA20OX* gibberellin synthesis genes is upregulated in response to leaf tip-derived auxin. (A - C) Expression profiles derived from the RNA sequencing experiment in **Chapter 4** of *GA20OX1* **(A)**, *GA20OX2* **(B)** and *GA20OX3* **(C)** in the leaf tip, adaxial and abaxial petiole during WL and FRtip treatment (asterisks indicate significant treatment effect, *: $p < 0.01$, **: $p < 0.001$, two-sided t-test). **(D)** Relative *GA20OX2* transcript abundance in abaxial and adaxial petiole samples after 2h mock and IAAtip treatments. Relative transcript abundance compared to the abaxial petiole in mock treatment. ($n = 4$ biological replicates, harvested from 8 plants per replicate, different letters indicate significant differences, Tukey HSD $p < 0.05$).

(Figure 6.1 C), confirming that the IAA response, and not IAA transport, is reduced in *pif4 pif5*. As we previously showed that FR-induced expression of *YUCCA* in the leaf tip is entirely PIF7-dependent (Pantazopoulou *et al.*, 2017, **Chapter 3**), we conclude that PIF7 is

required for YUCCA-mediated auxin synthesis in the leaf tip, while PIF4 and PIF5 regulate the auxin response in the petiole as members of the BAP/D module.

Gibberellin synthesis as a downstream target of auxin signalling mediates auxin-induced hyponasty

In addition to the auxin enrichment profiles, our transcriptome analysis showed enrichment for GA synthesis, specifically in the abaxial petiole, where expression of the rate-limiting GA synthesis genes *GA20 OXIDASE 1 (GA20OX1)* and *GA20OX2* was induced (Hedden, 2020; Figure 6.2 A, B). Interestingly, *GA20OX3* expression was mainly induced in the leaf tip (Figure 6.2 C). The abaxial induction of *GA20OX1* and *GA20OX2* expression seems to be a response to tip-derived auxin as similar asymmetric induction of *GA20OX2* was found in response to IAA_{tip} (Figure 6.2 D).

To further test the involvement of *GA20OX* genes we performed mutant analysis and found that the single mutants *ga20ox1* and *ga20ox2* showed reduced hyponastic responses to FR_{tip}, and the *ga20ox1 ga20ox2* double mutant lacked all petiole hyponasty (Figure 6.3 A). When we alleviated the gibberellin deficiency by GA application to the petiole, the hyponastic response to FR_{tip} was restored in *ga20ox1 ga20ox2* (Figure 6.3 B). Consistent with these mutant data, paclobutrazol (PAC) pre-treatment, which blocks GA biosynthesis, also inhibited the hyponastic response to FR_{tip} and this could again be rescued by exogenous GA application to the petiole (Figure 6.3 C). Thus, locally restoring GA deficiency in the petiole rescued FR_{tip}-induced hyponasty in otherwise GA deficient plants, suggesting that GA is needed in the petiole itself, and that it is induced via auxin coming from the leaf tip. Consistently, IAA_{tip} treatment did also not induce hyponasty in the GA-deficient *ga20ox1 ga20ox2* mutant (Figure 6.3 D). Interestingly, GA application to the leaf tip, rather than the petiole, stimulated hyponasty in both wild type and *ga20ox1 ga20ox2* without additional FR (Figure 6.3 E), implying that GA perhaps not only acts locally but also remotely to promote differential petiole growth.

We next decided to investigate whether GA signalling through DELLA degradation in the petiole is required for FR_{tip}-induced petiole hyponasty. We tested the global (pentuple) DELLA knockout mutant *dellaP*. Although leaf angles were constitutively high in *dellaP*, FR_{tip} and IAA_{tip} still induced further petiole hyponasty, resulting in nearly vertical leaves (Figure 6.4 A, B). When we studied DELLA abundance using the representative DELLA reporter *pRGA::GFP-RGA*, we observed RGA degradation in both sides of the petiole upon

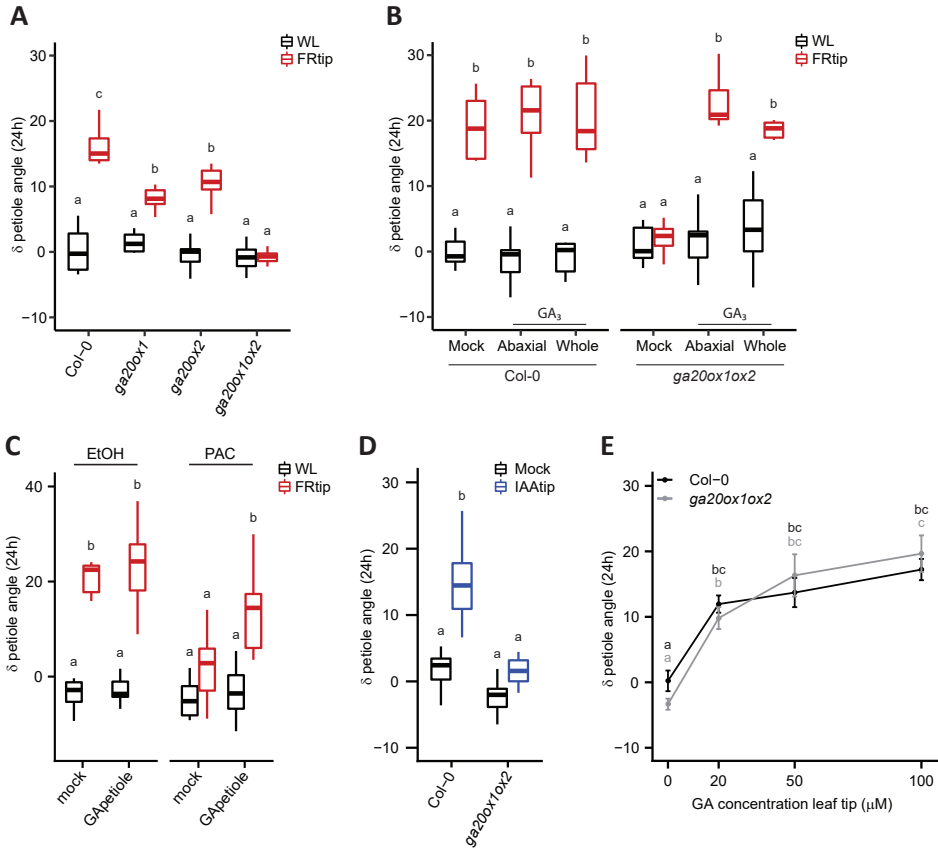


Figure 6.3. Gibberellin synthesis is required for the petiole hyponasty response to leaf tip-derived auxin. (A) Petiole angle change after 24h WL or FRtip treatment in Col-0, *ga20ox1*, *ga20ox2* and *ga20ox1 ga20ox2* (*ga20ox1ox2*). ($n = 9$ biological replicates per treatment group, different letters indicate significant differences, Tukey HSD $p < 0.05$). (B) Petiole angle change after 24h light treatment in Col-0 and *ga20ox1 ga20ox2* combined with 50 μM GA_3 or mock application to the petiole. When GA_3 was applied to the abaxial side of the petiole, the adaxial side was mock treated. ($n = 7$ biological replicates per treatment group, different letters indicate significant differences, Tukey HSD $p < 0.05$). (C) Petiole angle change after 24 h in mock or PAC pre-treated Col-0 plants treated with WL or FRtip and mock or 50 μM GA_3 to the abaxial petiole. ($n = 7$ biological replicates per treatment group, different letters indicate significant differences, Tukey HSD $p < 0.05$). (D) Petiole angle change after 24h mock or IAA:tip treatment in Col-0 and *ga20ox1 ga20ox2*. ($n = 10$ biological replicates per treatment group, different letters indicate significant differences, Tukey HSD $p < 0.05$). (E) Petiole angle change in Col-0 and *ga20ox1 ga20ox2* after 24 h mock or different concentrations of GA_3 treatment to the leaf tip. ($n = 7$ biological replicates per treatment group, different letters indicate significant differences with colours representing the corresponding genotype, Tukey HSD $p < 0.05$, data represent mean \pm SEM).

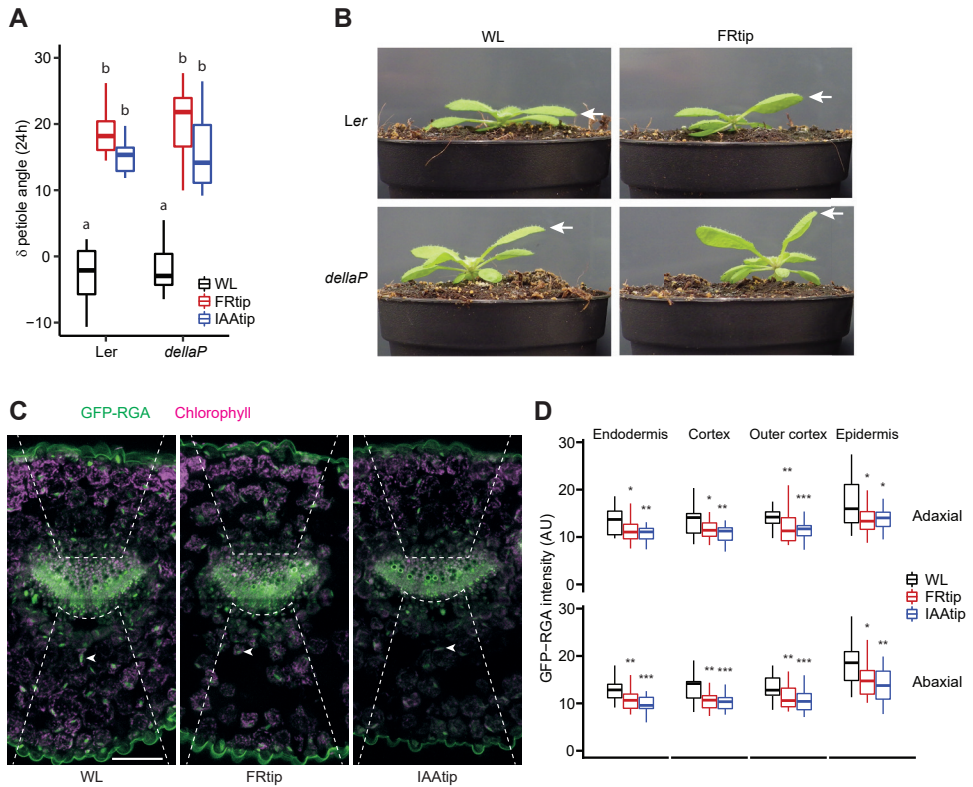


Figure 6.4. Involvement and degradation of DELLA proteins in the petiole hyponasty response to leaf tip-derived auxin. (A) Petiole angle change after 24h WL, FRtip or IAAtip treatment in *Ler* and *dellaP*. ($n = 7$ biological replicates per treatment group, different letters indicate significant differences, Tukey HSD $p < 0.05$). **(B)** Representative images of *Ler* and *dellaP* after 24 h in WL and FRtip. The leaf of interest is indicated with the arrows. **(C & D)** Representative images **(C)** and quantification **(D)** of GFP-RGA fluorescence in the petiole base. Plants were treated for 7h with mock, FRtip or IAAtip. ($n = 24$ samples per treatment, asterisks represent significant treatment effect compared to WL, *: $p < 0.05$, **: $p < 0.01$, ***: $p < 0.001$, two-sided t-test). Scale bar in **C** represent $100 \mu\text{m}$, dashed lines indicate the abaxial and adaxial regions where nuclear GFP signal was quantified, arrowheads point out an individual nucleus in the abaxial cortex in each image.

FRtip and IAAtip (Figure 6.4 C, D). RGA degradation was not tissue-specific but was observed for all tissues layers investigated, from endodermis to epidermis (Figure 6.4 C, D). These data together indicate that GA response in the petiole increases upon leaf tip-derived auxin and that GA is required to achieve petiole hyponasty.

Discussion

In this chapter, we show that GA functions in leaf hyponasty to permit auxin-induced differential petiole growth upon FR enrichment at the leaf tip. We postulate a controlling role for GA in the activation of the BAP/D module of interacting, growth-promoting transcription factors in the petiole. In our transcriptome analysis in **Chapter 4**, we revealed that far-red light enrichment at the leaf tip induces a rapid auxin response in the abaxial petiole, that also stimulates expression of *GA20OX* GA synthesis genes.

Upregulation of *GA20OX* expression during shade and auxin-induced growth was previously shown (Hisamatsu *et al.*, 2005; Frigerio *et al.*, 2006). However, it was not known that these genes are also responsive to remote FR or IAA signalling, and are required for the induction of petiole hyponasty in response to leaf tip-derived auxin. We observed that tip-derived auxin stimulates *GA20OX1* and *GA20OX2* expression in the growing abaxial petiole, suggesting local induction of GA biosynthesis (Figure 6.2). We also observed that a GA target, the growth-repressing DELLA protein RGA, is degraded upon these treatments (6.4C, D). In contrast to the specifically abaxial auxin accumulation and *GA20OX* expression, RGA degradation occurred non-specifically on both sides of the petiole (Figure 6.4 C, D). This implies that there would be abaxial-adaxial GA transport or diffusion that would result in non-differential GA signalling in the petiole in response to FRtip. Indeed, when we applied GA to both sides of the petiole in the GA-deficient, *ga20ox1 ga20ox2* mutant that is not responsive to FRtip, we found that the hyponastic response to FRtip was rescued in a similar manner compared to when GA was applied only to the abaxial side (Figure 6.3 B). Moreover, we found that GA application to the petiole in WL did not by itself affect petiole angles. In addition, in the *dellaP* mutant background, where GA signalling is highly active, tip-derived auxin still induced further hyponasty in response to tip-derived auxin (Figure 6.4 A, B), suggesting that GA signalling by itself does not induce maximal hyponasty. In conclusion, we propose that GA abundance and DELLA degradation in the petiole are required to allow for petiole cell growth, while the specifically abaxial auxin accumulation provides the directional cue that ensures differential petiole growth resulting in petiole hyponasty.

In contrast with *GA20OX1* and *GA20OX2*, a third member of the family *GA20OX3* was strongly induced specifically in the leaf tip by FRtip treatment (Figure 6.2 C). Our described mechanism for auxin-induced GA synthesis in the petiole via *GA20OX1* and *GA20OX2*, does not exclude the possibility that GA derived from the leaf tip would also be transported towards the petiole to enhance petiole hyponasty. Indeed, when we applied GA to the leaf tip in WL, this resulted in petiole hyponasty in both wild type and *ga20ox1 ga20ox2*

(Figure 6.3 E). Keeping in mind that GA treatment of the petiole does not stimulate petiole hyponasty in WL (Figure 6.3 B), it apparently makes an important difference if GA increases locally in the petiole, or remotely in the leaf tip. It is likely that GA treatment of the leaf tip would locally degrade DELLAs in the leaf tip. As DELLA degradation prevents their inhibition of various growth-promoting transcription factors, including PIFs (de Lucas *et al.*, 2008; Feng *et al.*, 2008), this would likely enhance PIF activity, which could promote auxin synthesis in the leaf tip, and this could then be transported towards the abaxial petiole to induce differential growth. In addition, GA might also be transported from the leaf tip to the petiole, but this by itself would not suffice to induce hyponasty as indicated by the local GA applications to the petiole (Figure 6.3 B), indicating that any putative movement of GA from tip to base, would also need auxin to be transported from tip to base in order to induce hyponasty. This is supported by the following observations: GA treatment of the leaf tip of the *ga20ox1 ga20ox2* mutant does induce hyponasty (Figure 6.3 E), putatively through increased IAA synthesis in the leaf tip, while IAA application to the leaf tip of these *ga20ox1 ga20ox2* mutants does not induce hyponasty (Figure 6.3 D). If we assume that indeed GA application to the leaf tip promotes leaf tip auxin synthesis, then the difference between the GA and IAA application is that in the GA application both IAA and GA are elevated in the tip, both hormones could then be transported to the petiole base, providing the auxin-derived positional information and the GA-dependent relieve of growth-restraint, together inducing hyponastic leaf movement.

Gibberellin signalling stimulates growth by activating the growth-promoting transcription factors of the BAP/D module, through removal of the repressive DELLAs (Oh *et al.*, 2014). Using mutant analysis, we found functional requirement for ARF6, ARF7 and ARF8, as well as PIF4 and PIF5 for the petiole hyponasty response to auxin and FR (Figure 6.1). In addition, we observed transcriptional activation of BR signalling in the petiole (**Chapter 4**). Our findings suggest that activation of the BAP/D module is required for auxin-mediated petiole hyponasty. It remains to be studied whether the specific members and interactions in the BAP/D module are the same in adult petioles as in seedling hypocotyls (Oh *et al.*, 2014). Over the last decade, a complex network of direct and indirect interactions of various photoreceptors with each of the growth-promoting members of the BAP/D module has been revealed (Hornitschek *et al.*, 2012; Li *et al.*, 2012; Hersch *et al.*, 2014; Pedmale *et al.*, 2016; Yang *et al.*, 2018; Wang *et al.*, 2018; Xu *et al.*, 2018; Dong *et al.*, 2019; He *et al.*, 2019; Mao *et al.*, 2020; reviewed in Küpers *et al.*, 2020, **Chapter 2**). In general, light-activated photoreceptors are shown to inhibit the growth-inducing activity of these transcription factors. To functionally validate this multitude of interactions, local

seedling studies could be combined with studies using our long-distance FRtip and IAAtip treatments as well as the local petiole elongation-inducing FR treatment of the petiole (**Chapter 3**).

Acknowledgements

We would like to thank Yasmin Salvatore for performing preliminary petiole hyponasty experiments.

Materials and Methods

Plant material and growth conditions

Genotypes used in this chapter: *ga20ox1-3, ga20ox2-1, ga20ox1-3 ga20ox2-1* (Rieu *et al.*, 2008), *arf6-2 nph4-1, nph4-1 arf8-3* (Reed *et al.*, 2018), *pif4-101 pif5-1* (Lorrain *et al.*, 2008), *pif7-1* (Leivar *et al.*, 2008) and *pif4-101 pif5-1 pif7-1* (de Wit *et al.*, 2015) were all in Col-0 background; *dellaP* (Feng *et al.*, 2008) and *pRGA::GFP-RGA* (Silverstone *et al.*, 2001) were in *Ler* background.

Seeds were sown on Primasta soil or agarose plates for germination and cold stratified for three days before transfer to short day white light (WL) conditions light/dark 9 h/15 h, 20 °C, 70 % humidity, 130-150 $\mu\text{M m}^{-2} \text{s}^{-1}$ PAR. Around eight days after germination, individual seedlings were transplanted to 70 mL round pots containing Primasta soil.

For all experiments, 28 days old plants were selected based on homogeneous development and the presence of a ~5 mm petiole on the 5th youngest leaf which would be used in the experiment. All experiments were started at 10:00 A.M. (ZT2). For phenotyping experiments, petiole angle before treatment and after 24 hours was determined in ImageJ using digital images taken from the side.

Light and pharmacological treatments

For FRtip light treatment, WL was supplemented with FR using EPITEX L730-06AU FR LEDs. These FR LEDs had peak emission at 730nm and locally reduced R/FR from ~2.0 in WL to below 0.1 in FRtip. For pharmacological treatments at the leaf tip, 5 μL solution was pipetted onto the leaf tip. IAA was provided at a standard concentration of 30 μM for IAAtip treatments. Pharmacological solutions and mocks for leaf tip application contained DMSO for IAA (0.03 %) or EtOH for GA_3 (0.05-0.1 %) as well as Tween-20 (0.1 %). For hormone application to the petiole, concentrated stocks were diluted in lanolin (95-97 %

lanolin, 0.03 % DMSO for IAA, 0.05 % EtOH for GA₃). The lanolin containing solutions were carefully applied to the petiole using a tooth pick. Paclobutrazol (PAC) pre-treatment was done two times at ten and five days before the experiment started. On both days, 20 mL 100 µM PAC or mock (0.3 % EtOH) was provided to the soil of each individual pot.

RNA isolation and RT-qPCR

RNA isolation and RT-qPCR were performed as described in **Chapter 3**. A total of 4 biological replicates were harvested from 8 plants per replicate of which the basal two-thirds of the leaf of interest was separated into an abaxial and adaxial sample as indicated in Figure 4.1. RT-qPCR primers can be found in Appendix 1.

Confocal microscopy

Confocal microscopy and data analysis on transverse GFP-RGA petiole cross-sections was performed as described in **Chapter 5** using the following lasers and filters; GFP – 488 nm laser, 510-525 nm filter, chlorophyll – 561 nm laser, 641-691 nm filter.

RNA sequencing data analysis

RNA sequencing data analysis was done as described in **Chapter 4**.

Statistical analyses and data visualisation

Specific details on statistical analyses can be found in the figure legends. In multi-comparison analyses, we performed multi-factorial ANOVA with Tukey's HSD post hoc correction. Elsewhere, we used two-sided t-test with $p < 0.05$ cut-off. Graphs were prepared in R and finetuned in Adobe Illustrator.



Chapter 7

Transient early weed competition reduces maize development and yield

Jesse J. Küpers, Pien de Wolff & Ronald Pierik

Plant Ecophysiology, Dept. Biology, Utrecht University, 3584CH Utrecht, The Netherlands

Abstract

Weeds are a major cause of worldwide losses of crop yield. Ongoing regulations continue to restrict herbicide usage, which means that crops may face greater competition by weeds. The yield of maize (*Zea mays*) is mainly reduced by weeds that occur during early plant growth, when the crop is still small and may be outgrown by the weeds. We performed a greenhouse experiment to study the effect of light competition by weeds during early development on later growth, development and yield in maize. We found that early light competition with weeds distorts early developmental parameters and that this is strongly correlated with final yield. We show that of these developmental parameters, the stem diameter, which is reduced in the presence of weeds and increased in lower crop density, correlates most strongly with final plant and ear dry weight.

Introduction

The world's population is expected to grow to around 9.7 billion people in 2050 (Binns *et al.*, 2020). This growing human population requires ever-increasing global food production. Simultaneously, the various and wide-spread effects of climate change reduce the amount of potentially arable land. Moreover, biodiversity is also being reduced as ever-more land is converted into crop fields to sustain the increasing food demands. Besides making efforts within the global food chain to change towards more plant-based diets, reduce food waste and spoilage and reverse the effects of climate change, improving crop productivity will help to sustainably feed the future world (Binns *et al.*, 2020).

Regarding worldwide agricultural land use, maize (*Zea mays*) farming is second only to wheat according to FAOSTAT (<https://www.fao.org/faostat/>). Increasing the sowing density of maize may increase yield per unit area (Marín & Weiner, 2014), but this cannot be taken too far because beyond a critical density intraspecific light competition will increase the risk of plant lodging (Shi *et al.*, 2016; Xue *et al.*, 2017). During early maize development, the relatively large spaces between maize seedlings, especially between the rows in the standard fields, provides ample growth opportunity for weeds, which can strongly reduce crop yield (Subedi & Ma, 2009). In addition, increased future regulation of herbicide usage combined with the occurrence of herbicide-resistant weeds provides new challenges in weed control (Westwood *et al.*, 2018; Kudsk & Mathiassen, 2020), making it important to develop more weed-resistant crops.

Maize rapidly responds to weeds when it perceives a relative enrichment of far-red (FR) light that is reflected from leaves and provides an early neighbour proximity signal (Ballaré *et al.*, 1990). In most young maize cultivars, perception of FR enrichment from nearby weeds leads to shade avoidance growth responses that include shoot elongation, which brings the maize leaves higher towards the sunlight but could also foster light penetration through the field, onto the weeds (Liu *et al.*, 2009; Page *et al.*, 2009; Shi *et al.*, 2019). A recent study in *Arabidopsis* indeed showed that inhibition of such shade avoidance responses can help prevent light penetration to the soil level where weeds would establish and grow (Pantazopoulou *et al.*, 2021). Although beneficial for plant survival, this early elongation growth response to outgrow weeds distorts later growth and development and leads to reduced yield (Liu *et al.*, 2009; Page *et al.*, 2009, 2012).

In this chapter, we investigate the effect of early neighbour detection through FR light signalling on the development and yield of three maize genotypes. We found that an early reduction in maize stem diameter negatively correlates with further development and final yield.

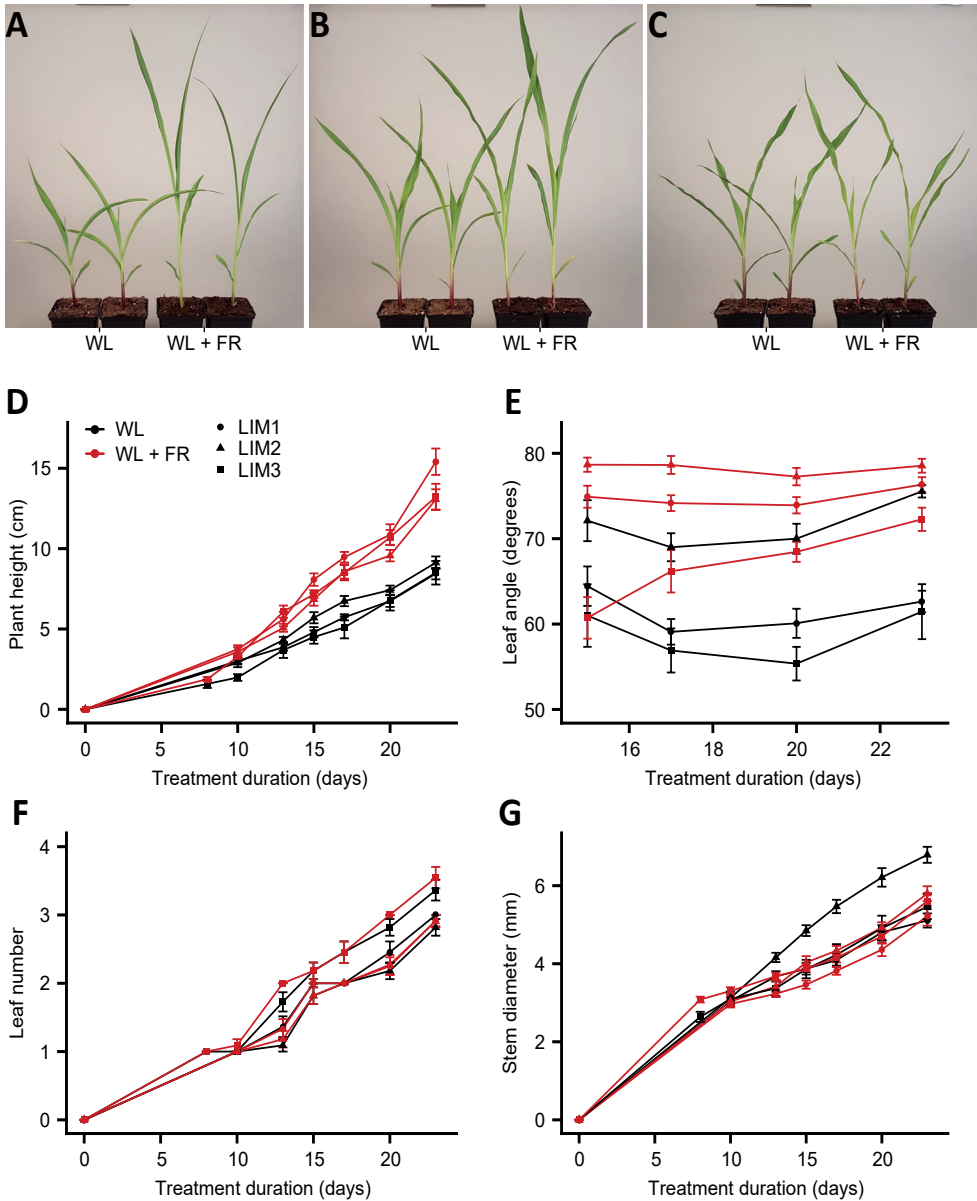


Figure 7.1. Three maize genotypes show adaptive growth responses to FR enrichment. (A - C) Representative pictures of LIM1 (A), LIM2 (B) and LIM3 (C) after 23 days of growth in a climate room in WL and WL + FR. **(D - G)** Plant height (D), leaf angle of the youngest developed leaf (E), leaf number (F) and stem diameter (G) of the three genotypes during the first 23 days of growth in WL and WL + FR. $n = 12$, error bars represent SEM.

Results

FR enrichment induces shade avoidance growth in maize

Three different maize inbred lines (LIM1-3, hereafter called genotypes) were selected to determine the response to FR enrichment in climate room conditions. The genotypes showed variation in growth phenotype in white light (WL) control conditions (Figure 7.1 A-C). When exposed to FR enrichment in WL background (WL + FR) during the first 23 days of treatment, plant height and leaf angle increased in all genotypes, while leaf number was unaffected (Figure 7.1 D-F, Table 7.1). A clear difference between the genotypes was found in stem diameter, which was reduced by FR in LIM1, but not in LIM2 and LIM3 (Figure 7.1 G, Table 7.1).

Table 7.1. ANOVA determined effects of treatment and time of development on plant height, leaf angle, leaf number and stem diameter in three maize genotypes. $n = 12$, asterisks indicate significant main or interaction effects of the two-way ANOVA, performed per genotype and growth parameter (*: $p < 0.05$, ***: $p < 0.001$).

	Height			Leaf angle			Leaf number			Diameter		
	LIM1	LIM2	LIM3	LIM1	LIM2	LIM3	LIM1	LIM2	LIM3	LIM1	LIM2	LIM3
Treatment	***	***	***	***	***	***	ns	ns	ns	ns	***	ns
Time	***	***	***	ns	ns	*	***	***	***	***	***	***
Treatment*Time	***	***	***	ns	ns	*	ns	ns	ns	ns	***	ns

Early neighbour detection reduces maize development and final yield

Based on these findings, a larger next experiment was designed to assess the effect of FR enrichment during the first 23 days after sowing on development and yield of the three genotypes (Figure 7.2 A, B). The three genotypes were grown in a greenhouse in control and three different treatments. In the FR enrichment treatment, a combination of a green and white filter was used to mimic FR light reflection by weeds (Figure 7.2 B). It is important to note that besides FR, the green filter also reflected a large portion of the green and yellow light in the 475-600 nm range (Figure 7.2 C).

In the weeds treatment, the mustard mizuna (*Brassica juncea* subsp. *integrifolia* var. *japonica*) was sown at a density of around 2000 seeds per m^2 around the maize plants. To prevent excessive light competition, the mizuna plants were trimmed back around the maize plants when they threatened to outgrow the maize. Light spectrum measurement revealed that this primarily led to reflection of FR light, with a much lower peak in the green light range than occurred in the FR enrichment treatment (Figure 7.2 C). All maize

plots of plants were surrounded by border plants of another maize genotype to buffer against edge effects. Lastly, a low density control was taken along in which the plants grew at one third of the regular planting density (Figure 7.2 A). After 23 days, the weeds and FR enrichment filter were removed and plants continued growing in control conditions.

At the end of the 23-day treatment, the presence of the weeds had caused a mild reduction in height in LIM2 and LIM3, and the FR enrichment had reduced plant height in LIM3 (Figure 7.3 A). At later timepoints, the plants that experienced early weeds remained shorter than control plants in all genotypes. FR-enriched plants also showed a, slightly, reduced overall plant height during the first 56 days of growth, which was recovered to control levels at later stages in LIM1 and LIM2. Interestingly, the plants grown at low density grew similarly tall as control at first, but growth in the low density slowed down relative to control in LIM2 and LIM3 after the first 56 days.

As another important factor of plant development, the number of leaves was measured over time (Figure 7.3 B). Both the weeds and FR enrichment caused an early reduction in leaf number, that persisted throughout the experiment and was strongest in the weeds treatment. Thus even long after the weeds and FR-enriching filters were removed, there was still a significant effect on rate of development. Low density grown plants developed leaves more quickly during the intermediate stage of development in LIM1 and LIM2 but had a similar number of leaves in all genotypes at the end of the growth period.

The most drastic and persistent treatment effects on plant development were found when regarding stem diameter (Figure 7.3 C). In all three genotypes, weeds caused an early and persistent reduction in stem diameter. FR enrichment caused an early reduction in stem diameter, but this was recovered after 43 days. At the same 43 day timepoint, plants grown in low density started to grow much thicker stems than in control. At the end of the experiment, there was large variation in stem diameter between the treatments in all three genotypes.

Besides reducing plant growth and development, the early presence of weeds also reduced final plant dry weight (DW) in all genotypes (Figure 7.4 A). In addition, the separately analysed dry weight of the ear (also known as the cob) was also reduced by weeds in LIM1 and LIM3 (Figure 7.4 B). Despite having some small effects on plant development, the FR enrichment did not affect final yield parameters. In contrast, the plants grown in low density had much higher individual yield than the control, regarding both plant and ear dry weight.

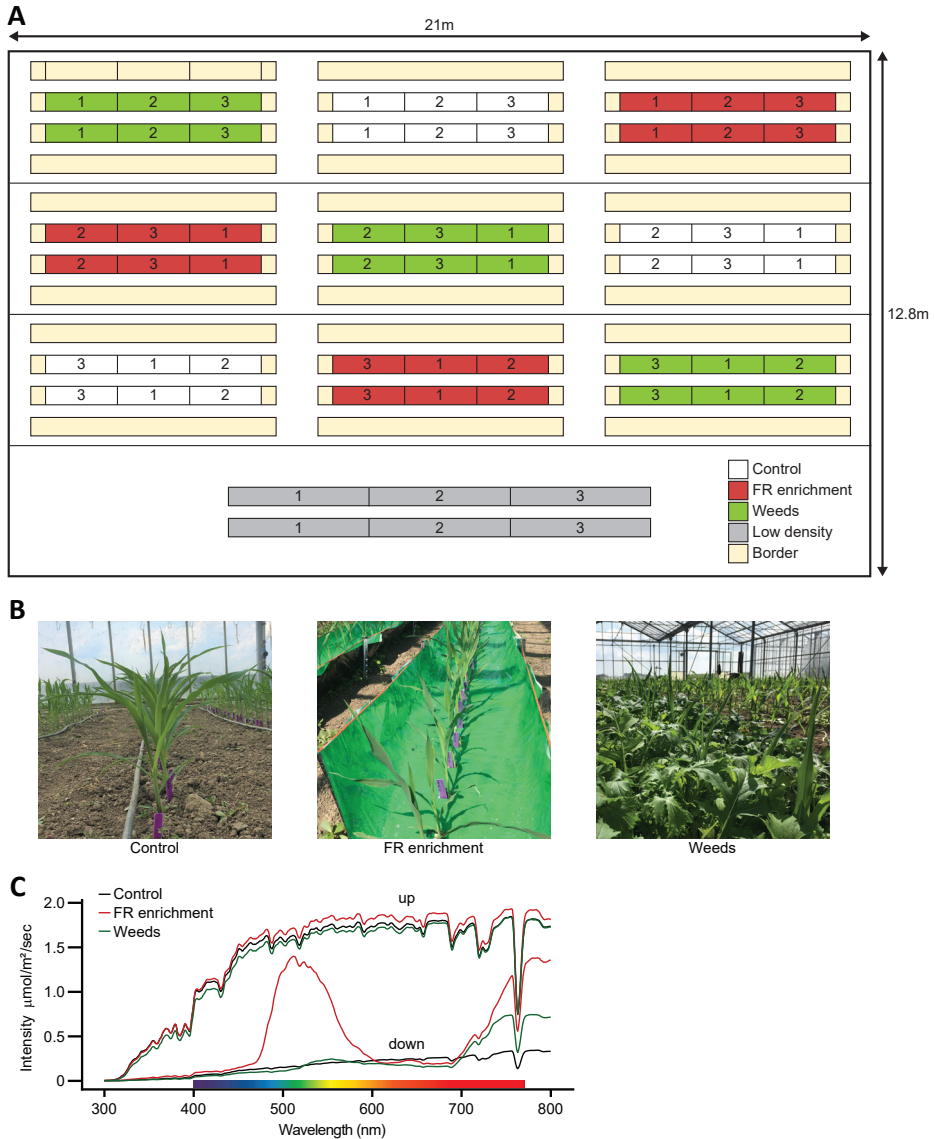


Figure 7.2. Description of design and treatments used in the greenhouse experiment. (A) Schematic representation of the distribution of treatments and genotypes (1: LIM1, 2: LIM2, 3: LIM3) over the greenhouse. **(B)** Representative photographs of plant growth after 22 days in control, FR and weeds conditions. **(C)** Representative light spectra measured upwards and downwards (pointing towards soil, filter or weeds) after 21 days in control, FR enrichment and weeds treatment.

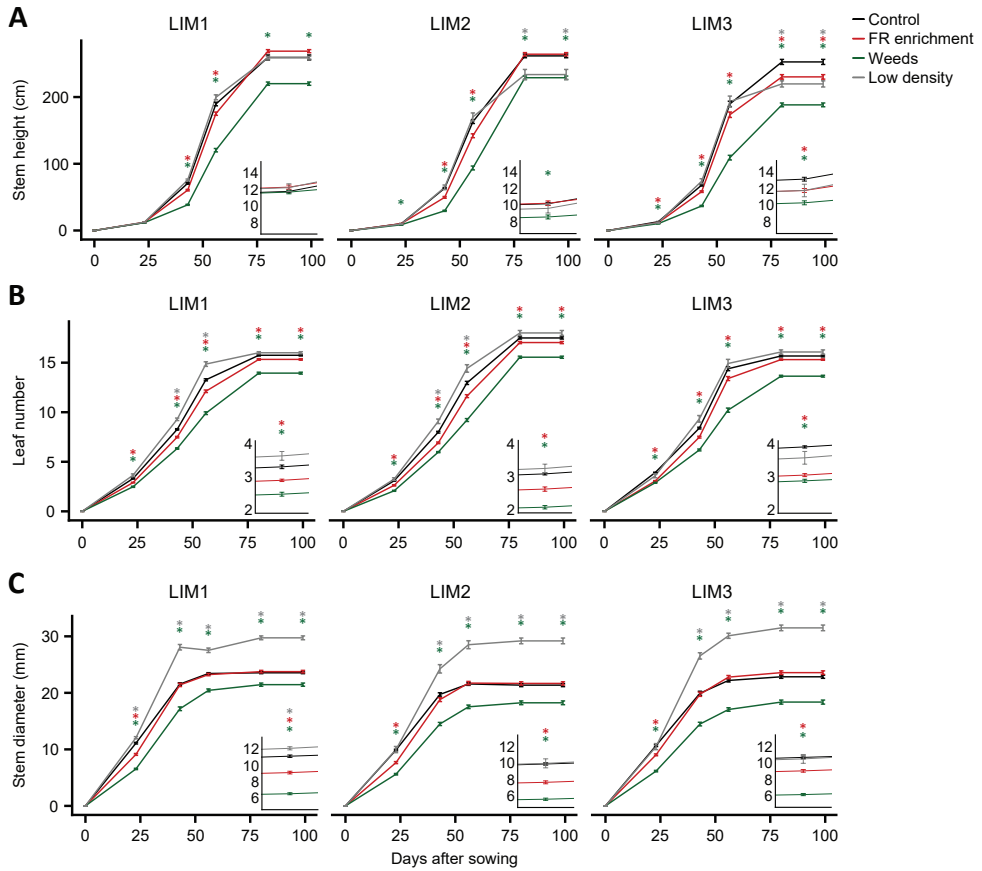


Figure 7.3. Early light competition slows down maize development. (A - C) Development over time of stem height (A), leaf number (B) and stem diameter (C) of the three genotypes in the indicated treatments. FR-enrichment and weeds treatments occurred during the first 22 days of growth and were removed afterwards. Inset graphs show a zoomed-in view of the corresponding graphs at 23 days after sowing. Coloured asterisks indicate significant treatment difference from control calculated per timepoint, Dunnett's test ($p < 0.01$), error bars represent SEM. Genotype name is indicated above each of the plots.

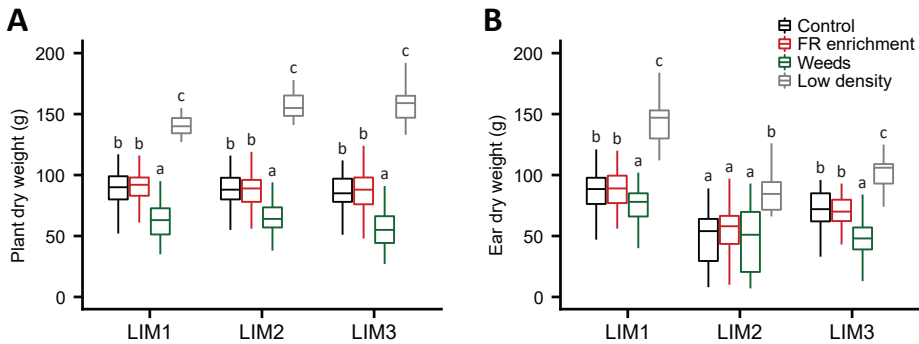


Figure 7.4. Light competition with weeds and neighbours reduces maize yield. (A & B) Final plant (A) and ear (B) dry weight per plant in the indicated treatments. Different letters indicate significant difference between treatments, calculated per genotype, according to two-way ANOVA + Tukey ($p < 0.01$). Genotype name is indicated on the x-axis.

Early reduction in stem diameter correlates with reduced yield

Using a correlation analysis, we verified if the overall variation in development is correlated with variation in yield (Figure 7.5 A). We observed that developmental parameters over time were correlated with each other as well as with the final yield. Positive correlations were found within and between the different tested parameters. Although plant height and leaf number both showed a significant positive correlation with plant and ear dry weight, the strongest and most consistent correlation with yield was found for stem diameter. In addition, there was a strong correlation between early stem diameter and later plant height and leaf number. Separate correlation analysis per genotype revealed that, among the tested developmental parameters, diameter again correlated most strongly with yield in each of the three genotypes (Figure 7.5 B).

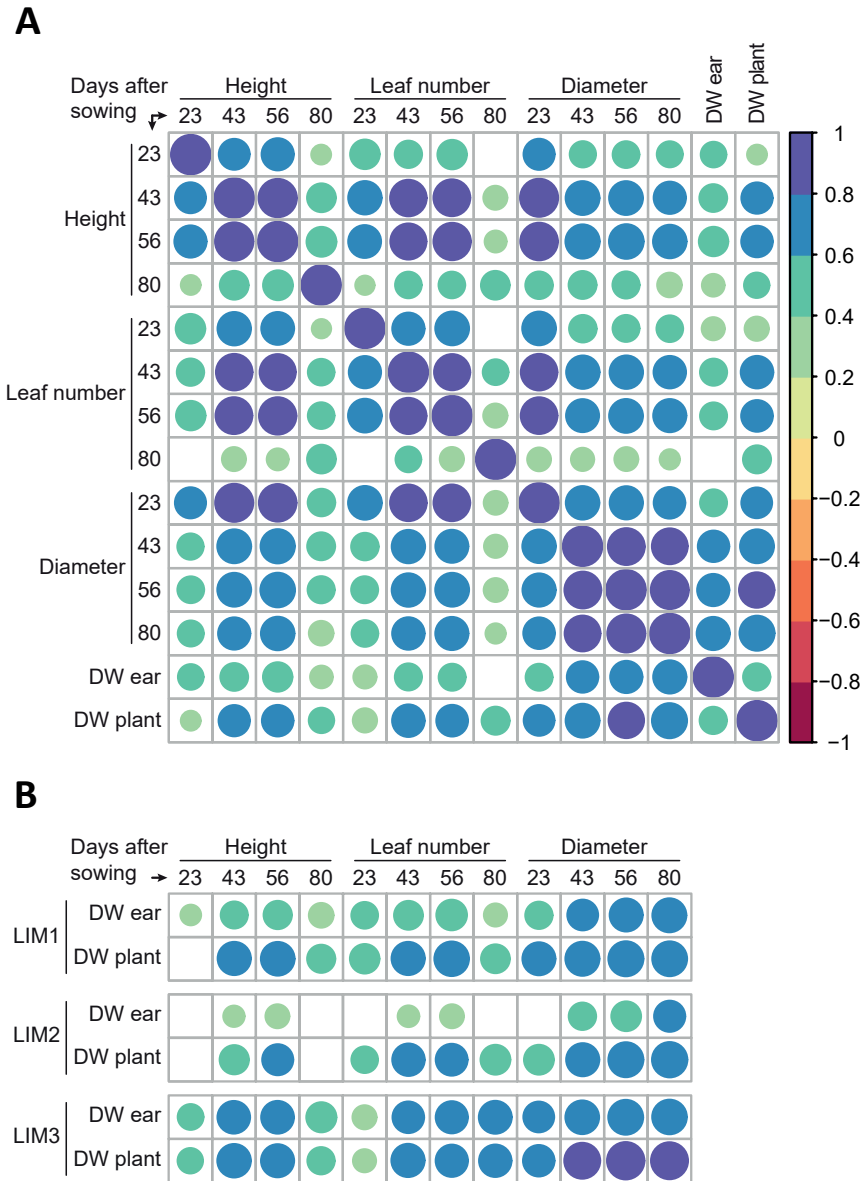


Figure 7.5. Correlation analysis of maize development and yield parameters. Pearson correlation analysis between developmental parameters and final yield. Correlation was performed using data derived from all four treatments (control, FR enrichment, weeds and low density) and all three genotypes (A) or separate per genotype (B). Colours represent direction and strength of the correlation, size also represents the strength of the correlation. Numbers on the axes represent measurement day (days after sowing). Non-significant correlations ($p < 0.001$) are indicated as empty cells.

Discussion

In maize farming, light competition by weeds, especially during early development, is an important yield-limiting factor (Liu *et al.*, 2009; Page *et al.*, 2009, 2012). In this chapter, we found that the presence of weeds during early growth, strongly reduces development and yield of three tested maize genotypes (Figure 7.3, 7.4). We found that early stem diameter, which was reduced by FR enrichment and weeds, had a strong positive correlation with later development regarding plant height and leaf number as well as final yield (Figure 7.5). The plants that were grown at the reduced density had thicker stems than under control conditions in all genotypes when measured 43 days after sowing, but only in genotype A at 23 days after sowing (Figure 7.3). This suggests that in this time period, the presence of nearby maize plants in control conditions reduced stem thickness compared to plants grown at low density. The observed positive correlation could indicate that thick stems are required for further development and yield. A functional explanation of this finding could be that thick stems contain more vascular bundles, or wider vascular channels through which water, nutrients and assimilates can be transported between source and sink tissues (Shi *et al.*, 2016). In addition, thicker stems are stronger than thinner stems, which can help prevent lodging and the associated loss of light capture in excessively tall plants (Shi *et al.*, 2016). The relatively mild reduction in stem diameter that was observed in FR-enriched plants did not coincide with reduced yield (Figure 7.3, 7.4). This suggests that a mild reduction in stem diameter had no persistent effects.

As mentioned above, plants grown at reduced density perform better, in terms of dry weight and yield, than those at the regular control density. Although this may suggest that a lower density would be preferable over the standard density that is practised in European agriculture, this is not the case. While the individual plants at lower density yielded about 50 % more than in the control density (Figure 7.4 A, B), this does not make up for the two-thirds reduction in number of individuals per square meter. In other words, yield per unit area of land is still substantially higher in the standard control density than in the low density and the optimal crop density is found when the maximal yield per unit area is achieved.

Although designed to mimic light reflected by weeds growing around the plants, the reflected light spectrum in our green filter setup that was used for FR enrichment was still different from the light that was actually reflected in the weeds treatment (Figure 7.2 C). The peak in reflection of light in the 475-600 nm range (primarily green and yellow) we observed using the FR-enriching filter could to some extent power photosynthesis and light signalling (Smith *et al.*, 2017), and was hardly observed in light reflected from weeds.

In addition, the amount of FR that was reflected in the FR-enrichment treatment was also higher than in the weeds treatment. The relative rich abundance of photosynthetically active light in the green filter reflection may (partially) explain why this treatment was less severely affecting long-term maize performance than the actual weed treatment over the same time period.

Other explanations, such as competition for water, nutrients and light between maize and weeds could also play a role, although we tried to limit such effects by growing the plants on nutrient-rich and well-watered soil and trimming the weeds back when they grew too tall. Other neighbour detection signals that are used by plants including leaf touching (de Wit *et al.*, 2012) and ethylene signalling (Pierik *et al.*, 2004b), could also explain part of the difference between the two treatments.

A well-described response to neighbour detection is stem elongation (Ballaré & Pierik, 2017). While we found a quick and persistent increase of stem height by additional FR treatment in a climate room experiment (Figure 7.1 D), this was not found after the 23 day FR-enrichment or weeds treatment in the greenhouse experiment (Figure 7.3 A). Other greenhouse studies have revealed that the presence of weeds leads to an increase in maize height early after emergence, which disappears at later stages of development (Liu *et al.*, 2009; Page *et al.*, 2009). A similar early growth response might have occurred in our greenhouse experiment prior to the first measuring timepoint. The different FR-enrichment responses observed between the two growing conditions can also be related to differences in environmental signals between the systems. Plants need to optimise their growth in response to the complex integration of light signals such as intensity, spectral distribution and daylength with environmental signals such as temperature, drought, salinity and pests (Courbier & Pierik, 2019).

Here we discussed how light signals derived from weeds and neighbours affect shoot architecture and yield of maize. To increase collective light capture and yield in weedy fields, suppressing weed growth is crucial. Changing sowing patterns from rows that have short distances between plants within rows and larger distance between rows towards a more uniform pattern in combination with optimizing sowing density can help suppress weeds by accelerating canopy closure (Weiner *et al.*, 2010; Marín & Weiner, 2014; Pantazopoulou *et al.*, 2021). Based on our results, developing maize cultivars that are less responsive to weeds regarding their growth and development would also help increase yields. Reducing FR-mediated inhibition of the phytochrome B (phyB) photoreceptor signalling pathway may lead to constitutively thick stems and help increase yields (Wies *et al.*, 2019). Also, it was shown in *Arabidopsis* that a canopy of non-shade avoiding plants

is better able to form a closed canopy that can shade out weeds (Pantazopoulou et al., 2021). However, maintaining some degree of flexibility would be desired to facilitate leaf movement and stem bending towards bright spots in the vegetation to ensure optimal collective light harvesting (Maddonna *et al.*, 2002).

Acknowledgements

We would like to thank Limagrain Rilland and the associated staff for providing materials and a greenhouse facility to perform the experiment. Specifically, Louis Vlaswinkel, Cornélie Noordam, Angelica Gonzalez and Jaimy Oudeman were invaluable with their help designing, preparing, executing and maintaining the experiment.

Materials and methods

Plant material, growth conditions and treatments

Three anonymised maize inbred lines (LIM1-3) were selected from the Limagrain seed stocks. For the climate room experiments, seeds were sown in Primasta soil and plants were grown in long day light conditions light/dark 16 h / 8 h, 20 °C, 70 % humidity, ~ 230 $\mu\text{M m}^{-2} \text{s}^{-1}$ PAR, R/FR ratio 2.2 in WL and 0.1 in WL + FR, R/FR reduction was generated using Philips GreenPower LED research modules far red.

The greenhouse experiment was performed in Rilland, the Netherlands (N 51.402640°, E 4.123002°) and started on the 23rd of May 2019. The soil consisted of clay and was enriched in nutrients with fertilizer and enriched in organic matter by ploughing a green manure crop into the soil prior to the start of the experiment. Drip irrigation provided a consistent water supply throughout the experiment. When the plants started to flower, pollen distribution was helped by gently shaking the plants several times a week. Pest control occurred throughout the experiment using *Ichneumon* wasps and *Scelta* (Royal Brinkman). Plants that were heavily infected regardless of these treatments were removed from the analysis.

Each plot contained one treatment and 26 plants of each of the three genotypes (greenhouse layout visually described in Figure 7.2). Maize seeds were sown in rows at normal field density with 75 cm between rows and 13 cm between plants within a row. Plots consisted of 4 parallel rows, the outermost of which were sown with a fourth genotype that was used as a border plant to minimise edge effects. The two middle rows, containing the three genotypes were again bordered on each end by two border plants. In between these border plants, 72 seeds of the three selected genotypes (24 per genotype) were sown over the two rows.

Five days before sowing the maize, seeds of mizuna mustard (*Brassica juncea* subsp. *integrifolia* var. *japonica*) were scattered around the middle two rows of the plots containing the weeds treatment. Weeds were manually trimmed when they threatened to grow taller than the maize. A green filter (LEE filter 122 Fern Green) was stuck on a reflective sheet of white plastic and this combination was hung in a concave shape around the base of the plant (Figure 7.2 B). The distance between the two ends of the concave filter was 40cm, and the highest point was 21 cm from the soil. Holes were cut into the filters to provide a space for the maize plants to grow. To generate the low density treatment, a total of 36 plants (12 per genotype) was sown at one-third of the

normal density (39cm between plants, 75 cm between rows). 23 days after sowing, the filters and mizuna weeds were removed. Remaining weeds were frequently removed throughout the rest of the experiment.

Measurements and statistical analyses

In both experiments, plant height was measured from the soil to the topmost fully developed leaf collar, leaf number was determined by counting the number of fully developed leaf collars and stem diameter was measured using a digital calliper at the base of the stem. In the climate room experiment, leaf angle was determined as the angle of the youngest counted leaf relative to the horizontal plane. At the end of the growing season, each plant was separately harvested for plant and ear dry weight measurements. Plants were dried at 40° C for 7 days, ears were dried at 105° C for 4-6 days. Light spectrum was measured using an Ocean Optics JAZ meter.

Data visualisation and analysis was performed in R. Specific details on statistical analyses can be found in the figure legends. In multi-comparison analyses, we performed multi-factorial ANOVA with Tukey's HSD post hoc correction. Correlation analysis were performed using "corrplot" and "Hmisc" packages, inspired by the MVapp (Julkowska *et al.*, 2019).



Chapter 8

General discussion

General discussion

Light is an essential resource for plant growth, as it powers photosynthesis. Various environmental factors influence light availability to the plant, including light competition with neighbours. In most species, light competition triggers an array of growth responses, collectively called shade avoidance (Ballaré & Pierik, 2017). These growth responses include adaptive shoot elongation and a more erect orientation of the leaves, helping to increase light capture. At the same time, shade signals reduce root growth and resistance against pests and pathogens (Ballaré & Pierik, 2017). Therefore, light competition between plants is undesired in crop systems, where collective performance of the field is more important than individual plant performance (Weiner *et al.*, 2010). However, not all shade avoidance responses are undesirable in cropping systems: retaining the ability to reposition leaves towards light gaps in the canopy is essential to optimise collective light harvesting (Maddonni *et al.*, 2002). Hence, it is of great importance to understand the mechanisms regulating shade avoidance and light foraging.

An important signal of neighbour proximity and shade is variation in the ratio of red (R) to far-red (FR) light (R/FR) (Fraser *et al.*, 2016). The R/FR is high (around 1.2) in full sunlight and decreases in shade (sometimes to less than 0.1), due to absorption of R and reflection of FR. In addition, horizontal FR reflection reduces the R/FR around the plant and provides an early neighbour proximity warning that precedes actual shade (Ballaré *et al.*, 1990). A reduction in R/FR leads to the inactivation of phytochrome (phy) photoreceptors, which stops the repression and degradation of PHYTOCHROME INTERACTING FACTOR (PIF) transcription factors (Leivar & Monte, 2014). PIFs are important regulators of shade-induced gene expression, including that of auxin synthesis and signalling genes (Hornitschek *et al.*, 2012; Li *et al.*, 2012). In *Arabidopsis*, the shoot response to FR enrichment, mimicking reflection by neighbour proximity, consists of elongation of the hypocotyl and petiole, as well as upward bending of the petiole (i.e. hyponasty) (Ballaré & Pierik, 2017).

Petiole growth responses to FR enrichment depend on the site of FR perception

In **Chapter 3** of this thesis, we studied *Arabidopsis* petiole growth responses to FR enrichment. We observed that local FR enrichment at the leaf tip (FRtip) leads to remote petiole hyponasty, while petiole elongation is triggered by local FR enrichment at the petiole itself. The long-distance induction of petiole hyponasty ensures that the plant

adaptively raises its leaves in response to early neighbour detection at the outermost part of the leaf, the leaf tip (Pantazopoulou *et al.*, 2017). In addition, the lack of hyponasty upon FR enrichment at the petiole itself prevents self-shading by newly developing leaves. This prevents an unnecessary increase of the leaf angle, which would limit leaf area exposure to sunlight coming from above, thus preventing a potential decrease in light interception. A recent study showed that, in *Arabidopsis* monocultures, low R/FR-induced petiole hyponasty reduces whole-canopy closure (Pantazopoulou *et al.*, 2021). Combining experimental work and mathematical modelling, it was observed that this increases light penetration between the plants, facilitating growth of plants invading the monoculture and decreasing biomass production of the monoculture individuals.

We used various methods to investigate the molecular mechanisms controlling the induction of petiole hyponasty upon FRtip, and showed that FRtip stimulates auxin synthesis in the leaf tip via PIF7-mediated activation of *YUCCA* gene expression (Chapter 3, Figure 8.1). Auxin is subsequently transported towards the petiole base to induce differential growth.

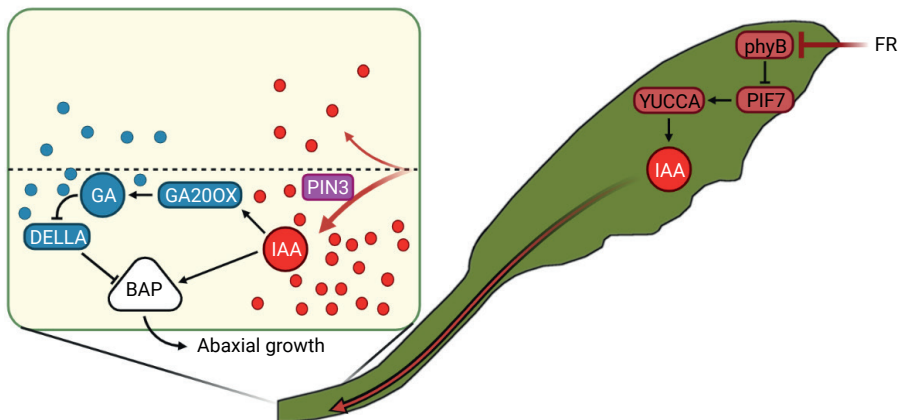


Figure 8.1. Proposed mechanism of how long-distance phytochrome signalling from tip to base orchestrates petiole hyponasty. Reflected FR is first detected at the outermost leaf tip. This induces local inactivation of phyB, followed by auxin synthesis via PIF7 and YUCCAs. Auxin is then transported towards the petiole and directed towards the abaxial side by PINs. In the abaxial petiole, auxin stimulates gibberellin synthesis via *GA20OX* expression, leading to the breakdown of DELLAs in the petiole. DELLA inactivation releases their repression of the BAP module and reinforces auxin-mediated cell elongation. The asymmetric auxin distribution and signalling ensures abaxial cell elongation which results in adaptive petiole hyponasty. Round shapes represent auxin (IAA, red) and gibberellin (GA, blue). Image was created using BioRender.com.

Abscisic acid signalling can reduce petiole hyponasty

In our transcriptome analysis in **Chapter 4**, we found that abscisic acid (ABA) signalling was also induced by FRtip, albeit mostly locally in the sensing leaf tip. ABA signalling is important in stress responses to, among others, salt, drought and general osmotic stress (Zhu, 2016). When we studied the effect of ABA in more detail, we found that ABA treatment to the leaf tip inhibited petiole hyponasty, as well as auxin synthesis and signalling (**Chapter 3**). In correspondence with this observation, our transcriptome analysis suggests a negative temporal correlation between the significance of ABA- and auxin-related gene ontology (GO) terms. Interestingly, none of the ABA synthesis, perception and signalling mutants we tested showed a strongly deviating FRtip-induced petiole hyponasty response compared to wild-type. ABA signalling of soil salinity was recently shown to inhibit PIF-mediated hypocotyl elongation in low R/FR as well (Hayes *et al.*, 2019), suggesting that the stress signal may overrule the urge to grow excessively tall in unfavourable abiotic conditions. In support of this hypothesis of decision making, it was found that constitutively shade avoiding *phyB* mutants are intolerant to drought, despite the fact that they accumulate higher levels of ABA in well-watered conditions (González *et al.*, 2012). Moreover, plants that contain reduced levels of growth-promoting gibberellins are more resistant to drought (Colebrook *et al.*, 2014). To further test the involvement of ABA signalling in FRtip-induced petiole hyponasty, it would be interesting to test mutants for *9-CIS-EPOXYCAROTENOID DIOXYGENASE 3 (NCED3)* and *NCED5*, that show transcriptional induction by FRtip in the leaf tip and petiole, respectively and of which *NCED3* is linked to the suppression of branching in low R/FR (González-Grandío *et al.*, 2017). Nevertheless, it is quite possible that ABA is not *per se* a major regular in shade avoidance under standard conditions, but it's coregulation may serve as a point of crosstalk for abiotic stress signalling pathways to suppress shade avoidance if needed. An example would be a dry soil where water availability would not allow excessive growth and shade avoidance investments would need to be suppressed.

Hormonal regulation of petiole hyponasty upon neighbour detection in the leaf tip

We designed the RNA sequencing experiment in **Chapter 4** based on analysis of the kinetics and location of petiole hyponasty. Using cell-size analysis of the abaxial and adaxial petiole epidermis, we showed that FR enrichment at the leaf tip increases abaxial cell length. This abaxial petiole-specific growth was also reflected in the transcriptome, as were auxin and brassinosteroid signalling and synthesis of ethylene and gibberellin.

As part of the strong abaxial induction of ethylene synthesis-related GO terms, *ACC SYNTHASE* genes were strongly regulated and these are well-known auxin targets (Lee *et al.*, 2017). Induction of ethylene synthesis in low R/FR has been shown in various species and settings (Pierik *et al.*, 2004b; Kegge *et al.*, 2013; Courbier *et al.*, 2021), and ethylene signalling is linked to hypocotyl elongation and petiole hyponasty (Polko *et al.*, 2012, 2015; Das *et al.*, 2016). A specific role for ethylene in low R/FR-induced hyponasty is, however, not well-established and previous work on the matter generated ambiguous insights between different ethylene mutants (Kegge, 2013). Brassinosteroid signalling has also been associated with various light signalling-induced growth responses, often alongside auxin (Kozuka *et al.*, 2010; Keuskamp *et al.*, 2011; Procko *et al.*, 2016; Hayes *et al.*, 2019). The transcriptional response to brassinosteroid requires signalling via the transcription factors BRASSINAZOLE RESISTANT 1 (BZR1) and its homolog BRI EMS SUPPRESSOR 1 (BES1). BZR1 can interact with AUXIN RESPONSE FACTOR 6 (ARF6) and PIF4 to stimulate growth through trans-activation and expression of shared and unique target genes (Oh *et al.*, 2012, 2014). These interacting transcription factors are all inhibited by DELLA proteins in the BZR1-ARF6-PIF4/DELLA (BAP/D) module. The degradation of DELLAs in the presence of gibberellin (Sun, 2010) allows the BAP/D module to induce cell elongation and hypocotyl growth (Oh *et al.*, 2014).

In **Chapter 6** we investigated whether the BAP/D module also affects petiole hyponasty in adult *Arabidopsis* and found functional requirement for PIFs and ARFs for auxin-induced petiole hyponasty. Moreover, we found evidence to suggest that leaf tip-derived auxin stimulates gibberellin synthesis, likely via increased expression of *GA20 OXIDASE 1* (*GA20OX1*) and *GA20OX2* in the abaxial petiole and that this leads to degradation of the DELLA protein REPRESSOR OF GA (RGA), as observed by confocal microscopy using the *pRGA::GFP-RGA* reporter (Figure 8.1). Gibberellin synthesis is required for petiole hyponasty, as gibberellin deficiency through paclobutrazol treatment or mutation of *GA20OX1* and *GA20OX2* inhibits FRtip-induced petiole hyponasty, and this can be rescued when gibberellin is applied exogenously. Interestingly, the degradation of GFP-RGA was observed on both sides of the petiole, in contrast with the abaxial *GA20OX* expression pattern and auxin accumulation we found in **Chapter 5**. This led us to propose gibberellin is a requirement for petiole hyponasty to occur, but not the positional cue defining where exactly cell growth happens.

Directional PIN-mediated auxin transport to the abaxial petiole translates long-distance phytochrome signalling into differential growth

To answer the question of how the non-differential FR enrichment signal, coming from the leaf tip, can so specifically induce abaxial cell elongation in the petiole, we analysed auxin distribution in **Chapter 5**. LC-MS analysis of petiole and leaf tip material revealed increased auxin concentration in the leaf tip and abaxial petiole in FRtip treatment, while such an increase was not found in the adaxial petiole. To improve the spatial resolution of our auxin concentration analysis, we decided to use a confocal fluorescence microscopy approach of the newly generated auxin reporter C3PO. Chlorophyll autofluorescence in the leaf complicates the use of fluorescent protein (FP)-based reporters (Donaldson, 2020). Combining recent improvements to FP fixation and optical clearing techniques with physical sectioning of the petiole (Kurihara *et al.*, 2015; Skopelitis *et al.*, 2017), allowed us to adequately visualise and quantify FP fluorescence of C3PO. This approach revealed that leaf tip-derived auxin accumulates in the abaxial petiole, in a process that requires PIN-FORMED 3 (PIN3), PIN4 and PIN7 auxin efflux proteins (Figure 8.1). Using *pPIN3::PIN3-GFP*, we show that in the petiole endodermis, PIN3 primarily localises on the abaxial side and that this asymmetry is reinforced by leaf tip auxin treatment (IAAtip). Endodermal PIN3 distribution has previously been suggested to be required for correctly distributing auxin from the vasculature towards the required surrounding cell layers for hypocotyl elongation in low R/FR (Keuskamp *et al.*, 2010) and phototropism towards unilateral blue (B) light (Ding *et al.*, 2011) as well as PIF4-mediated petiole hyponasty in elevated temperature (Park *et al.*, 2019). Unlike in these examples, the redistribution of PIN3 in the petiole endodermis in IAAtip treatment does not include local treatment to the tissue where PIN3 localisation is affected but depends on long-distance signalling. The expression and abundance of PIN3 are increased by auxin signalling (Keuskamp *et al.*, 2010), but this does not explain the occurrence of abaxial-adaxial PIN3 asymmetry in control conditions, which could be explained in various other ways.

Possible mechanisms controlling auxin and PIN3 asymmetry in the petiole

Firstly, in the hypocotyl endodermis, PIN3 localisation is strongly influenced by gravity (Rakusová *et al.*, 2011). In hypocotyls that are placed at a 90 ° angle, PIN3 accumulates on the bottom side of the hypocotyl and directs auxin flow towards that side, resulting in upward hypocotyl bending. In such conditions, the direction of gravity is sensed by

amyloplasts that accumulate on the bottom side of endodermal cells in both hypocotyls and inflorescence stems (Morita, 2010; Kim *et al.*, 2011). In the petiole endodermis gravity sensing may direct endodermal PIN3 towards the abaxial petiole, resulting in preferentially abaxial auxin transport.

An alternative explanation could be the asymmetrical shape of the leaf vasculature. Long-distance auxin flow has previously been shown to go through the phloem (Kramer & Bennett, 2006), which is primarily located on the abaxial side of the leaf vasculature (Bou-torrent *et al.*, 2012). This asymmetry could mean that leaf tip-derived auxin flowing through the phloem would be predestined to preferentially end up in the abaxial petiole. As *PIN3* expression is induced by auxin, leaf tip-derived auxin may create a positive feedback loop that directs auxin towards the abaxial side. It is possible that this anatomical asymmetry between the abaxial and adaxial side of the petiole, together with the gravity vector determining PIN localisation are combined: much of the phloem is already on the abaxial side of the vasculature and a gravity-based relative high abundance of PIN3 on the same side would further polarise auxin abundance towards the abaxial petiole.

The abaxial-adaxial asymmetry of leaf and vasculature shape is determined by developmental regulators including abaxially expressed *KANADI* (*KAN*) and adaxially expressed *REVOLUTA* (*REV*). *KAN* and *REV* determine abaxial and adaxial identity by oppositely regulating expression of target genes including *HOMEODOMAIN PROTEIN 1* (*HDP1*) and *ARABIDOPSIS THALIANA HOMEODOMAIN PROTEIN 1* (*ATH1*) genes (reviewed in Merelo *et al.*, 2017). The adaxial identity is reinforced by *ASYMMETRIC LEAVES 1* (*AS1*) and *AS2* (reviewed in Iwakawa *et al.*, 2020; Machida *et al.*, 2021). These leaf polarity proteins are also involved in auxin biology and shade avoidance responses (Izhaki & Bowman, 2007; Bou-torrent *et al.*, 2012; Brandt *et al.*, 2012; Merelo *et al.*, 2013; Reinhart *et al.*, 2013; Huang *et al.*, 2014; Xie *et al.*, 2015; Kuhlemeier & Timmermans, 2016). Using the RNA sequencing dataset (**Chapter 4**) we found that these genes that determine leaf polarity in developing leaves retain their differential expression between the abaxial and adaxial domains in the adult petiole (Figure. 8.2). Residual differential activity of these proteins may therefore influence auxin synthesis, distribution and signalling and the hyponastic response to FRtip in our adult petioles. Unfortunately, mutants for the leaf polarity genes mentioned here typically have strong developmental defects, making them rather unsuitable for analyses of hyponastic response to low R/FR. Although the timeframe of this study did not allow it, it would be very interesting to generate inducible expression or knockout lines for these leaf polarity genes, such that the severe mutant phenotypes of the constitutive lines may be circumvented.

A final possible explanation of the asymmetrical PIN3 distribution could be the existence of a light signalling gradient within the petiole tissue. Light gradients have been shown to exist and direct growth in thin and seemingly transparent hypocotyls during hypocotyl phototropism towards a weak light source in darkness, via asymmetrical auxin distribution through PIN3 localisation (Ding *et al.*, 2011). Light gradients also steer stem and petiole phototropism (Kagawa *et al.*, 2009; Vanhaelewyn *et al.*, 2019) and leaf flattening, which is reduced in *pin3 pin4 pin7* mutants (Kozuka *et al.*, 2013; Legris *et al.*, 2021). These light gradients are mainly signalled by the UV-B and B light photoreceptors UV-B RESISTANCE LOCUS 8 (UVR8) and phototropin (Legris & Boccaccini, 2020). However, in light-grown plants, cryptochrome and phytochrome inactivation are required to provide auxin flow from cotyledons to the hypocotyl to ensure that asymmetrical phototropin signalling generates asymmetrical growth towards an unilateral light source (Goyal *et al.*, 2016; Boccaccini *et al.*, 2020).

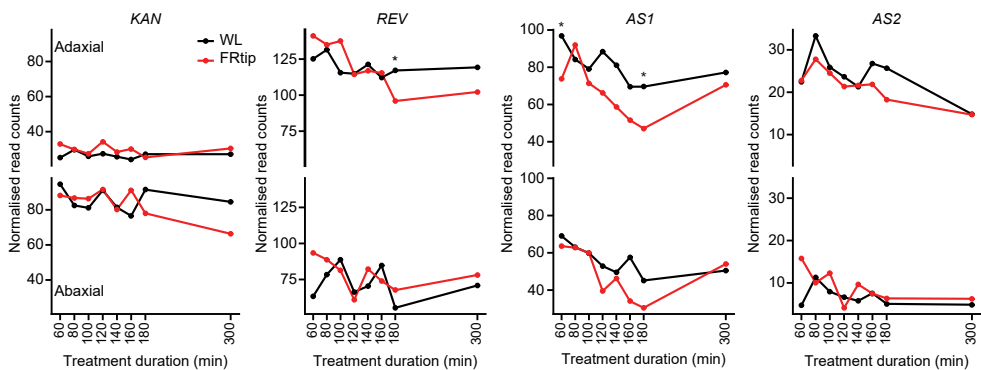


Figure 8.2. Leaf polarity genes remain to be differentially expressed between the adaxial and abaxial side in adult petioles. Expression profiles derived from the RNA sequencing experiment in Chapter 4 of the leaf polarity genes *KAN*, *REV*, *AS1* and *AS2* in the adaxial (top panels) and abaxial (bottom panels) petiole during WL and FRtip treatment (asterisks indicate significant treatment effect, *: $p < 0.01$, two-sided t-test).

A possible mechanism of light gradient sensing via phytochromes and cryptochromes could involve a gradient of BAP/D activation, as BZR, ARF and PIF have all been shown to directly or indirectly be inhibited by these photoreceptors (Hornitschek *et al.*, 2012; Li *et al.*, 2012; Hersch *et al.*, 2014; de Wit *et al.*, 2016; Pedmale *et al.*, 2016; Wang *et al.*, 2018; Xu *et al.*, 2018; Dong *et al.*, 2019; He *et al.*, 2019; Mao *et al.*, 2020). Phytochromes and cryptochromes may be more active on the lit adaxial side of the petiole, than the shaded

abaxial side. Initial experiments to test whether light signalling gradients in the petiole may affect petiole hyponasty in response to FR enrichment or auxin treatment at the leaf tip should include localised (monochromatic) light treatment to the abaxial petiole. This approach has previously been used to show that petiole hyponasty through leaf tip touching is not affected by abaxial green or R light supplementation (de Wit *et al.*, 2012).

Finally, a combination of the hypotheses discussed here may exist. For example, light gradients and gravity are directional cues that work in the same direction under natural sunlight conditions and may thus sustain each other's putative effect. Furthermore, if such gradients indeed set-up PIN polarity, this may still interact with the developmental differences of the abaxial and adaxial side of the petiole as set up through KAN and REV, as well as the anatomical asymmetry of the vasculature.

Concluding remarks

To meet the challenge of sustainably feeding an ever-growing human population, improvements to crops and cropping systems are essential (Binns *et al.*, 2020). As highly productive agriculture requires dense cropping, optimising light use is essential in all crop fields. An important aspect of light use efficiency is the photosynthetic efficiency with which light is used to fixate carbon dioxide. Recent developments in photosynthesis research, such as improving the recovery from energy-costly photoprotection from high light (Kromdijk *et al.*, 2016), could help to drastically improve the light use efficiency in crops. Regarding light and shade signalling, the shade avoidance growth response to neighbour detection can seriously distort plant development and reduce final yield (**Chapter 7**). Moreover, excessive growth during shade avoidance reduces resistance to other environmental stresses such as drought and infection (González *et al.*, 2012; De Wit *et al.*, 2013; Ballaré, 2014; Courbier *et al.*, 2020). However, the inability to physically move away from stress has, through evolution, created incredibly intricate and sophisticated organisms that are able to optimise growth and development to any changes in their environment. Simply inactivating a major light signalling pathway to reduce light competition between crops, may hamper adaptive light foraging and suppressive shading of weeds (Maddonni *et al.*, 2002; Weiner *et al.*, 2010; Pantazopoulou *et al.*, 2021). The benefits and negative effects of shade avoidance growth responses on individual and communal photosynthesis, survival and yield should continue to be studied using a combination of modelling and experimental approaches, such that we can create crops that use the limited supply of light to the fullest.

References

- Adamowski M, Friml J. 2015.** PIN-Dependent Auxin Transport: Action, Regulation, and Evolution. *The Plant Cell* **27**: 20–32.
- Arsuffi G, Braybrook SA. 2018.** Acid growth: an ongoing trip. *Journal of Experimental Botany* **69**: 137–146.
- Atamian HS, Creux NM, Brown EA, Garner AG, Blackman BK, Harmer SL. 2016.** Circadian regulation of sunflower heliotropism, floral orientation, and pollinator visits. *Science* **353**: 587–590.
- Bai M-Y, Shang J-X, Oh E, Fan M, Bai Y, Zentella R, Sun T, Wang Z-Y. 2012.** Brassinosteroid, gibberellin and phytochrome impinge on a common transcription module in Arabidopsis. *Nature cell biology* **14**: 810–817.
- Ballaré CL. 2014.** Light regulation of plant defense. *Annual review of plant biology* **65**: 335–63.
- Ballaré CL, Pierik R. 2017.** The shade-avoidance syndrome: Multiple signals and ecological consequences. *Plant Cell and Environment* **40**: 2530–2543.
- Ballaré CL, Scopel AL, Sánchez RA. 1990.** Far-Red Radiation Reflected from Adjacent Leaves: An Early Signal of Competition in Plant Canopies. *Science* **247**: 329–332.
- Barbosa ICR, Hammes UZ, Schwechheimer C. 2018.** Activation and Polarity Control of PIN-FORMED Auxin Transporters by Phosphorylation. *Trends in Plant Science* **23**: 523–538.
- Beall FD, Yeung EC, Pharis RP. 1996.** Far-red light stimulates internode elongation, cell division, cell elongation, and gibberellin levels in bean. *Canadian Journal of Botany* **74**: 743–752.
- Bhatia N, Ahl H, Jönsson H, Heisler MG. 2019.** Quantitative analysis of auxin sensing in leaf primordia argues against proposed role in regulating leaf dorsoventrality. *eLife* **8**: e39298.
- Binns CW, Lee MK, Maycock B, Torheim LE, Nanishi K, Duong DTT. 2020.** Climate Change, Food Supply, and Dietary Guidelines. *Annual Review of Public Health* **42**: 233–255.
- Black M, Shuttleworth JE. 1974.** The role of the cotyledons in the photocontrol of hypocotyl extension in *Cucumis sativus* L. *Planta* **117**: 57–66.
- Boccaccini A, Legris M, Krahmer J, Allenbach-Petrolati L, Goyal A, Galvan-Ampudia C, Vernoux T, Karayekov EE, Casal JJ, Fankhauser C, et al. 2020.** Low blue light enhances phototropism by releasing cryptochrome 1-mediated inhibition of PIF4 expression. *Plant Physiology* **183**: 1780–1793.
- Bou-Torrent J, Galstyan A, Gallemí M, Cifuentes-Esquivel N, Molina-Contreras MJ, Salla-Martret M, Jikumaru Y, Yamaguchi S, Kamiya Y, Martínez-García JF. 2014.** Plant proximity perception dynamically modulates hormone levels and sensitivity in Arabidopsis. *Journal of Experimental Botany* **65**: 2937–2947.
- Bou-Torrent J, Roig-Villanova I, Martínez-García JF. 2008.** Light signaling: back to space. *Trends in Plant Science* **13**: 108–114.
- Bou-torrent J, Salla-martret M, Brandt R, Musielak T, Palauqui J, Martínez-garcía JF, Wenkel S. 2012.** ATHB4 and HAT3, two class II HD-ZIP transcription factors, control leaf development in Arabidopsis. *Plant signaling & behavior* **7**: 1382–1387.
- Brandt R, Salla-Martret M, Bou-Torrent J, Musielak T, Stahl M, Lanz C, Ott F, Schmid M, Greb T, Schwarz M, et al. 2012.** Genome-wide binding-site analysis of REVOLUTA reveals a link between leaf patterning and light-mediated growth responses. *Plant Journal* **72**: 31–42.
- Buti S, Hayes S, Pierik R. 2020.** The bHLH network underlying plant shade-avoidance. *Physiologia Plantarum*: 1–13.

- Casal JJ, Smith H. 1988a.** Persistent effects of changes in phytochrome status on internode growth in light-grown mustard: Occurrence, kinetics and locus of perception. *Planta* **175**: 214–220.
- Casal JJ, Smith H. 1988b.** The loci of perception for phytochrome control of internode growth in light-grown mustard: Promotion by low phytochrome photoequilibria in the internode is enhanced by blue light perceived by the leaves. *Planta* **176**: 277–282.
- Casanova-Sáez R, Voß U. 2019.** Auxin Metabolism Controls Developmental Decisions in Land Plants. *Trends in Plant Science* **24**: 741–754.
- Cerdán PD, Chory J. 2003.** Regulation of flowering time by light quality. *Nature* **423**: 881–885.
- Chaiwanon J, Wang W, Zhu J-Y, Oh E, Wang Z-Y. 2016.** Information Integration and Communication in Plant Growth Regulation. *Cell* **164**: 1257–1268.
- de Chaumont F, Dallongeville S, Chenouard N, Hervé N, Pop S, Provoost T, Meas-Yedid V, Pankajakshan P, Lecomte T, Le Montagner Y, et al. 2012.** Icy: An open bioimage informatics platform for extended reproducible research. *Nature Methods* **9**: 690–696.
- Chelle M, Evers JB, Combes D, Varlet-Grancher C, Vos J, Andrieu B. 2007.** Simulation of the three-dimensional distribution of the red:far-red ratio within crop canopies. *New Phytologist* **176**: 223–234.
- Chen L, Huang XX, Zhao SM, Xiao DW, Xiao LT, Tong JH, Wang WS, Li YJ, Ding Z, Hou BK. 2020.** IPyA glucosylation mediates light and temperature signaling to regulate auxin-dependent hypocotyl elongation in Arabidopsis. *Proceedings of the National Academy of Sciences of the United States of America* **117**: 6910–6917.
- Chen X, Yao Q, Gao X, Jiang C, Harberd NP, Fu X. 2016.** Shoot-to-Root Mobile Transcription Factor HY5 Coordinates Plant Carbon and Nitrogen Acquisition. *Current Biology* **26**: 640–646.
- Christie JM, Yang H, Richter GL, Sullivan S, Thomson CE, Lin J, Titapiwatanakun B, Ennis M, Kaiserli E, Lee OR, et al. 2011.** Phot1 inhibition of ABCB19 primes lateral Auxin Fluxes in the Shoot Apex required for Phototropism. *PLoS Biology* **9**: e1001076.
- Colebrook EH, Thomas SG, Phillips AL, Hedden P. 2014.** The role of gibberellin signalling in plant responses to abiotic stress. *Journal of Experimental Biology* **217**: 67–75.
- Courbier S, Grevink S, Sluijs E, Bonhomme PO, Kajala K, Van Wees SCM, Pierik R. 2020.** Far-red light promotes Botrytis cinerea disease development in tomato leaves via jasmonate-dependent modulation of soluble sugars. *Plant Cell and Environment* **43**: 2769–2781.
- Courbier S, Pierik R. 2019.** Canopy Light Quality Modulates Stress Responses in Plants. *iScience* **22**: 441–452.
- Courbier S, Snoek BL, Kajala K, Li L, van Wees SCM, Pierik R. 2021.** Mechanisms of far-red light-mediated dampening of defense against Botrytis cinerea in tomato leaves. *Plant Physiology* **187**: 1250–1266.
- Crawford AJ, McLachlan DH, Hetherington AM, Franklin KA. 2012.** High temperature exposure increases plant cooling capacity. *Current Biology* **22**: R396–R397.
- Darwin C, Darwin F. 1880.** The power of movement in plants. *John Murray*.
- Das D, St Onge KR, Voeselek LACJ, Pierik R, Sasidharan R. 2016.** Ethylene- and shade-induced hypocotyl elongation share transcriptome patterns and functional regulators. *Plant Physiology* **172**: 718–733.
- Deal RB, Henikoff S. 2011.** The INTACT method for cell type-specific gene expression and chromatin profiling in Arabidopsis thaliana. *Nature Protocols* **6**: 56–68.
- Ding Z, Galván-Ampudia CS, Demarsy E, Łangowski Ł, Kleine-Vehn J, Fan Y, Morita MT, Tasaka M, Fankhauser C, Offringa R, et al. 2011.** Light-mediated polarization of the PIN3 auxin transporter for the phototropic response in Arabidopsis. *Nature cell biology* **13**: 447–452.

- Djakovic-Petrovic T, de Wit M, Voeselek LACJ, Pierik R. 2007.** DELLA protein function in growth responses to canopy signals. *The Plant Journal* **51**: 117–126.
- Donaldson L. 2020.** Autofluorescence in Plants. *Molecules* **25**: 2393.
- Dong H, Liu J, He G, Liu P, Sun J. 2019.** Photoexcited phytochrome B interacts with brassinazole resistant 1 to repress brassinosteroid signaling in Arabidopsis. *Journal of Integrative Plant Biology* **62**: 652–667.
- Endo M, Araki T, Nagatani A. 2016.** Tissue-specific regulation of flowering by photoreceptors. *Cellular and Molecular Life Sciences* **73**: 829–839.
- Endo M, Nakamura S, Araki T, Mochizuki N, Nagatani A. 2005.** Phytochrome B in the mesophyll delays flowering by suppressing FLOWERING LOCUS T expression in Arabidopsis vascular bundles. *The Plant Cell* **17**: 1941–1952.
- FAOSTAT 2021.** Food and Agriculture Organization of the United Nations. <https://www.fao.org/faostat/>
- Fankhauser C, Christie JM. 2015.** Plant phototropic growth. *Current Biology* **25**: R384–R389.
- Fendrych M, Leung J, Friml J. 2016.** TIR1/AFB-Aux/IAA auxin perception mediates rapid cell wall acidification and growth of Arabidopsis hypocotyls. *eLife* **5**: e19048.
- Feng S, Martinez C, Gusmaroli G, Wang Y, Zhou J, Wang F, Chen L, Yu L, Iglesias-Pedraz JM, Kircher S, et al. 2008.** Coordinated regulation of Arabidopsis thaliana development by light and gibberellins. *Nature* **451**: 475–479.
- Fernández-Milmanda GL, Ballaré CL. 2021.** Shade Avoidance: Expanding the Color and Hormone Palette. *Trends in Plant Science* **26**: 509–523.
- Fernández-Milmanda GL, Crocco CD, Reichelt M, Mazza CA, Köllner TG, Zhang T, Cargnel MD, Lichy MZ, Fiorucci AS, Fankhauser C, et al. 2020.** A light-dependent molecular link between competition cues and defence responses in plants. *Nature Plants* **6**: 223–230.
- Fiorucci AS, Galvão VC, Ince YÇ, Boccaccini A, Goyal A, Allenbach Petrolati L, Trevisan M, Fankhauser C. 2020.** PHYTOCHROME INTERACTING FACTOR 7 is important for early responses to elevated temperature in Arabidopsis seedlings. *New Phytologist* **226**: 50–58.
- Franklin KA. 2008.** Shade avoidance. *New Phytologist* **179**: 930–944.
- Franklin KA, Lee SH, Patel D, Kumar SV, Spartz AK, Gu C, Ye S, Yu P, Breen G, Cohen JD, et al. 2011.** PHYTOCHROME-INTERACTING FACTOR 4 (PIF4) regulates auxin biosynthesis at high temperature. *Proceedings of the National Academy of Sciences of the United States of America* **108**: 20231–20235.
- Fraser DP, Hayes S, Franklin KA. 2016.** Photoreceptor crosstalk in shade avoidance. *Current Opinion in Plant Biology* **33**: 1–7.
- Frigerio M, Alabadí D, Pérez-Gómez J, García-Cárcel L, Phillips AL, Hedden P, Blázquez MA. 2006.** Transcriptional regulation of gibberellin metabolism genes by auxin signaling in Arabidopsis. *Plant Physiology* **142**: 553–563.
- Friml J, Benková E, Blilou I, Wisniewska J, Hamann T, Ljung K, Woody S, Sandberg G, Scheres B, Jürgens G, et al. 2002a.** AtPIN4 mediates sink-driven auxin gradients and root patterning in Arabidopsis. *Cell* **108**: 661–673.
- Friml J, Wisniewska J, Benkova E, Mendgen K, Palme K. 2002b.** Lateral relocation of auxin efflux regulator PIN3 mediates tropism in Arabidopsis. *Nature* **415**: 806–809.
- Fujii H, Verslues PE, Zhu JK. 2007.** Identification of two protein kinases required for abscisic acid regulation of seed germination, root growth, and gene expression in Arabidopsis. *Plant Cell* **19**: 485–494.

- Gallei M, Luschnig C, Friml J. 2020.** Auxin signalling in growth: Schrödinger's cat out of the bag. *Current Opinion in Plant Biology* **53**: 43–49.
- Galvão VC, Fankhauser C. 2015.** Sensing the light environment in plants: Photoreceptors and early signaling steps. *Current Opinion in Neurobiology* **34**: 46–53.
- Gao C, Liu X, De Storme N, Jensen KH, Xu Q, Yang J, Liu X, Chen S, Martens HJ, Schulz A, et al. 2020.** Directionality of Plasmodesmata-Mediated Transport in Arabidopsis Leaves Supports Auxin Channeling. *Current Biology* **30**: 1970–1977.
- Geisler M, Aryal B, Di Donato M, Hao P. 2017.** A critical view on ABC transporters and their interacting partners in auxin transport. *Plant and Cell Physiology* **58**: 1601–1604.
- van Gelderen K, Kang C, Paalman R, Keuskamp DH, Hayes S, Pierik R. 2018.** Far-red Light Detection in the Shoot Regulates Lateral Root Development through the HY5 Transcription Factor. *The Plant Cell* **30**: 101–116.
- Gommers CMM, Keuskamp DH, Buti S, van Veen H, Koevoets IT, Reinen E, Voesenek LACJ, Pierik R. 2017.** Molecular Profiles of Contrasting Shade Response Strategies in Wild Plants: Differential Control of Immunity and Shoot Elongation. *The Plant Cell* **29**: 331–344.
- Gommers CMM, Visser EJW, St Onge KR, Voesenek LACJ, Pierik R. 2013.** Shade tolerance: when growing tall is not an option. *Trends in plant science* **18**: 65–71.
- González-Grandío E, Pajoro A, Franco-Zorrilla JM, Tarancón C, Immink RGH, Cubas P. 2017.** Abscisic acid signaling is controlled by a BRANCHED1/HD-ZIP I cascade in Arabidopsis axillary buds. *Proceedings of the National Academy of Sciences* **114**: E245–E254.
- González-Grandío E, Poza-Carrión C, Sorzano COS, Cubas P. 2013.** BRANCHED1 Promotes Axillary Bud Dormancy in Response to Shade in Arabidopsis. *The Plant Cell* **25**: 834–850.
- González CV, Ibarra SE, Piccoli PN, Botto JF, Boccalandro HE. 2012.** Phytochrome B increases drought tolerance by enhancing ABA sensitivity in Arabidopsis thaliana. *Plant, Cell and Environment* **35**: 1958–1968.
- Goyal A, Karayekov E, Galvão VC, Ren H, Casal JJ, Fankhauser C. 2016.** Shade Promotes Phototropism through Phytochrome B-Controlled Auxin Production. *Current Biology* **26**: 3280–3287.
- Gühl K, Holmer R, Xiao TT, Shen D, Wardhani TAK, Geurts R, van Zeijl A, Kohlen W. 2021.** The Effect of Exogenous Nitrate on LCO Signalling, Cytokinin Accumulation, and Nodule Initiation in *Medicago truncatula*. *Genes* **12**: 988.
- Haga K, Frank L, Kimura T, Schwechheimer C, Sakai T. 2018.** Roles of AGCVIII Kinases in the Hypocotyl Phototropism of Arabidopsis Seedlings. *Plant and Cell Physiology* **59**: 1060–1071.
- Haga K, Hayashi KI, Sakai T. 2014.** Pinoid AGC Kinases Are Necessary for Phytochrome-Mediated Enhancement of Hypocotyl Phototropism in Arabidopsis. *Plant Physiology* **166**: 1535–1545.
- Haga K, Sakai T. 2012.** PIN auxin efflux carriers are necessary for pulse-induced but not continuous light-induced phototropism in Arabidopsis. *Plant Physiology* **160**: 763–776.
- Haga K, Tsuchida-Mayama T, Yamada M, Sakai T. 2015.** Arabidopsis ROOT PHOTOTROPISM2 Contributes to the Adaptation to High-Intensity Light in Phototropic Responses. *The Plant Cell* **27**: 1098–1112.
- Hayes S, Pantazopoulou CK, van Gelderen K, Reinen E, Tween AL, Sharma A, de Vries M, Prat S, Schuurink RC, Testerink C, et al. 2019.** Soil Salinity Limits Plant Shade Avoidance. *Current Biology* **29**: 1669–1676.
- Hayes S, Sharma A, Fraser DP, Trevisan M, Cragg-Barber CK, Tavridou E, Fankhauser C, Jenkins GI, Franklin KA. 2017.** UV-B Perceived by the UVR8 Photoreceptor Inhibits Plant Thermomorphogenesis. *Current Biology* **27**: 120–127.

- Hayes S, Velanis CN, Jenkins GI, Franklin KA. 2014.** UV-B detected by the UVR8 photoreceptor antagonizes auxin signaling and plant shade avoidance. *Proceedings of the National Academy of Sciences of the United States of America* **111**: 11894–11899.
- He G, Liu J, Dong H, Sun J. 2019.** The Blue-Light Receptor CRY1 Interacts with BZR1 and BIN2 to Modulate the Phosphorylation and Nuclear Function of BZR1 in Repressing BR Signaling in Arabidopsis. *Molecular Plant* **12**: 689–703.
- Hedden P. 2020.** The current status of research on gibberellin biosynthesis. *Plant and Cell Physiology* **61**: 1832–1849.
- Hersch M, Lorrain S, de Wit M, Trevisan M, Ljung K, Bergmann S, Fankhauser C. 2014.** Light intensity modulates the regulatory network of the shade avoidance response in Arabidopsis. *Proceedings of the National Academy of Sciences* **111**: 6515–6520.
- Herud-Sikimić O, Stiel AC, Kolb M, Shanmugaratnam S, Berendzen KW, Feldhaus C, Höcker B, Jürgens G. 2021.** A biosensor for the direct visualization of auxin. *Nature* **592**: 768–772.
- Hisamatsu T, King RW, Helliwell CA, Koshioka M. 2005.** The involvement of gibberellin 20-oxidase genes in phytochrome-regulated petiole elongation of Arabidopsis. *Plant Physiology* **138**: 1106–1116.
- Holalu S V., Finlayson SA. 2017.** The ratio of red light to far red light alters Arabidopsis axillary bud growth and abscisic acid signalling before stem auxin changes. *Journal of Experimental Botany* **68**: 943–952.
- Hornitschek P, Kohnen M V., Lorrain S, Rougemont J, Ljung K, López-Vidriero I, Franco-Zorrilla JM, Solano R, Trevisan M, Pradervand S, et al. 2012.** Phytochrome interacting factors 4 and 5 control seedling growth in changing light conditions by directly controlling auxin signaling. *Plant Journal* **71**: 699–711.
- Hornitschek P, Lorrain S, Zoete V, Michielin O, Fankhauser C. 2009.** Inhibition of the shade avoidance response by formation of non-DNA binding bHLH heterodimers. *The EMBO Journal* **28**: 3893–902.
- Huang T, Harrar Y, Lin C, Reinhart B, Newell NR, Talavera-Rauh F, Hokin SA, Kathryn Barton M, Kerstetter RA. 2014.** Arabidopsis KANADI1 acts as a transcriptional repressor by interacting with a specific cis-element and regulates auxin biosynthesis, transport, and signaling in opposition to HD-ZIPIII factors. *Plant Cell* **26**: 246–262.
- Iwakawa H, Takahashi H, Machida Y, Machida C. 2020.** Roles of ASYMMETRIC LEAVES2 (AS2) and nucleolar proteins in the adaxial-abaxial polarity specification at the perinucleolar region in arabidopsis. *International Journal of Molecular Sciences* **21**: 7314.
- Izaguirre MM, Mazza CA, Astigueta MS, Ciarla AM, Ballaré CL. 2013.** No time for candy: Passionfruit (*Passiflora edulis*) plants down-regulate damage-induced extra floral nectar production in response to light signals of competition. *Oecologia* **173**: 213–221.
- Izhaki A, Bowman JL. 2007.** KANADI and class III HD-Zip gene families regulate embryo patterning and modulate auxin flow during embryogenesis in Arabidopsis. *Plant Cell* **19**: 495–508.
- Jaeger KE, Wigge PA. 2007.** FT Protein Acts as a Long-Range Signal in Arabidopsis. *Current Biology* **17**: 1050–1054.
- Julkowska MM, Saade S, Agarwal G, Gao G, Pailles Y, Morton M, Awlia M, Tester M. 2019.** MV app-multivariate analysis application for streamlined data analysis and curation. *Plant Physiology* **180**: 1261–1276.
- Jung JH, Domijan M, Klose C, Biswas S, Ezer D, Gao M, Khattak AK, Box MS, Charoensawan V, Cortijo S, et al. 2016.** Phytochromes function as thermosensors in Arabidopsis. *Science* **354**: 886–889.

- Kagawa T, Kimura M, Wada M. 2009.** Blue light-induced phototropism of inflorescence stems and petioles is mediated by phototropin family members phot1 and phot2. *Plant and Cell Physiology* **50**: 1774–1785.
- Kegge W. 2013.** Above ground plant interactions: Consequences for growth and volatile emission. *PhD thesis*.
- Kegge W, Weldegergis BT, Soler R, Vergeer van Eijk M, Dicke M, Voeselek LACJ, Pierik R. 2013.** Canopy light cues affect emission of constitutive and methyl jasmonate-induced volatile organic compounds in *Arabidopsis thaliana*. *New Phytologist* **200**: 861–874.
- Keller MM, Jaillais Y, Pedmale U V., Moreno JE, Chory J, Ballaré CL. 2011.** Cryptochrome 1 and phytochrome B control shade-avoidance responses in *Arabidopsis* via partially independent hormonal cascades. *Plant Journal* **67**: 195–207.
- Keuskamp DH, Pollmann S, Voeselek LACJ, Peeters AJM, Pierik R. 2010.** Auxin transport through PIN-FORMED 3 (PIN3) controls shade avoidance and fitness during competition. *Proceedings of the National Academy of Sciences of the United States of America* **107**: 22740–22744.
- Keuskamp DH, Sasidharan R, Vos I, Peeters AJM, Voeselek LACJ, Pierik R. 2011.** Blue-light-mediated shade avoidance requires combined auxin and brassinosteroid action in *Arabidopsis* seedlings. *The Plant Journal* **67**: 208–217.
- Kim S, Hwang G, Kim S, Thi TN, Kim H, Jeong J, Kim J, Kim J, Choi G, Oh E. 2020.** The epidermis coordinates thermoresponsive growth through the phyB-PIF4-auxin pathway. *Nature Communications* **11**: 1–13.
- Kim K, Shin J, Lee S-H, Kweon H-S, Maloof JN, Choi G. 2011.** Phytochromes inhibit hypocotyl negative gravitropism by regulating the development of endodermal amyloplasts through phytochrome-interacting factors. *Proceedings of the National Academy of Sciences* **108**: 1729–1734.
- Kim J, Song K, Park E, Kim K, Bae G, Choi G. 2016.** Epidermal Phytochrome B Inhibits Hypocotyl Negative Gravitropism Non-Cell-Autonomously. *The Plant Cell* **28**: 2770–2785.
- Kohnen M V, Schmid-Siegert E, Trevisan M, Allenbach Petrolati L, Sénéchal F, Müller-Moulé P, Maloof J, Xenarios I, Fankhauser C. 2016.** Neighbor detection induces organ-specific transcriptomes, revealing patterns underlying hypocotyl-specific growth. *Plant Cell* **28**: 2889–2904.
- Kozuka T, Kobayashi J, Horiguchi G, Demura T, Sakakibara H, Tsukaya H, Nagatani A. 2010.** Involvement of Auxin and Brassinosteroid in the Regulation of Petiole Elongation under the Shade. *Plant Physiology* **153**: 1608–1618.
- Kozuka T, Suetsugu N, Wada M, Nagatani A. 2013.** Antagonistic regulation of leaf flattening by phytochrome B and phototropin in *Arabidopsis thaliana*. *Plant and Cell Physiology* **54**: 69–79.
- Kramer EM, Bennett MJ. 2006.** Auxin transport: a field in flux. *Trends in Plant Science* **11**: 382–386.
- Kramer EM, Rutschow HL, Mabie SS. 2011.** AuxV: A database of auxin transport velocities. *Trends in Plant Science* **16**: 461–463.
- Kromdijk J, Głowacka, Katarzyna Leonelli L, Gabilly ST, Iwai M, Niyogi KK, Long SP. 2016.** Improving photosynthesis and crop productivity by accelerating recovery from photoprotection. *Nature* **354**: 857–861.
- de Kroon H, Huber H, Stuefer JF, van Groenendael JM. 2005.** A modular concept of phenotypic plasticity in plants. *New Phytologist* **166**: 73–82.
- Kudsk P, Mathiassen SK. 2020.** Pesticide regulation in the European Union and the glyphosate controversy. *Weed Science* **68**: 214–222.

- Kuhlemeier C, Timmermans MCP. 2016.** The Sussex signal: Insights into leaf dorsiventrality. *Development* **143**: 3230–3237.
- Küpers JJ, van Gelderen K, Pierik R. 2018.** Location Matters: Canopy Light Responses over Spatial Scales. *Trends in Plant Science* **23**: 865–873.
- Küpers JJ, Oskam L, Pierik R. 2020.** Photoreceptors regulate plant developmental plasticity through auxin. *Plants* **9**: 940.
- Kurihara D, Mizuta Y, Sato Y, Higashiyama T. 2015.** ClearSee: a rapid optical clearing reagent for whole-plant fluorescence imaging. *Development* **142**: 4168–4179.
- Kutschera U, Niklas KJ. 2007.** The epidermal-growth-control theory of stem elongation: An old and a new perspective. *Journal of Plant Physiology* **164**: 1395–1409.
- Laby RJ, Kincaid MS, Kim D, Gibson SI. 2000.** The Arabidopsis sugar-insensitive mutants *sis4* and *sis5* are defective in abscisic acid synthesis and response. *Plant Journal* **23**: 587–596.
- Lee HY, Chen YC, Kieber JJ, Yoon GM. 2017.** Regulation of the turnover of ACC synthases by phytohormones and heterodimerization in Arabidopsis. *Plant Journal* **91**: 491–504.
- Lee H, Ha J, Kim S, Choi H, Kim ZH, Han Y, Kim J, Oh Y, Fragoso V, Shin K, et al. 2016.** Stem-piped light activates phytochrome B to trigger light responses in Arabidopsis thaliana roots. *Science Signaling* **9**: ra106.
- Legris M, Boccaccini A. 2020.** Stem phototropism toward blue and ultraviolet light. *Physiologia Plantarum* **169**: 357–368.
- Legris M, Ince YÇ, Fankhauser C. 2019.** Molecular mechanisms underlying phytochrome-controlled morphogenesis in plants. *Nature Communications* **10**: 1–15.
- Legris M, Klose C, Burgie ES, Rojas CC, Neme M, Hiltbrunner A, Wigge PA, Schäfer E, Vierstra RD, Casal JJ. 2016.** Phytochrome B integrates light and temperature signals in Arabidopsis. *Science* **354**: 897–900.
- Legris M, Szarzynska-Erden BM, Trevisan M, Allenbach Petrolati L, Fankhauser C. 2021.** Phototropin-mediated perception of light direction in leaves regulates blade flattening. *Plant Physiology* **187**: 1235–1249.
- Leivar P, Monte E. 2014.** PIFs: Systems integrators in plant development. *Plant Cell* **26**: 56–78.
- Leivar P, Monte E, Al-Sady B, Carle C, Storer A, Alonso JM, Ecker JR, Quail PH. 2008.** The Arabidopsis phytochrome-interacting factor PIF7, together with PIF3 and PIF4, regulates responses to prolonged red light by modulating phyB levels. *Plant Cell* **20**: 337–352.
- Léon-Kloosterziel KM, Alvarez Gil M, Ruijs GJ, Jacobsen SE, Olszewski NE, Schwartz SH, Zeevaart JAD, Koornneef M. 1996.** Isolation and characterization of abscisic acid-deficient Arabidopsis mutants at two new loci. *The Plant Journal* **10**: 655–661.
- Li L, Ljung K, Breton G, Schmitz RJ, Pruneda-Paz J, Cowing-Zitron C, Cole BJ, Ivans LJ, Pedmale U V, Jung H-S, et al. 2012.** Linking photoreceptor excitation to changes in plant architecture. *Genes & Development* **26**: 785–790.
- Liang T, Yang Y, Liu H. 2019.** Signal transduction mediated by the plant UV-B photoreceptor UVR8. *New Phytologist* **221**: 1247–1252.
- Liao C, Smet W, Brunoud G, Yoshida S, Vernoux T, Weijers D. 2015.** Reporters for sensitive and quantitative measurement of auxin response. *Nature Methods* **12**: 207–210.
- Lin R, Wang H. 2005.** Two homologous ATP-binding cassette transporter proteins, AtMDR1 and AtPGP1, regulate Arabidopsis photomorphogenesis and root development by mediating polar auxin transport. *Plant Physiology* **138**: 949–964.

- Liu JG, Mahoney KJ, Sikkema PH, Swanton CJ. 2009.** The importance of light quality in crop-weed competition. *Weed Research* **49**: 217–224.
- López-Juez E, Kobayashi M, Sakurai A, Kamiya Y, Kendrick RE. 1995.** Phytochrome, gibberellins, and hypocotyl growth. *Plant Physiology* **107**: 131–140.
- Lorrain S, Allen T, Duek PD, Whitelam GC, Fankhauser C. 2008.** Phytochrome-mediated inhibition of shade avoidance involves degradation of growth-promoting bHLH transcription factors. *The Plant Journal* **53**: 312–323.
- de Lucas M, Davière J-M, Rodríguez-Falcón M, Pontin M, Iglesias-Pedraz JM, Lorrain S, Fankhauser C, Blázquez MA, Titarenko E, Prat S. 2008.** A molecular framework for light and gibberellin control of cell elongation. *Nature* **451**: 480–484.
- Ma D, Li X, Guo Y, Chu J, Fang S, Yan C, Noel JP, Liu H. 2016.** Cryptochrome 1 interacts with PIF4 to regulate high temperature-mediated hypocotyl elongation in response to blue light. *Proceedings of the National Academy of Sciences of the United States of America* **113**: 224–229.
- Machida Y, Suzuki T, Sasabe M, Iwakawa H, Kojima S, Machida C. 2021.** Arabidopsis ASYMMETRIC LEAVES2 (AS2): roles in plant morphogenesis, cell division, and pathogenesis. *Journal of Plant Research*: 1–12.
- Maddoni GA, Otegui ME, Andrieu B, Chelle M, Casal JJ. 2002.** Maize leaves turn away from neighbors. *Plant Physiology* **130**: 1181–1189.
- Mao Z, He S, Xu F, Wei X, Jiang L, Liu Y, Wang W, Li T, Xu P, Du S, et al. 2020.** Photoexcited CRY1 and phyB interact directly with ARF6 and ARF8 to regulate their DNA-binding activity and auxin-induced hypocotyl elongation in Arabidopsis. *New Phytologist* **225**: 848–865.
- Marín C, Weiner J. 2014.** Effects of density and sowing pattern on weed suppression and grain yield in three varieties of maize under high weed pressure. *Weed Research* **54**: 467–474.
- Martínez-García JF, Gallemí M, Molina-Contreras MJ, Llorente B, Bevilacqua MRR, Quail PH. 2014.** The shade avoidance syndrome in Arabidopsis: The antagonistic role of phytochrome A and B differentiates vegetation proximity and canopy shade. *PLoS ONE* **9**: e109275.
- Mashiguchi K, Tanaka K, Sakai T, Sugawara S, Kawaide H, Natsume M, Hanada A, Yaeno T, Shirasu K, Yao H, et al. 2011.** The main auxin biosynthesis pathway in Arabidopsis. *Proceedings of the National Academy of Sciences of the United States of America* **108**: 18512–18517.
- Merelo P, Paredes EB, Heisler MG, Wenkel S. 2017.** The shady side of leaf development: the role of the REVOLUTA/KANADI1 module in leaf patterning and auxin-mediated growth promotion. *Current Opinion in Plant Biology* **35**: 111–116.
- Merelo P, Xie Y, Brand L, Ott F, Weigel D, Bowman JL, Heisler MG, Wenkel S. 2013.** Genome-Wide Identification of KANADI1 Target Genes. *PLoS ONE* **8**: e77341.
- Michaud O, Fiorucci A, Xenarios I, Fankhauser C. 2017.** Local auxin production underlies a spatially restricted neighbor-detection response in Arabidopsis. *Proceedings of the National Academy of Sciences* **114**: 7444–7449.
- Moreno-Risueno MA, Van Norman JM, Moreno A, Zhang J, Ahnert SE, Benfey PN. 2010.** Oscillating gene expression determines competence for periodic Arabidopsis root branching. *Science* **329**: 1306–1311.
- Morita MT. 2010.** Directional gravity sensing in gravitropism. *Annual review of plant biology* **61**: 705–720.
- Müller-Moulé P, Nozue K, Pytlak ML, Palmer CM, Covington MF, Wallace AD, Harmer SL, Maloof JN. 2016.** YUCCA auxin biosynthetic genes are required for Arabidopsis shade avoidance. *PeerJ* **4**: e2574.

- Mustroph A, Zanetti ME, Jang CJH, Holtan HE, Repetti PP, Galbraith DW, Girke T, Bailey-Serres J. 2009.** Profiling translatoemes of discrete cell populations resolves altered cellular priorities during hypoxia in Arabidopsis. *Proceedings of the National Academy of Sciences of the United States of America* **106**: 18843–18848.
- Nagashima A, Suzuki G, Uehara Y, Saji K, Furukawa T, Koshiba T, Sekimoto M, Fujioka S, Kuroha T, Kojima M, et al. 2008.** Phytochromes and cryptochromes regulate the differential growth of Arabidopsis hypocotyls in both a PGP19-dependent and a PGP19-independent manner. *Plant Journal* **53**: 516–529.
- Nito K, Kajiyama T, Unten-Kobayashi J, Fujii A, Mochizuki N, Kambara H, Nagatani A. 2015.** Spatial regulation of the gene expression response to shade in Arabidopsis seedlings. *Plant and Cell Physiology* **56**: 1306–1319.
- Notaguchi M, Abe M, Kimura T, Daimon Y, Kobayashi T, Yamaguchi A, Tomita Y, Dohi K, Mori M, Araki T. 2008.** Long-Distance, Graft-Transmissible Action of Arabidopsis FLOWERING LOCUS T Protein to Promote Flowering. *Plant and Cell Physiology* **49**: 1645–1658.
- Nozue K, Tat A V., Kumar Devisetty U, Robinson M, Mumbach MR, Ichihashi Y, Lekkala S, Maloof JN. 2015.** Shade Avoidance Components and Pathways in Adult Plants Revealed by Phenotypic Profiling. *PLoS Genetics* **11**: e1004953.
- Oh E, Zhu JY, Bai MY, Arenhart RA, Sun Y, Wang ZY. 2014.** Cell elongation is regulated through a central circuit of interacting transcription factors in the Arabidopsis hypocotyl. *eLife* **3**: e03031.
- Oh E, Zhu J-Y, Wang Z-Y. 2012.** Interaction between BZR1 and PIF4 integrates brassinosteroid and environmental responses. *Nature cell biology* **14**: 802–809.
- Pacin M, Semmoloni M, Legris M, Finlayson SA, Casal JJ. 2016.** Convergence of CONSTITUTIVE PHOTOMORPHOGENESIS 1 and PHYTOCHROME INTERACTING FACTOR signalling during shade avoidance. *New Phytologist* **211**: 967–979.
- Page ER, Cerrudo D, Westra P, Loux M, Smith K, Foresman C, Wright H, Swanton CJ. 2012.** Why Early Season Weed Control Is Important in Maize. *Weed Science* **60**: 423–430.
- Page ER, Tollenaar M, Lee EA, Lukens L, Swanton CJ. 2009.** Does the shade avoidance response contribute to the critical period for weed control in maize (*Zea mays*)? *Weed Research* **49**: 563–571.
- Pantazopoulou CK, Bongers FJ, Küpers JJ, Reinen E, Das D, Evers JB, Anten NPR, Pierik R. 2017.** Neighbor detection at the leaf tip adaptively regulates upward leaf movement through spatial auxin dynamics. *Proceedings of the National Academy of Sciences* **114**: 7450–7455.
- Pantazopoulou CK, Bongers FJ, Pierik R. 2021.** Reducing shade avoidance can improve Arabidopsis canopy performance against competitors. *Plant Cell and Environment* **44**: 1130–1141.
- Park S-Y, Fung P, Nishimura N, Jensen DR, Fujii H, Zhao Y, Lumba S, Santiago J, Rodrigues A, Chow TF, et al. 2009.** Abscisic acid inhibits type 2C protein phosphatases via the PYR/PYL family of START proteins. *Science* **324**: 1068–1071.
- Park YJ, Lee HJ, Gil KE, Kim JY, Lee JH, Lee H, Cho HT, Vu LD, Smet I De, Park CM. 2019.** Developmental programming of thermonastic leaf movement. *Plant Physiology* **180**: 1185–1197.
- Pedmale U V., Huang SSC, Zander M, Cole BJ, Hetzel J, Ljung K, Reis PAB, Sridevi P, Nito K, Nery JR, et al. 2016.** Cryptochromes Interact Directly with PIFs to Control Plant Growth in Limiting Blue Light. *Cell* **164**: 233–245.
- Pedmale U V., Liscum E. 2007.** Regulation of phototropic signaling in Arabidopsis via phosphorylation state changes in the phototropin 1-interacting protein NPH3. *Journal of Biological Chemistry* **282**: 19992–20001.

- Péret B, Swarup K, Ferguson A, Seth M, Yang Y, Dhondt S, James N, Casimiro I, Perry P, Syed A, et al. 2012.** AUX/LAX genes encode a family of auxin influx transporters that perform distinct functions during arabidopsis development. *Plant Cell* **24**: 2874–2885.
- Petrášek J, Friml J. 2009.** Auxin transport routes in plant development. *Development* **136**: 2675–2688.
- Petrášek J, Mravec J, Bouchard R, Blakeslee JJ, Abas M, Seifertová D, Wiśniewska J, Tadele Z, Kubeš M, Čovanová M, et al. 2006.** PIN Proteins Perform a Rate-Limiting Function in Cellular Auxin Efflux. *Science* **312**: 914–918.
- Pierik R, Cuppens MLC, Voeselek LACJ, Visser EJW. 2004a.** Interactions between ethylene and gibberellins in phytochrome-mediated shade avoidance responses in tobacco. *Plant Physiology* **136**: 2928–2936.
- Pierik R, Djakovic-Petrovic T, Keuskamp DH, de Wit M, Voeselek LACJ. 2009.** Auxin and ethylene regulate elongation responses to neighbor proximity signals independent of gibberellin and della proteins in Arabidopsis. *Plant physiology* **149**: 1701–1712.
- Pierik R, Testerink C. 2014.** The Art of Being Flexible: How to Escape from Shade, Salt and Drought. *Plant Physiology* **166**: 5–22.
- Pierik R, Whitelam GC, Voeselek LACJ, De Kroon H, Visser EJW. 2004b.** Canopy studies on ethylene-insensitive tobacco identify ethylene as a novel element in blue light and plant-plant signalling. *Plant Journal* **38**: 310–319.
- Pierik R, De Wit M. 2014.** Shade avoidance: phytochrome signalling and other aboveground neighbour detection cues. *Journal of Experimental Botany* **65**: 2815–2824.
- Polko JK, van Rooij JA, Vanneste S, Pierik R, Ammerlaan AMH, Vergeer-van Eijk MH, McLoughlin F, Gühl K, Van Isterdael G, Voeselek LACJ, et al. 2015.** Ethylene-Mediated Regulation of A2-Type CYCLINs Modulates Hyponastic Growth in Arabidopsis. *Plant Physiology* **169**: 194–208.
- Polko JK, van Zanten M, van Rooij JA, Marée AFM, Voeselek LACJ, Peeters AJM, Pierik R. 2012.** Ethylene-induced differential petiole growth in Arabidopsis thaliana involves local microtubule reorientation and cell expansion. *New Phytologist* **193**: 339–348.
- Porco S, Pěňčík A, Rasheda A, Vo U, Casanova-Sáez R, Bishopp A, Golebiowska A, Bhosale R, Swarupa R, Swarup K, et al. 2016.** Dioxygenase-encoding AtDAO1 gene controls IAA oxidation and homeostasis in arabidopsis. *Proceedings of the National Academy of Sciences of the United States of America* **113**: 11016–11021.
- Preuten T, Hohm T, Bergmann S, Fankhauser C. 2013.** Defining the Site of Light Perception and Initiation of Phototropism in Arabidopsis. *Current Biology* **23**: 1934–1938.
- Procko C, Burko Y, Jaillais Y, Ljung K, Long JA, Chory J. 2016.** The epidermis coordinates auxin-induced stem growth in response to shade. *Genes & Development* **30**: 1529–1541.
- Procko C, Crenshaw CM, Ljung K, Noel JP, Chory J. 2014.** Cotyledon-Generated Auxin Is Required for Shade-Induced Hypocotyl Growth in Brassica rapa. *Plant Physiology* **165**: 1285–1301.
- Pucciariello O, Legris M, Rojas CC, Iglesias MJ, Hernando CE, Dezar C, Vazquez M, Yanovsky MJ, Finlayson SA, Prat S, et al. 2018.** Rewiring of auxin signaling under persistent shade. *Proceedings of the National Academy of Sciences of the United States of America* **115**: 5612–5617.
- Rakusová H, Gallego-Bartolome J, Vanstraelen M, Robert HS, Alabadí D, Blázquez MA, Benková E, Friml J. 2011.** Polarization of PIN3-dependent auxin transport for hypocotyl gravitropic response in Arabidopsis thaliana. *The Plant Journal* **67**: 817–826.
- Rauf M, Arif M, Fisahn J, Xue G-P, Balazadeh S, Mueller-Roeber B. 2013.** NAC Transcription Factor SPEEDY HYPONASTIC GROWTH Regulates Flooding-Induced Leaf Movement in Arabidopsis. *The Plant Cell* **25**: 4941–4955.

- Reed JW, Wu MF, Reeves PH, Hodgens C, Yadav V, Hayes S, Pierik R. 2018. Three Auxin Response Factors Promote Hypocotyl Elongation. *Plant Physiology* **178**: 864–875.
- Regnault T, Davière J-M, Wild M, Sakvarelidze-Achard L, Heintz D, Carrera Bergua E, Lopez Diaz I, Gong F, Hedden P, Achard P. 2015. The gibberellin precursor GA12 acts as a long-distance growth signal in Arabidopsis. *Nature Plants* **1**: 1–6.
- Reinhart BJ, Liu T, Newell NR, Magnani E, Huang T, Kerstetter R, Michaels S, Barton MK. 2013. Establishing a framework for the ad/abaxial regulatory network of Arabidopsis: Ascertaining targets of class III HOMEODOMAIN LEUCINE ZIPPER and KANADI regulation. *Plant Cell* **25**: 3228–3249.
- Rieu I, Ruiz-Rivero O, Fernandez-Garcia N, Griffiths J, Powers SJ, Gong F, Linhartova T, Eriksson S, Nilsson O, Thomas SG, et al. 2008. The gibberellin biosynthetic genes AtGA20ox1 and AtGA20ox2 act, partially redundantly, to promote growth and development throughout the Arabidopsis life cycle. *Plant Journal* **53**: 488–504.
- Roberts D, Pedmale U V., Morrow J, Sachdev S, Lechner E, Tang X, Zheng N, Hannink M, Genschik P, Liscum E. 2011. Modulation of Phototropic Responsiveness in Arabidopsis through Ubiquitination of Phototropin 1 by the CUL3-Ring E3 Ubiquitin Ligase CRL3NPH3. *The Plant Cell* **23**: 3627–3640.
- Roig-Villanova I, Martínez-García JF. 2016. Plant Responses to Vegetation Proximity: A Whole Life Avoiding Shade. *Frontiers in Plant Science* **7**: 236.
- Ruiz Rosquete M, Barbez E, Kleine-Vehn J. 2012. Cellular auxin homeostasis: Gatekeeping is housekeeping. *Molecular Plant* **5**: 772–786.
- Ruyter-Spira C, Kohlen W, Charnikhova T, van Zeijl A, van Bezouwen L, de Ruijter N, Cardoso C, Lopez-Raez JA, Matusova R, Bours R, et al. 2011. Physiological effects of the synthetic strigolactone analog GR24 on root system architecture in arabidopsis: Another belowground role for strigolactones? *Plant Physiology* **155**: 721–734.
- Sah SK, Reddy KR, Li J. 2016. Abscisic acid and abiotic stress tolerance in crop plants. *Frontiers in Plant Science* **7**: 1–26.
- Salehin M, Bagchi R, Estelle M. 2015. SCF TIR1/AFB -Based Auxin Perception: Mechanism and Role in Plant Growth and Development. *The Plant Cell* **27**: 9–19.
- Salisbury FJ, Hall A, Grierson CS, Halliday KJ. 2007. Phytochrome coordinates Arabidopsis shoot and root development. *The Plant Journal* **50**: 429–438.
- Sasidharan R, Chinnappa CC, Staal M, Elzenga JTM, Yokoyama R, Nishitani K, Voesenek LACJ, Pierik R. 2010. Light Quality-Mediated Petiole Elongation in Arabidopsis during Shade Avoidance Involves Cell Wall Modification by Xyloglucan Endotransglucosylase/Hydrolases. *Plant Physiology* **154**: 978–990.
- Sasidharan R, Chinnappa CC, Voesenek LACJ, Pierik R. 2008. The regulation of cell wall extensibility during shade avoidance: A study using two contrasting ecotypes of *Stellaria longipes*. *Plant Physiology* **148**: 1557–1569.
- Sasidharan R, Keuskamp DH, Kooke R, Voesenek LACJ, Pierik R. 2014. Interactions between auxin, microtubules and XTHs mediate green shade- induced petiole elongation in Arabidopsis. *PLoS ONE* **9**: e90587.
- Sauer M, Kleine-Vehn J. 2019. PIN-FORMED and PIN-LIKES auxin transport facilitators. *Development* **146**: dev168088.
- Schiessl K, Lilley JLS, Lee T, Tamvakis I, Kohlen W, Bailey PC, Thomas A, Luptak J, Ramakrishnan K, Carpenter MD, et al. 2019. NODULE INCEPTION Recruits the Lateral Root Developmental Program for Symbiotic Nodule Organogenesis in *Medicago truncatula*. *Current Biology* **29**: 3657–3668.

- Shalitin D, Yang H, Mockler TC, Maymon M, Guo H, Whitelam GC, Lin C. 2002.** Regulation of Arabidopsis cryptochrome 2 by blue-light-dependent phosphorylation. *Nature* **417**: 763–767.
- Sharma A, Sharma B, Hayes S, Kerner K, Hoecker U, Jenkins GI, Franklin KA. 2019.** UVR8 disrupts stabilisation of PIF5 by COP1 to inhibit plant stem elongation in sunlight. *Nature Communications* **10**: 1–10.
- Sheerin DJ, Menon C, zur Oven-Krockhaus S, Enderle B, Zhu L, Johnen P, Schleifenbaum F, Stierhof Y-D, Huq E, Hiltbrunner A. 2015.** Light-Activated Phytochrome A and B Interact with Members of the SPA Family to Promote Photomorphogenesis in Arabidopsis by Reorganizing the COP1/SPA Complex. *The Plant Cell* **27**: 189–201.
- Shi Q, Kong F, Zhang H, Jiang Y, Heng S, Liang R, Ma L, Liu J, Lu X, Li P, et al. 2019.** Molecular mechanisms governing shade responses in maize. *Biochemical and Biophysical Research Communications* **516**: 112–119.
- Shi DY, Li YH, Zhang JW, Liu P, Zhao B, Dong ST. 2016.** Effects of plant density and nitrogen rate on lodging-related stalk traits of summer maize. *Plant, Soil and Environment* **62**: 299–306.
- Silva-Navas J, Moreno-Risueno MA, Manzano C, Pallero-Baena M, Navarro-Neila S, Téllez-Robledo B, Garcia-Mina JM, Baigorri R, Gallego FJ, Del Pozo JC. 2015.** D-Root: a system for cultivating plants with the roots in darkness or under different light conditions. *The Plant Journal* **84**: 244–255.
- Silverstone AL, Jung HS, Dill A, Kawaide H, Kamiya Y, Sun TP. 2001.** Repressing a Repressor: Gibberellin-Induced Rapid Reduction of the RGA Protein in Arabidopsis. *Plant Cell* **13**: 1555–1565.
- Singh G, Retzer K, Vosolsobě S, Napier R. 2018.** Advances in understanding the mechanism of action of the auxin permease AUX1. *International Journal of Molecular Sciences* **19**: 3391.
- Skopelitis DS, Benkovics AH, Husbands AY, Timmermans MCP. 2017.** Boundary Formation through a Direct Threshold-Based Readout of Mobile Small RNA Gradients. *Developmental Cell* **43**: 265–273.
- Smith HL, McAusland L, Murchie EH. 2017.** Don't ignore the green light: Exploring diverse roles in plant processes. *Journal of Experimental Botany* **68**: 2099–2110.
- Spartz AK, Lee SH, Wenger JP, Gonzalez N, Itoh H, Inzé D, Peer WA, Murphy AS, Overvoorde PJ, Gray WM. 2012.** The SAUR19 subfamily of SMALL AUXIN UP RNA genes promote cell expansion. *The Plant Journal* **70**: 978–990.
- Spartz AK, Ren H, Park MY, Grandt KN, Lee SH, Murphy AS, Sussman MR, Overvoorde PJ, Gray WM. 2014.** SAUR Inhibition of PP2C-D Phosphatases Activates Plasma Membrane H⁺-ATPases to Promote Cell Expansion in Arabidopsis. *The Plant Cell* **26**: 2129–2142.
- Staswick PE, Serban B, Rowe M, Tiryaki I, Maldonado MT, Maldonado MC, Suza W. 2005.** Characterization of an Arabidopsis Enzyme Family That Conjugates Amino Acids to Indole-3-Acetic Acid. *The Plant Cell* **17**: 616–627.
- Stepanova AN, Robertson-Hoyt J, Yun J, Benavente LM, Xie D-Y, Dolezal K, Schlereth A, Jürgens G, Alonso JM. 2008.** TAA1-mediated auxin biosynthesis is essential for hormone crosstalk and plant development. *Cell* **133**: 177–91.
- Stepanova AN, Yun J, Robles LM, Novak O, He W, Guo H, Ljung K, Alonso JM. 2011.** The Arabidopsis YUCCA1 Flavin Monooxygenase functions in the Indole-3-Pyruvic acid branch of Auxin Biosynthesis. *Plant Cell* **23**: 3961–3973.
- Subedi KD, Ma BL. 2009.** Assessment of some major yield-limiting factors on maize production in a humid temperate environment. *Field Crops Research* **110**: 21–26.

- Sullivan S, Kharshiing E, Laird J, Sakai T, Christie JM. 2019.** Deetiolation Enhances Phototropism by Modulating Phosphorylation Status. *Plant Physiology* **180**: 1119–1131.
- Sun T. 2010.** Gibberellin-GID1-DELLA: a pivotal regulatory module for plant growth and development. *Plant Physiology* **154**: 567–570.
- Sun J, Qi L, Li Y, Chu J, Li C. 2012.** PIF4-mediated activation of YUCCA8 expression integrates temperature into the auxin pathway in regulating arabidopsis hypocotyl growth. *PLoS Genetics* **8**: e1002594.
- Sun Q, Yoda K, Suzuki M, Suzuki H. 2003.** Vascular tissue in the stem and roots of woody plants can conduct light. *Journal of Experimental Botany* **54**: 1627–1635.
- Tal I, Zhang Y, Jørgensen ME, Pisanty O, Barbosa ICR, Zourelidou M, Regnault T, Crocoll C, Erik Olsen C, Weinstain R, et al. 2016.** The Arabidopsis NPF3 protein is a GA transporter. *Nature Communications* **7**: 11486.
- Tanaka S-I, Nakamura S, Mochizuki N, Nagatani A. 2002.** Phytochrome in Cotyledons Regulates the Expression of Genes in the Hypocotyl through Auxin-Dependent and -Independent Pathways. *Plant and Cell Physiology* **43**: 1171–1181.
- Tao Y, Ferrer J-L, Ljung K, Pojer F, Hong F, Long J a., Li L, Moreno JE, Bowman ME, Ivans LJ, et al. 2008.** Rapid Synthesis of Auxin via a New Tryptophan-Dependent Pathway Is Required for Shade Avoidance in Plants. *Cell* **133**: 164–176.
- Tavridou E, Pireyre M, Ulm R. 2020.** Degradation of the transcription factors PIF4 and PIF5 under UV-B promotes UVR8-mediated inhibition of hypocotyl growth in Arabidopsis. *Plant Journal* **101**: 507–517.
- Townsley BT, Covington MF, Ichihashi Y, Zumstein K, Sinha NR. 2015.** BrAD-seq: Breath Adapter Directional sequencing: A streamlined, ultra-simple and fast library preparation protocol for strand specific mRNA library construction. *Frontiers in Plant Science* **6**: 366.
- Vandenbussche F, Van Der Straeten D. 2014.** Differential accumulation of ELONGATED HYPOCOTYL5 correlates with hypocotyl bending to ultraviolet-B light. *Plant Physiology* **166**: 40–43.
- Vandenbussche F, Tilbrook K, Fierro AC, Marchal K, Poelman D, Van Der Straeten D, Ulm R. 2014.** Photoreceptor-Mediated Bending towards UV-B in Arabidopsis. *Molecular Plant* **7**: 1041–1052.
- Vanhaelewyn L, Viczián A, Prinsen E, Bernula P, Serrano AM, Arana MV, Ballaré CL, Nagy F, van der Straeten D, Vandenbussche F. 2019.** Differential UVR8 signal across the stem controls UV-B-induced inflorescence phototropism. *Plant Cell* **31**: 2070–2088.
- Wan Y, Jasik J, Wang L, Hao H, Volkmann D, Menzel D, Mancuso S, Baluska F, Lin J. 2012.** The Signal Transducer NPH3 Integrates the Phototropin1 Photosensor with PIN2-Based Polar Auxin Transport in Arabidopsis Root Phototropism. *The Plant Cell* **24**: 551–565.
- Wang W, Lu X, Li L, Lian H, Mao Z, Xu P, Guo T, Xu F, Du S, Cao X, et al. 2018.** Photoexcited CRYPTOCHROME1 interacts with dephosphorylated bes1 to regulate brassinosteroid signaling and photomorphogenesis in arabidopsis. *Plant Cell* **30**: 1989–2005.
- Wang X, Yu R, Wang J, Lin Z, Han X, Deng Z, Fan L, He H, Deng XW, Chen H. 2020.** The Asymmetric Expression of SAUR Genes Mediated by ARF7/19 Promotes the Gravitropism and Phototropism of Plant Hypocotyls. *Cell Reports* **31**: 107529.
- Weijers D, Wagner D. 2016.** Transcriptional Responses to the Auxin Hormone. *Annual review of plant biology* **67**: 539–574.

- Weiner J, Andersen SB, Wille WKM, Griepentrog HW, Olsen JM. 2010. Evolutionary Agroecology: The potential for cooperative, high density, weed-suppressing cereals. *Evolutionary Applications* 3: 473–479.
- Went FW, Thimann K V. 1937. Phytohormones. *New York: The MacMillan Company* 1: 1–316.
- Westwood JH, Charudattan R, Duke SO, Fennimore SA, Marrone P, Slaughter DC, Swanton C, Zollinger R. 2018. Weed Management in 2050: Perspectives on the Future of Weed Science. *Weed Science* 66: 275–285.
- Wies G, Mantese AI, Casal JJ, Maddonni GÁ. 2019. Phytochrome B enhances plant growth, biomass and grain yield in field-grown maize. *Annals of Botany* 123: 1079–1088.
- Wigge PA, Kim MC, Jaeger KE, Busch W, Schmid M, Lohmann JU, Weigel D. 2005. Integration of Spatial and Temporal Information During Floral Induction in Arabidopsis. *Science* 309: 1056–1059.
- Willige BC, Ahlers S, Zourelidou M, Barbosa ICR, Demarsy E, Trevisan M, Davis PA, Roelfsema MRG, Hangarter R, Fankhauser C, et al. 2013. D6PK AGCVIII kinases are required for auxin transport and phototropic hypocotyl bending in Arabidopsis. *Plant Cell* 25: 1674–1688.
- Wisniewska J, Xu J, Seifartová D, Brewer PB, Růžička K, Blilou L, Rouquié D, Benková E, Scheres B, Friml J. 2006. Polar PIN localization directs auxin flow in plants. *Science* 312: 883.
- de Wit M, Kegge W, Evers JB, Vergeer-van Eijk MH, Gankema P, Voeselek LACJ, Pierik R. 2012. Plant neighbor detection through touching leaf tips precedes phytochrome signals. *Proceedings of the National Academy of Sciences* 109: 14705–14710.
- de Wit M, Keuskamp DH, Bongers FJ, Hornitschek P, Gommers CMM, Reinen E, Martínez-Cerón C, Fankhauser C, Pierik R. 2016. Integration of Phytochrome and Cryptochrome Signals Determines Plant Growth during Competition for Light. *Current Biology* 26: 3320–3326.
- de Wit M, Ljung K, Fankhauser C. 2015. Contrasting growth responses in lamina and petiole during neighbor detection depend on differential auxin responsiveness rather than different auxin levels. *New Phytologist* 208: 198–209.
- de Wit M, Lorrain S, Fankhauser C. 2014. Auxin-mediated plant architectural changes in response to shade and high temperature. *Physiologia Plantarum* 151: 13–24.
- De Wit M, Spoel SH, Sanchez-Perez GF, Gommers CMM, Pieterse CMJ, Voeselek LACJ, Pierik R. 2013. Perception of low red:far-red ratio compromises both salicylic acid- and jasmonic acid-dependent pathogen defences in Arabidopsis. *The Plant Journal* 75: 90–103.
- Won C, Shen X, Mashiguchi K, Zheng Z, Dai X, Cheng Y, Kasahara H, Kamiya Y, Chory J, Zhao Y. 2011. Conversion of tryptophan to indole-3-acetic acid by TRYPTOPHAN AMINOTRANSFERASES OF ARABIDOPSIS and YUCCAs in Arabidopsis. *Proceedings of the National Academy of Sciences* 108: 18518–18523.
- Woodley of Menie MA, Pawlik P, Webb MT, Bruce KD, Devlin PF. 2019. Circadian leaf movements facilitate overtopping of neighbors. *Progress in Biophysics and Molecular Biology* 146: 104–111.
- Xie Y, Straub D, Eguen T, Brandt R, Stahl M, Martínez-García JF, Wenkel S. 2015. Meta-analysis of arabidopsis KANADI1 direct target genes identifies a basic growth-promoting module acting upstream of hormonal signaling pathways. *Plant Physiology* 169: 1240–1253.
- Xu F, He S, Zhang J, Mao Z, Wang W, Li T, Hua J, Du S, Xu P, Li L, et al. 2018. Photoactivated CRY1 and phyB Interact Directly with AUX/IAA Proteins to Inhibit Auxin Signaling in Arabidopsis. *Molecular Plant* 11: 523–541.
- Xue J, Xie R, Zhang W, Wang K, Hou P, Ming B, Gou L, Li S. 2017. Research progress on reduced lodging of high-yield and -density maize. *Journal of Integrative Agriculture* 16: 2717–2725.

- Yang C, Xie F, Jiang Y, Li Z, Huang X, Li L. 2018.** Phytochrome A Negatively Regulates the Shade Avoidance Response by Increasing Auxin/Indole Acetic Acid Protein Stability. *Developmental Cell* **44**: 29–41.
- Yoshida T, Fujita Y, Maruyama K, Mogami J, Todaka D, Shinozaki K, Yamaguchi-Shinozaki K. 2015.** Four Arabidopsis AREB/ABF transcription factors function predominantly in gene expression downstream of SnRK2 kinases in abscisic acid signalling in response to osmotic stress. *Plant, Cell and Environment* **38**: 35–49.
- Žádníková P, Petrášek J, Marhavý P, Raz V, Vandenbussche F, Ding Z, Schwarzerová K, Morita MT, Tasaka M, Hejatko J, et al. 2010.** Role of PIN-mediated auxin efflux in apical hook development of Arabidopsis thaliana. *Development* **137**: 607–617.
- Zanetti ME, Chang IF, Gong F, Galbraith DW, Bailey-Serres J. 2005.** Immunopurification of polyribosomal complexes of Arabidopsis for global analysis of gene expression. *Plant Physiology* **138**: 624–635.
- Zhang Y, Yu Q, Jiang N, Yan X, Wang C, Wang Q, Liu J, Zhu M, Bednarek SY, Xu J, et al. 2017.** Clathrin regulates blue light-triggered lateral auxin distribution and hypocotyl phototropism in Arabidopsis. *Plant Cell and Environment* **40**: 165–176.
- Zheng Z, Guo Y, Novák O, Chen W, Ljung K, Noel JP, Chory J. 2016.** Local auxin metabolism regulates environment-induced hypocotyl elongation. *Nature Plants* **2**: 1–9.
- Zheng Z, Guo Y, Novak O, Dai X, Zhao Y, Ljung K, Noel JP, Chory J. 2013.** Coordination of auxin and ethylene biosynthesis by the aminotransferase VAS1. *Nature chemical biology* **9**: 244–246.
- Zhu JK. 2016.** Abiotic Stress Signaling and Responses in Plants. *Cell* **167**: 313–324.
- Zourelidou M, Müller I, Willige BC, Nill C, Jikumaru Y, Li H, Schwechheimer C. 2009.** The polarly localized D6 PROTEIN KINASE is required for efficient auxin transport in Arabidopsis thaliana. *Development* **136**: 627–636.

Appendix

Appendix 1. Primer sequences used in this thesis.

Primer set	Forward	Reverse	Purpose
ACS4	GGAGCCACTTCCGCAAAC	GCTTGCTCGTAGGCTTCTTC	RT-qPCR
GA200X2	AGTAGCTTCACCGGCAGATT	ACGCCTAAACTTAAGCCCAGA	RT-qPCR
IAA19	TAAGCTCTTCGGTTTCCGTG	ACATCCCCCAAGGTACATCA	RT-qPCR
IAA29	AAGATGGATGGTGTGGCAAT	GTCACCCTCTTCCCTTGGA	RT-qPCR
PEX4	TGCAACCTCCTCAAGTTCGA	TGAGTCGCAGTTAAGAGGACT	RT-qPCR
PIL1	AGACCACCTACGATGTTGCC	TAGCATTTGTGGTGGTGCAT	RT-qPCR
PIN3	CTTATTTGGGCTCTCGTCGC	AACGTTGCCACTGAATTCCC	RT-qPCR
RD20	GTCAGCGAAAAGTACGGAAC	TCGTGACCTTCTGTTCCATT	RT-qPCR
RHIP1	ATTGGTGTCTGCTAGTCT	TAAAGCCGCTCTCAAGCA	RT-qPCR
TAA1	TGTCCGATTTCTGGTCAATCTGG	CACAAGTTCGTCATGTCGCTGAAG	RT-qPCR
YUC8	TGCGGTTGGGTTTACGAGGAAAG	GCGTTTCGTGGGTTGTTTTG	RT-qPCR
YUC9	AGTCCGGCGAGAAATTCAGA	AACCGAGCTTCTAACGACCA	RT-qPCR
mTurquoise2 + STOP	TTTTGGATCCGGTGGTATGGT GAGCAAGGGCGAGGA	TTTTAGATCTTTACTTGTACA GCTCGTCCATGC	Cloning C3PO
mTurquoise2 non-STOP	TTTTGGATCCGGTGGTATGGT GAGCAAGGGCGAGGA	TTTTAGATCTCTTGTACAGCT CGTCCATGCC	Cloning C3PO
NLS-mTurquoise2 non-STOP	TTTTGGATCCCATGGCTCCAA AGAAGAAGAGAAAGGTCATG GTGAGCAAGGGCGAGGA	TTTTAGATCTCTTGTACAGCT CGTCCATGCC	Cloning C3PO
Additional Ascl	CTAGATTAATTAAGACACAGG CGCGCCT	CTAGAGGCGCGCCTGTGTCT TAATTAAT	Cloning C3PO

Samenvatting

Planten zijn een belangrijk onderdeel van de koolstofcyclus. Ze nemen koolstofdioxide (CO_2) uit de lucht op en zetten het, samen met water, om in suikers en zuurstof in het proces genaamd fotosynthese. Deze omzetting vergt energie die de plant verkrijgt uit de absorptie van zonlicht in chlorofyl (bladgroen) in de bladeren. Voornamelijk blauw (400-500 nm) en rood (R, 600-700 nm) licht worden efficiënt geabsorbeerd door chlorofyl, terwijl andere kleuren zoals groen (500-550 nm) en ver-rood (far-red, FR, 700-800 nm) licht minder worden geabsorbeerd maar juist door het blad heen schijnen of er van weerkaatsen. De weerkaatsing van groen licht maakt dat bladeren voor het menselijk oog groen zijn. Planten "zien" hun buurplanten daarentegen voornamelijk door de weerkaatsing van ver-rood licht. Het rood en ver-rood gevoelige lichtreceptoreiwit fytochroom B (phyB) bestaat in een actieve en inactieve vorm. In vol zonlicht, waar de hoeveelheden rood en ver-rood licht vergelijkbaar zijn, is phyB voornamelijk actief. Door de specifieke absorptie van rood licht door bladeren is er onder een bladerdek een relatieve verlaging van de hoeveelheid rood ten opzichte van ver-rood licht, dit wordt een lage rood:ver-rood ratio (R:FR) genoemd. Bij een afnemende R:FR neemt de activiteit van phyB ook af. Behalve onder een bladerdek verandert de R:FR ook rondom planten. In dit geval komt dat niet door absorptie van rood licht maar door horizontale weerkaatsing van ver-rood licht. Op deze manier kan een plant bepalen waar er andere planten in de buurt staan en zijn groei er op aanpassen. Deze adaptieve groei is essentieel voor planten die dichtbij andere planten groeien vanwege de beperkte hoeveelheid zonlicht.

De lage R:FR die planten ervaren bij hoge dichtheid zorgt voor inactivatie van phyB. Inactief phyB verliest zijn remmende invloed op de groeistimulerende PHYTOCHROME INTERACTING FACTOR (PIF) eiwitten, waardoor celgroei in gang wordt gezet. Als gevolg van deze celgroei strekken planten zich in laag R:FR. Deze strekking en opwaartse groei brengt de bladeren van de plant omhoog en zorgt ervoor dat de plant minder snel in de schaduw van diens buurplanten komt te staan en wordt daarom schaduw vermijding genoemd. Hoewel deze groeireactie op het waarnemen van burenen een voordeel oplevert voor de lichtinterceptie van de individuele plant kleven er ook nadelen aan. Zo verhogen lange dunne stengels het risico op omwaaien. Ook kan de productie van vruchten en zaden verminderen, groeit het wortelsysteem minder en is er verminderde resistentie tegen plagen en infecties. Daarnaast kan er een kettingreactie optreden waarin strekking van een enkel individu zorgt voor strekking van diens buurplanten en vice versa. In de voedselproductie is de opbrengst per hectare belangrijker dan de opbrengst van individuele planten. Door beter te begrijpen hoe schaduw vermijding wordt gereguleerd,

kunnen gewassen worden gecreëerd die minder lichtconcurrentie vertonen waardoor de opbrengst geoptimaliseerd wordt.

Aangezien de R:FR bepaald wordt door zowel absorptie van rood als reflectie van ver-rood licht door buurplanten, kan er grote variatie bestaan in de R:FR die wordt waargenomen in verschillende delen van de plant. In **hoofdstuk 3** wordt beschreven hoe de rozetplant *Arabidopsis thaliana* (*Arabidopsis*, zandraket) reageert op lokale veranderingen in de R:FR in specifieke delen van het blad. Wanneer de R:FR lokaal wordt verlaagd door FR licht toediening op de bladsteel (petiool) zal deze strekken. Daarentegen zorgt FR toediening op de bladpunt (FRtip) voor opwaartse beweging van de petiool (hyponastie). Deze hyponastie vindt plaats door asymmetrische groei tussen de onder- en bovenkant van de petiool basis, waarbij de onderkant sneller groeit dan de bovenkant. Zowel de strekking als de hyponastie van de petiool vindt alleen plaats in het blad waar respectievelijk de petiool of de bladpunt FR toediening krijgen. In dit hoofdstuk wordt verder beschreven dat FRtip behandeling zorgt voor verhoogde transcriptie van de *YUCCA* auxine synthese genen in de bladpunt via PIF7. Auxine is een plantenhormoon dat bekend staat om zijn groeistimulerende werking. Ook laten we zien dat phyB, PIF7 en YUCCA eiwitten nodig zijn voor de hyponastie, net als de PIN auxine transporteiwitten. Directe toediening van auxine op de bladpunt (IAAtip) stimuleert net als FRtip petiool hyponastie. Dit suggereert dat auxine transport van de bladpunt naar de petiool nodig is voor hyponastie in reactie op FRtip behandeling. In tegenstelling tot auxine lijkt het hormoon abscisinezuur (ABA) de hyponastie en PIF signalering in FRtip te remmen.

Hoofdstuk 4 beschrijft een weefsel-specifieke genexpressieanalyse waarin wordt onderzocht hoe de lokale FR behandeling in de bladpunt een distale en asymmetrische groeirespons kan stimuleren in de basis van de petiool. Hyponastie wordt al zichtbaar binnen 4 uur FRtip behandeling. Om te achterhalen welke moleculaire processen er hiervoor geactiveerd worden in de bladpunt, alsook de onder- en bovenkant van de bladsteel, zijn er 9 tijdstippen geselecteerd van 40 minuten tot 5 uur FRtip behandeling. Deze genexpressieanalyse laat een duidelijke auxine respons zien in elk van de weefsels, terwijl signalering van licht en ABA voornamelijk plaatsvindt in de bladpunt. Tussen de twee kanten van de petiool is er een verschillende inductie van auxine- en groeirespons die sterker is in de groeiende onderzijde van de petiool. Daarnaast is er in de onderkant van de petiool een sterkere inductie van signalering door de groeistimulerende hormonen brassinosteroid (BR) en gibberellinezuur (GA). De bevindingen in dit hoofdstuk vormen de basis van verdere analyse in hoofdstukken 5 en 6.

In **hoofdstuk 5** wordt de verdeling van auxine door het blad in verder detail beschreven. Door middel van confocale fluorescentiemicroscopie met een nieuw ontwikkelde auxine reporter wordt de verdeling van auxine op celtype-specifiek niveau in de petiool onderzocht. Hieruit blijkt dat auxine wordt getransporteerd naar de onderzijde van de bladsteel en dat de PIN auxine transporteiwitten daarvoor essentieel zijn. Van deze PINs wordt beschreven dat PIN3 zich in de endodermis, de cellaag rondom de centrale vaatbundel, voornamelijk bevindt aan de onderzijde. Deze asymmetrie wordt nog sterker wanneer er auxine vanaf de bladpunt naar de basis van de petiool beweegt. Dit suggereert dat asymmetrie in PIN3 verdeling zorgt voor auxine transport naar de onderzijde van de petiool, wat de eerder genoemde PIN3 asymmetrie weer versterkt.

De rol van het hormoon GA die in de genexpressieanalyse van hoofdstuk 4 werd gesuggereerd wordt verder onderzocht in **hoofdstuk 6**. Hier laten we zien dat de GA synthese genen *GA20OX1* en *GA20OX2* specifiek geïnduceerd worden door FRtip en IAAtip in de onderzijde van de petiool. Het inactiveren van GA productie door mutatie van *GA20OX* genen of toediening van paclobutrazol remt de hyponastie in reactie op FRtip. De suggestie dat GA synthese plaatsvindt in de petiool in reactie op auxine dat komt vanuit de bladpunt wordt verder bevestigd door de gemeten afname van het DELLA eiwit RGA in de petiool. DELLAs zijn groei remmende eiwitten die worden afgebroken in de aanwezigheid van GA. DELLAs remmen de groei door inhibitie van de zogenaamde BAP module eiwitten BZR1, ARF en PIF die respectievelijk groei stimuleren in reactie op BR, auxine en laag R:FR. In dit hoofdstuk wordt aangetoond dat ARFs en PIFs essentieel zijn voor de hyponastie respons op auxine uit de bladpunt. Hieruit concluderen we in dit hoofdstuk dat auxine in de onderzijde van de petiool een groeireactie in gang zet doordat de DELLA remmer van de BAP module wordt afgebroken.

Het grootste deel van dit proefschrift focust op het ontrafelen van de onderliggende moleculaire mechanismen van petiool hyponastie in *Arabidopsis*. Daarentegen geeft **hoofdstuk 7** een beschrijving van het onderzoek dat is gedaan naar het effect van vroege lichtconcurrentie in maïs (*Zea mays*). Met het oog op ontwikkelingen rondom strengere wetgeving omtrent het gebruik van herbiciden in de akkerbouw bestaat de kans dat gewassen in de toekomst meer last zullen ondervinden van lichtconcurrentie door onkruiden. Vooral in de vroege ontwikkeling zijn maïsplanten nog dusdanig klein dat zulke concurrentie grote effecten kan hebben op de uiteindelijke opbrengst. Door maïs te groeien in een omgeving met óf zonder onkruiden die na de eerste drie weken van groei werden weggehaald is onderzocht hoe de ontwikkeling van maïs door deze onkruiden werd beïnvloed. Hieruit bleek dat de onkruiden bij de maïsplanten zorgen

voor een relatief dunnere stengel, een kortere plant en een kleiner aantal bladeren. Deze verschillen ontstaan al binnen de eerste drie weken en blijven daarna bestaan, ook al zijn de onkruiden weggehaald. Uiteindelijk zorgt deze competitie ook voor een lager drooggewicht van de plant en kolf. Uit correlatieanalyse is gebleken dat vooral de vroege stengeldikte sterk correleert met de uiteindelijke opbrengst van de plant en dus een goed aanknopingspunt kan vormen voor verdere veredeling van dit gewas.

In dit proefschrift laten we zien dat de locatie van laag R:FR perceptie bepaalt welke groeirespons er wordt geïnduceerd. Wanneer een blad laag R:FR waarneemt op de bladpunt vindt er daar lokaal auxine synthese plaats. Deze auxine wordt zorgvuldig getransporteerd naar de onderzijde van de petiool waar signalering van auxine, samen met gibberelline, zorgt voor versterkte celgroei aan de onderzijde van de petiool, terwijl de bovenzijde niet sneller groeit. Dit onderzoek maakt duidelijk dat auxine een belangrijke rol speelt in de spatiale controle van lichtsignalering op bladbeweging.

Acknowledgements

Het is af. Na jaren werk en maanden schrijven kom ik uit mijn schrijvershol en presenteer ik met trots... mijn proefschrift!

'Ben je nu dan klaar met studeren, kan je nu gaan werken?' Juist.

Hoewel mijn promotie door vertragingen langer heeft geduurd dan van tevoren gedacht heb ik geen moment spijt gehad van mijn keuze om in 2015 met **Ronald** een onderzoeksvoorstel te schrijven. Dankzij je gigantische vertrouwen heb ik me altijd vrij en gewaardeerd gevoeld. Daardoor was het echt mijn project en heb ik ontzettend veel geleerd. Ik blijf diep onder de indruk van hoe je in groot detail betrokken bent bij alle projecten in de groep en hoe snel je kan schakelen tussen de meest complexe data en relevante literatuur. Je bent een groot voorbeeld voor me.

Ook **Rens** wil ik graag bedanken voor alle jaren van gastvrijheid, die begonnen in mijn eerste week als BSc student: *'Nee, ik ben geen u!'*. De zomerbarbecues en kerstdiners bij jou en Carla thuis zorgden er voor dat ik me heel snel thuis voelde bij EvP. Ook de scherpe vragen tijdens werkbesprekingen of de koffiepauze heb ik altijd erg gewaardeerd. **Rashmi**, I remember having our first conversation many years ago while cycling through the floodplains around Nijmegen during an EvP outing. Thank you for always having a ready laugh, and supporting first myself and later many of my students as second thesis reviewer. **Kaisa**, when you came to the lab you brought a lot of experience that was very welcome indeed. This was mainly regarding scripting in R and confocal microscopy, which turned out to be essential parts of my work and this thesis. Things got even better when you ordered a vibratome and taught me how to use it. I also really enjoyed the boardgame nights at your place.

Science is hard and slow work, but it's made a lot easier when you are supported by great technical staff like those I got to work with at EvP over the last years. **Ankie, Rob, Emilie, Diederik, Sara, Liao, Muthanna** and **Yorrit**, thank you for organising the lab and phytotron and helping and supporting me in all kinds of ways. Ik wil specifiek Emilie bedanken, je hebt me ontzettend veel geleerd in het lab, hebt het pipetteerwerk gedaan dat de basis is van hoofdstuk 4 en hebt zelfs mijn goddelijke bruidstaart gebakken (Mo en ik eten nog steeds elk jaar een stukje uit de vriezer). **Anton** en **Otto**, bedankt voor al het werk dat jullie hebben gedaan aan het maken en repareren van de octopuslampen en de spiegelende FR lichtbox.

Dan gaan we verder met de collega's van de shady side of EvP. Ik zou nooit bij EvP terecht zijn gekomen als **Paulien** en **Franca** me niet welkom hadden geheten om als student bij ze aan de slag te gaan. Jullie hebben me de belangrijke basis van het onderzoek in de plantenbiologie geleerd en hebben de vonk bij mij doen overslaan. Franca, je talent om vragen te stellen en blijven stellen totdat er duidelijkheid is vind ik bewonderenswaardig. Van het team dat er toen zat was ook **Lot** een inspiratie met de slimme proeven en mooie visualisaties. Ik vind het heel leuk dat ik jou als EPS talentje heb mogen aflossen, en je de afgelopen jaren tijdens allerlei meetings telkens weer tegen ben gekomen. Nog leuker vind ik het dat ik in april bij je ga beginnen aan mijn eerste postdoc, spannend!

When I started my PhD and moved into room Z303 I found that the shade team had attracted some talented new people. **Sarah**, how amazing it was to meet someone for the first time and immediately become friends. I loved our conversations through the cupboard that ranged from in-depth data discussions, to sharing stories of Yolo and Ilka. Having you as my office neighbour really helped to get me excited on good days and keep me sane on the worse ones. I really missed you when you finished your PhD before me! **Scott**, you are the smartest person I have ever talked science with. I keep on being amazed by how quick you come up with new ideas and hypotheses, and really enjoyed discussing them at conferences, in bars and even while driving home after my informal job application with Lot. **Chia-Kai**, your relaxed attitude, warm heart and great sense of humour were great distractions on the tough days. Thank you for being so kind. **Chrysa**, I like how we went from working together to finish your paper in 2017 to doing the same for my paper last year. I keep on being impressed with how you take on massive loads of work for cool new projects and how quickly you can transplant seedlings. **Kasper**, je hebt me ontzettend geholpen op het lange pad om een aardige microscopist te worden en was in het lab een erg behulpzaam aanspreekpunt. Ook bij het samen schrijven van het review heb ik veel van je geleerd, je was streng wanneer dat nodig was om het proces op gang te krijgen maar hielp geduldig bij de stukken waar ik geen ervaring had. **Sara**, your great knowledge of molecular biology and technically challenging project have always made you an impressive member of the group. I also really enjoyed eating and travelling through Japan together. **Diederik**, toen ik je voor het eerst tegenkwam was ik een klein beetje *starstruck*. *'Is dit de Keuskamp van Keuskamp et al., 2010?'* Later leerde ik je kennen als een behulpzame collega met veel passie voor je werk.

During my PhD, the shade team continued to grow. **Martina**, you replaced Chia-Kai's place in the office and we quickly became friends. Thank you for helping me with data discussions and analysis in R, those were always nice. But more than that, I appreciated

how we could share the frustrations and joys of simultaneously writing reviews, papers and our theses. I am sure your thesis will turn out great! Also, thanks for the tasty Eierlikör you brought me after your holidays in Austria. **Valérie**, ik leerde je kennen toen je als MSc student werkte in onze groep, toen spatte het talent er al van af! Ik heb altijd heerlijk met je kunnen lachen, maar vond de meer serieuze gesprekken zeker ook fijn. Veel plezier met je nieuwe baan in Wageningen, we zien elkaar vast nog wel eens lopen... of de bosjes induiken. **Mariana**, you brought new life to the lab when you joined. It was inspiring to speak with you about anything ranging from LEA proteins and hairy roots to diversity and equality matters. **Linge**, I have never met anyone more dedicated to their project. I wish you all the best in finishing your interesting work that is so very different from all the other projects in the group. **Nicole**, als ik opnieuw een stage zou moeten doen zou ik dat graag bij jou doen. Je vriendelijkheid en heerlijke humor maken je een heel fijne collega om te hebben. **Lisa**, wat was het leuk om met jou steeds verder de diepte in te gaan tijdens onze discussies over de regulatie van bladbeweging. We hebben samen een goed review geschreven, en coole technieken ontwikkeld om de regulatie van bladbeweging in steeds meer detail te onderzoeken, dank daarvoor. **Sanne**, tijdens je stages heb je belangrijke data en methodes ontwikkeld die rechtstreeks het proefschrift in zijn gegaan. Maar nog fijner vond ik dat je altijd klaar stond om waar nodig een handje of twee te helpen. Daarbij was het altijd gezellig, zelfs als we tot 's avonds laat plakjes moesten snijden bij de vibratoom. Ik vind het leuk dat je nu mijn collega en ook zelfs paranimf bent! **Kyra**, wat heeft EvP een geluk gehad dat je bij ons je PhD bent komen doen. Bedankt voor de mooie herinnering van rode wijn op de achterbank. **Pierre**, we only worked together for a couple of months but in this time I was very impressed with your passion for science. I am sure your project will turn out well because of your level of dedication!

Ook de mensen van de flooding groep moet ik om allerlei redenen bedanken. Allereerst **Sjon**, mijn maatje sinds de middelbare school. Ik ben ontzettend trots om te zien hoe jij door de carrière ladder heen knalt en weet zeker dat je er een succes van gaat maken in Freiburg. **Tom**, jij bent in staat om altijd ontspannen over te komen terwijl je bergen werk verzet. Bedankt voor alle onzelfzuchtige hulp die je me tijdens mijn promotie hebt geboden. **Hans**, bedankt voor je scherpe vragen tijdens discussies en inzichten in andere methoden van data analyse. Het R klasje dat je samen met Kaisa organiseerde heeft me over de laatste weerstand geholpen en doen besluiten al mijn data analyse vanaf dat moment met R te doen. To the other members of the flooding team, **Elaine, Shanice, Zeguang, Nikita, Justine, JZ, Melissa, Angelica, Natalia, Ava** and **Putri** (although you

didn't really work on flooding): Thank you for helping with all of those petiole harvest parties and all the nice coffee breaks, borrels and other moments we shared. **Andres, Daan, Gabriele** and **Leo**, you joined the Plant Ecophysiology group after I left the lab. I wish you the best of luck with all your projects!

Further thanks need to go to my students (I am starting to wonder whether I did anything myself). **Marco, Sanne, Yasmin, Pien, Sanne** (again), **Eline** and **Harold**, thank you for trusting me as your supervisor and for all the work you contributed to my project. You taught me a lot about supervising and working together with a variety of different people.

Tijdens mijn promotieonderzoek had ik het geluk om ook samen te mogen werken met mensen van buiten de Universiteit Utrecht. **Wouter**, bedankt voor het meedenken over en uitvoeren van de auxine metingen die nu Figuur 5.1 A vormen. **Dolf** and **Liao**, thank you for sharing the unpublished C3PO auxin reporter and helping me optimise the microscopy using this reporter. Het grootste deel van het werk dat in hoofdstuk 7 beschreven wordt is gedaan in de kassen van Limagrain Nederland. **Cornélie** en **Louis**, bedankt voor het helpen uitdenken en organiseren van het kaswerk. **Angelica, Jaimy** en alle anderen die Pien en mij in en om de kas hebben geholpen, heel hartelijk bedankt. Zonder jullie hulp en vriendelijkheid was het ons nooit gelukt om ons ambitieuze project goed uit te voeren.

Outside the lab, I got to be part of both the **EPSR organising committee** and the **EPS PhD council**. I enjoyed working together with these two very different teams of people to create events of which I am still proud to this day. Celebrating my birthday with all of Europe's brightest PhD students at the EPSR is something I will never forget. Ook heb ik meerdere keren meegedaan aan **Science Battles**. Het was heel leuk en leerzaam om in theaters van Boxmeer tot Amsterdam en Diepenheim tot Middelharnis te vertellen over bewegende bladeren en plantenhormonen. Bedankt voor die kans **René** en **Suzanne**.

Om af en toe stoom af te blazen waren daar de voetbalteams van de Basis en Ody 5/ DHSC 7/ Wijkers 3. Heerlijk om mezelf na een zware dag in het lab ook fysiek echt moe te krijgen, al zullen de biertjes achteraf daar ook aan hebben bijgedragen. Ook wil ik mijn vrienden bedanken voor alle lekkere etentjes, leuke uitjes en fijne vakanties. Vooral **Yuta, Jessie, Anouk** en de Lullo's **Thijs, Lennart, Daniël** en **Sjon**: dat we maar voor altijd vrienden mogen blijven!

En dan de mensen die ik al het langste ken, mijn familie. Lieve **papa** en **mama**, hoewel het er tijdens de middelbare school tijd misschien anders uitzag ben ik studeren toch leuk

gaan vinden. Zo leuk zelfs dat er een PhD in zat, wie had dat twaalf jaar geleden gedacht? Het was ontzettend fijn om jullie als collega's te hebben tijdens mijn schrijfmaanden in jullie werkkamer, soms om te klagen, op andere momenten om enthousiast te overleggen over hoe ik mijn auxine reporter werk moet visualiseren of een stuk tekst te laten lezen. En dan heerlijk eten uit eigen tuin en samen 2 voor 12 kijken. Jullie zijn ongelooflijk lieve en slimme mensen, geen wonder dat jullie zulke leuke kinderen hebben gekregen, mijn vier lieve grote zussen. **Marlijn**, wat is het bijzonder om terug te denken aan hoe ik als jochie bij mijn grote zus op bezoek ging in de grote stad Maastricht. Samen euro's (!) uit de muur halen, vanillecola en chocolademelk drinken en schaatsen op het Vrijthof, dat studeren leek mij ook wel wat! Ook **Tom**, **Niene**, **Elin** en **June** zijn schatten, ik vind het heel fijn om bij jullie langs te komen en onze hondjes samen te zien spelen. **Arieke** en **Lin**, wat was het fijn om laatst samen te gaan wintersporten, inclusief de Yetibar en kaasfondue. Ik ben altijd trots om te vertellen over het mooie werk dat jullie doen met jullie opleidingshonden. **Leanne**, mijn wetenschappelijke voorbeeld en paranimf. Wat een weg heb je afgelegd om te staan waar je nu staat en wat vind ik het fijn om met je te kunnen praten over de zin en onzin van de wetenschap. Bijzonder hoe we toen ik je laatst een data-analyse probeerde uit te leggen samen tot een nog beter idee kwamen voor diezelfde analyse. Ik vind het heel fijn om samen met Mo bij jou, **Thijs**, **Floris** en langs te komen om te schilderen, op te passen of simpelweg voor de gezelligheid. Lieve **Eselien**, hoewel we elkaar vroeger wel eens de tanden uit de mond sloegen (hij zat al heel erg los hoor!) heb ik je altijd een lieve zus gevonden. Ik vind het mooi en inspirerend om te zien hoe bewust jij en **Edwin** jullie leven indelen en de prioriteit hebben liggen op dat was echt belangrijk is, jullie eigen geluk met **Jibbe** en **Cato**.

Ook mijn schoonfamilie wil ik graag bedanken. Lieve **Bernie** en **Frank**, bedankt voor alle ontspannen weekenden in Winterswijk en ook de vakanties naar de Ardennen, Valencia en waar dan ook. Het heeft me altijd goed gedaan om bij jullie tot rust te komen en mijn zinnen te verzetten van werk. **Sue**, ik vind het heerlijk om met je te ouwehoeren en lachen. Bedankt voor alle leuke momenten samen over de afgelopen jaren van festival tot chicken & waffle lunch, met jou is het altijd fijn en gezellig. Ook wil ik nog oma **Diny** bedanken voor het teruggeven van het warme gevoel van grootouders die ik zelf al veel te lang niet meer heb.

En dan ben ik eindelijk bij jou, lieve **Mo**. Het is moeilijk in woorden samen te vatten hoe belangrijk je voor me bent geweest de afgelopen jaren. Dankzij jouw steun heb ik al die tijd zo hard aan dit project kunnen werken. De keren dat we in de weekenden samen naar het lab gingen om dingen af te krijgen heb ik altijd leuk en stiekem ook romantisch

gevonden. Doordeweeks thuiskomen bij jou is elke dag weer tot rust komen. Je weet precies wanneer je me ruimte moet geven of juist liefde. Met jou achter me kan ik de meest complexe situaties aan en komt alles goed. Ik heb zo ontzettend veel zin in de rest van ons leven samen, ook met onze lieve **Ilka**. Ik hou van je.

Curriculum Vitae

Jesse Jaap Küpers was born on the 5th of July 1992 in Winterswijk. He obtained his gymnasium higher education diploma at De Driemark in Winterswijk in June 2010. Afterwards Jesse studied Biology at Utrecht University where he finished his BSc studies in February 2014 with a short internship at the research group of Prof. Dr. Ronald Pierik in Plant Ecophysiology. He continued studying at Utrecht University and finished his MSc studies on Environmental Biology in June 2016. During his MSc studies, Jesse returned to the Plant Ecophysiology group to perform a 9-month research project with Dr. Paulien Gankema and Dr. Franca Bongers in which he studied plastic responses to changing light quality in *Arabidopsis thaliana*. For a second MSc research project, Jesse went to the Department of Comparative Development and Genetics at the Max Planck Institute for Plant Breeding Research in Cologne, headed by Prof. Dr. Miltos Tsiantis. In this 6-month project he worked with Dr. Bjorn Pieper to study the role of SPL9 in *Cardamine hirsuta* leaf development. During his MSc studies, Jesse also worked as a student assistant in the BSc course Plant Biology and Ecology at Utrecht University and later translated the course manual of this course from Dutch to English. At the end of his MSc studies, Jesse participated in the Experimental Plant Sciences (EPS) MSc talent programme to write a research proposal with Prof. Dr. Ronald Pierik. This research proposal was awarded with a personal grant by the Netherlands Organisation for Scientific Research (NWO) in August 2015 and allowed Jesse to start his PhD in July 2016. During his PhD research, Jesse was a member of the EPS PhD council in 2017-2018 and also helped organise the European Plant Science Retreat (EPSR) in 2018. Jesse also participated in several public outreach events including several Science Battle theatre shows throughout the Netherlands. The results of his PhD research are summarised in this thesis.

Publications

Küpers JJ, Snoek LB, Oskam L, Pantazopoulou CK, Matton SEA, Reinen E, Liao C-Y, Eggermont EDC, Weekamp H, Kohlen W, Weijers D, Pierik R. Local light signalling at the leaf tip drives remote differential petiole growth through auxin-gibberellin dynamics. *Under review in Current Biology*.

Küpers JJ, van Gelderen K, Pierik R. **2018**. Location Matters: Canopy Light Responses over Spatial Scales. *Trends in Plant Science* **23**: 865–873.

Küpers JJ, Oskam L, Pierik R. **2020**. Photoreceptors regulate plant developmental plasticity through auxin. *Plants* **9**: 940.

Pantazopoulou CK, Bongers FJ, **Küpers JJ**, Reinen E, Das D, Evers JB, Anten NPR, Pierik R. **2017**. Neighbor detection at the leaf tip adaptively regulates upward leaf movement through spatial auxin dynamics. *Proceedings of the National Academy of Sciences of the United States of America* **114**: 7450–7455.

van der Horst S, van Butselaar T, Zhang H, Vismans G, Steenbergen M, Courbier S, Neilen M, **Küpers JJ**. **2019**. Bringing together Europe's young plant scientists. *New Phytologist* **222**: 29–32.